Mapping and identifying genes for drought tolerance in barley (*Hordeum vulgare* L.)

Dissertation

zur Erlangung des

Doktorgrades der Agrarwissenschaften (Dr. agr.)

der

Naturwissenschaftlichen Fakultät III
Agrar- und Ernährungswissenschaften,
Geowissenschaften und Informatik

der Martin-Luther-Universität Halle-Wittenberg

vorgelegt von

Frau Rasha A. Tarawneh, M.Sc.

geb. am: 22.07.1983 in Al-Karak, Jordan

Gutachter:

1. Prof. Dr. Klaus Pillen
2. Priv. Doz. Dr. Andreas Börner
3. Prof. Elena Khlestkina

Verteidigt am: 20.01.2020

Printed and/or published with the support of the German Academic Exchange Service

ACKNOWLEDGMENTS

Taking a decision to start a Ph.D. study was not easy, especially when you need to leave your family, your country and start new experience. The journey during my study period was full of challenges, happy and sad moments. All the praises and thanks be to Allah first and the presence of many people who were always beside me and being my family; without them my journey would not be completed.

First of all, I would like to express my appreciation to my supervisor Pd. Dr. Habil Andreas Börner for accepting me in his group, for his supervision, advices and fruitful discussions. I learned from him how to be patient, how to face the difficulties and solve problems in a proper way. I cannot find enough words to thank him and without his support. I will not be as I am today.

Sincere thanks to Prof. Dr. Klaus Pillen for accepting me as a Ph.D. student in Martin Luther University Halle-Wittenberg. I appreciate his kindness and encouragement. I would like also to thank Dr. Marion Röder for being my monitor. Thanks to Prof. Elena Khlestkina, whom I had the honor to have her as a reviewer for my dissertation.

Special thanks to Dr. Ahmad Alqudah for his expert advices, his valuable input and suggestions. Thank you for your time, support and generosity. Many thanks to Dr. Manuela Nagel, who was beside me from the first day in IPK, for her encouragement, advices, help and support.

I would like to thank Dr. Kerstin Neuman for willing to help me in my dissertation, for her support, advices and valuable suggestions.

I am indebted to Dr. Adel Abdel-Ghani for his support and encouragement to complete my study in Germany, to Dr. Abdelfattah Badr and his great wife Dr. Hanaa Hijazi for the helpful suggestions and discussion and for the family atmosphere. Thanks a lot to Dr. Matias Schierenbeck for his help during my fieldwork and for the useful discussion and Dr. Helmy Yousef for his support.

Many thanks to my colleagues in RGR group, Dr. Tikhenko, Dr. Lohwasser for their encouragement; Sibylle, Gabriele, Josefine, Anette, Claudia, Mr. Grau, Anna Kodich, Anna Marta, Stefan, Laila Bershi and all other colleges for their technical assistance, the family and friendly working atmosphere. Special thanks to my colleague and friend, Stefani Thum for her unlimited help. I never asked her for help and she said no. I am lucky to have a friend like her. I would like to thank Mr. Peter Schreiber and his team, the greenhouse staff for their help during greenhouse and field experiments.

My sincere gratitude to Dr. Britt Leps for her time, encouragement and help during my stay at IPK. She is the perfect example of kindness and generosity.

I gratefully acknowledge the German Academic Exchange Service (Deutscher Akademischer Austauschdienst DAAD) for the financial support and the opportunity to start my Ph.D. in Germany. This opportunity increased my knowledge, allowed me to learn new techniques and skills and improve my career.

I would like to dedicate this dissertation to my big family, my parents, my brothers, Jaffar, Yazid, Mohamed and my sisters Shahd and Doaa, my brother in law Saqer, Dena, my aunt Yousra and to spirit of aunt Samar. Without their unconditional love, help, encouragement and trust I could not complete this stage. They encouraged my insistence and determination by their support and advice. My thanks to them for being beside me to achieve my dream, no words can express how much I am indebted to you all. I am lucky for having you in my life. You are the best gift anyone could ever ask for.

I am grateful to my friends Lubna, Zobeada, Tasnem, Razan and all others, to Mr. Ali Al-Soub, for being always beside me, for their support and encouragement. You all made me sure that “a strong friendship doesn't need daily conversation or being together. As long as the relationship lives in the heart, true friends are never apart”. I am happy that I could make new friends during my stay in

Germany. Jumana, Dalia, Sara, Iyad and Philip thank you so much for your support and being such good friends. Doaa, Faiza, Laila, Radwa, Mai and Mona thanks for the nice time.

Table of Contents

List of Abbreviation

AFLPs	Amplified fragment length polymorphisms
ANOVA	Analysis of variance
CV	Coefficient of variation
DB	Digital biomass
DS	Drought Stress
DTH	Days to heading
GDD	Growing degree days
H^2	Broad-sense heritability
HI	Harvest index
IAP	Integrated analysis platform
KClO	Potassium chlorate
MAF	Minor allele frequency
$Mg\ (ClO4)_2$	Magnesium chlorate
NS	Normal seedlings
RAPDs	Randomly amplified polymorphic DNAs
RILs	Recombinant inbred lines
%	Percentage
BLUE	Best Linear Unbiased Estimate
bp	base pair
C	Control
CD	Chemical desiccation
cM	centimorgan
cm	centimeter
D	Drought
DArT	Diversity Array Technology
DAS	Days after sowing
DH	Double haploid
DSI	Drought sensitivity index
FC	Field capacity
FDR	False discovery rate
FLUO	Fluorescence
g	gram
G x E	Genotyoe by enviroment
GB	Gigabyte
GBS	Genotyping-By-Sequencing
GLM	General linear model
GWAS	Genome-Wide Association Studies
H^2	Heritability
$K2SO_4$	Potassium sulphate
KI	Potassium iodide
kLx	kilolux

KN	Kernel number
KW	Kernel weight
L	Liter
LD	Linkage disequilibrium
LSD	Least significant difference
m	meter
Max	Maximum
$MgCO_3$	Magnesium carbonate
Min	Minimum
MLM	Mixed linear model
mm	millimeter
MTA	Marker Trait Association
NaCl	Sodium chloride
$NaClO_3$	Sodium chlorate
NIR	Near-infrared
^{O}C	degree Celsius
PCA	Principle component analysis
PEG	Polyethylene glycol
PH	Plant height
QTL	Quantitative trait loci
R	Repeatability
REML	Residual maximum likelihood
RFLPs	Restriction fragment length polymorphisms
SD	Standard deviation
SNP	Single Nucleotide Polymorphism
SPKL	Spike length
SSRs	Single Sequence Repeats
SY	Straw yield
TB	Total biomass
TG	Total germination
TKW	Thousand kernel weight
TN	Tiller number
w/v	Weight to volume

List of figures

List of tables

Supplementary information

All supplementary figures and tables are on the attached CD of the thesis.

1 Introduction

1.1 Abiotic stresses affecting plants

Plants encounter a wide range of external factors which affect their growth, development and productivity the so-called stress (unfavorable conditions). Stresses can be divided into two main types (categories), biotic factors such as pathogens, insects and weeds or abiotic factors resulted of climate and soil conditions (Wardlaw, 1972). Abiotic stress is a vast term including different stresses such as drought, salinity, heat, chilling and mineral deficiency. These stresses such as drought have a potential to reduce the average yield of different crops by 50 % (Singh et al., 2015b). Stresses can influence plant growth and yield at different developmental stages where plants show complex responses especially when different stresses are combined at the same time (Chinnusamy et al., 2003). Plants have been adapted/acclimated to abiotic stress by different strategies occurring at all plant structural levels started from anatomical and morphological levels to cellular, physiological, biochemical and molecular levels (Maiti and Satya, 2014).

1.1.1 Drought stress a serious threat to plants

Among all stresses, drought is the most damaging stress disrupting today's agriculture and causes crop yield losses (Gupta et al., 2017), due to its unpredictability of occurrence, severity, timing, and duration (Cattivelli et al., 2011). Drought is an inherent characteristic of climate, depends on rainfall variability and mostly occurs in combination with heat stress. From agricultural point of view, drought simply occurs when there is inadequate water available including rainfall and soil moisture to meet the needs of a particular crop at a particular time, a situation which restricts the expression of the full genetic potential of the plant (Mitra, 2001;Singh et al., 2015b).

Better understanding how drought affects plants is important to improve breeding efforts and management practices in presence of climate change and increasing world population in order to meet global food demands (Chaves et al., 2003;Rollins et al., 2013b), where the global yield loss of the major crops wheat, maize and barley due to increase in temperature from the year 1981 to 2002 was estimated around $5 billion per year (David and Christopher, 2007).

Plants have various protective mechanisms to cope drought stress upon the status of plant water potential as a response to water stress. Three main mechanisms of drought resistance have been identified, drought escape, drought avoidance and drought tolerance (Wardlaw, 1972;Gupta et al., 2017). Drought escape is defined as the ability of a plant to complete its life cycle before drought and/or heat stress become too severe. Drought avoidance is the ability of plants to maintain relatively high tissue water potential despite a shortage of soil-moisture, involving a rapid morphological development, leaf rolling, leaf shading, reduced leaf area, and increased stomata and cuticular resistance. Whereas drought tolerance is the ability to withstand water deficit with low tissue water potential (Maroco et al., 2000;Chaves et al., 2003;Fang and Xiong, 2015). However, plants use more than one mechanism at a time to adapt to drought (Fang and Xiong, 2015). Actually, the ability of the plant to tolerate drought

and to grow under water stress condition is important as finally drought affected the yield (Tuberosa and Salvi, 2006).

1.1.2 Drought affected plant growth at different stages

The response of plants to drought stress depends on it is genetic potential to adaptation, the duration and intensity of water stress and also on the developmental stage at which the stress occurred. In some stages plants can cope with such stress, where as other stages are considered to be more susceptible to an extent that result in yield losses (Szira et al., 2008;Maiti and Satya, 2014). Crops require different levels of moisture and temperature in order to grow, in addition to the nutrients and CO_2, which all increase with plant development starting from germination until maturity (Farooq et al., 2009). The increase in the growth requirement is a need to achieve energy for photosynthesis, evapotranspiration and respiration increment (Blum, 2011).

Plant growth, cell division, elongation and differentiation are impaired by drought, due to turgor reduction, where low water flow from xylem vessels to the surrounding cells affecting leaves number and size. This is resulting in a decrease of photosynthesis rate and assimilate supply (Lazar, 2003).

Drought has a profound effect on plant growth, development, yield and yield quality traits. Several studies documented the impact of drought stress in different crops at different developmental phases. The first developmental phase is seed germination that can be affected by drought stress which enhance or inhibit seed germination and affect seedling development as demonstrated by Abdel-Ghani et al. (2014), where 233 barley genotypes were exposed to early drought stress using 15 % and 18 % polyethylene glycol (PEG), resulting in delaying the time to reach 50 % of germination and affecting the seedling traits. Accordingly, in a durum wheat panel consisting of 114 recombinant inbred lines (RILs) germinated under moisture deficiency imposed by 12 % PEG, the germination percentage, root length, shoot length and normal seedlings percentage were reduced as shown by Nagel et al. (2014).

Applying drought stress at different stages of plant vegetative growth phase may result in leaf chlorophyll break down, affects photosynthesis, reduces carbon fixation rate through stomatal closure and induces leaf senescence (Chaves et al., 2003).

Wehner et al. (2015) studied the effect of drought stress in 156 winter barley genotypes at juvenile stage (from sowing until tillering). The authors recorded a reduction in total biomass, a differentiation in leaf color and an increase in proline content.

Exposing two barley genotypes at the vegetative phase to drought stress of 15 % field capacity (FC), under greenhouse conditions caused a significant reduction in plant height, spike number, thousand kernel weight (TKW) and biomass, while the reduction was not significant for harvest index and grain number (Rollins et al., 2013b).

Further, drought stress at early developmental stages is considered as a critical factor for many developmental and agronomic traits such as days to heading, plant height, tiller number and total biomass. In spring wheat, plant height was reduced in plants under rain-fed conditions compared to the fully irrigated plants (Edae et al., 2014) and a reduction in yield

potential was observed (Farooq et al., 2009). Drought stress at pre-anthesis stage shortens the time to flowering, while applying drought after anthesis reduces the period of grain filling in cereals such as triticale (Estrada-Campuzano et al., 2008) and the yield (Farooq et al., 2014). On the other hand, the remobilization of pre-anthesis stored carbohydrates from the stem and leaves is increased in order to develop grains that may compensate senescence induced losses in grain yield (Plaut et al., 2004;Yang and Zhang, 2006).

At reproductive stage limited water viability as under Mediterranean environmental conditions, reduces grain number, size and weight resulting in yield losses in barley, due to a low number of formed endosperms cells (Honsdorf et al., 2017) and a reduction in starch accumulation due to less assimilates which also was confirmed by Blum (1998).

Yield reduction as a result of leaf senescence was observed when drought occurred during the reproductive phase in wheat as described by Nawaz et al. (2013). In wild barley introgression lines, the number of grains, grain weight per spike, TKW, plant biomass and finally the grain yield were significantly reduced by drought stress ten days after anthesis under controlled greenhouse conditions as a result of shortening the grain filling duration (Honsdorf et al., 2017).

Alqudah et al. (2011) reported that the reduction in crop yield and yield components under drought stress during the reproductive stage is related to early flowering, short grain filling duration and reduction in dry matter accumulation which led to spike and floret sterility.

In barley, clear reduction in the grain yield and TKW under late drought condition was reported by Samarah et al. (2009) due to a low number of fertile grains which confirmed his previous findings (Samarah, 2005), that applying drought stress at post anthesis reduce grain yield due to low tiller number, in addition to lower number of spikes and grains per plant compared with plants under control conditions.

Similar to barley, Plaut et al. (2004) showed that wheat grain number was not affected by drought stress after anthesis, while grain filling rate was changed due to the shortening in grain filling duration causing a reduction in grain dry weight. Grain number is determined during the flowering stage as the plant depends on its assimilates to determine the final yield, grain number is considered as a consequence of yield rather than a determinant (Sinclair and Jamieson, 2006).

1.2 Chemical desiccation as a simulator for post-anthesis drought stress

Efficient screening techniques are required to select for superior drought tolerant genotypes from genetically diverse resources and environments at a specific developmental stage, in order to help breeders improving high yielding cultivars (Fang et al., 2017). Screening can be implemented under natural drought stress (rain-fed field conditions) or under optimum conditions (Ceccarelli et al., 1998). Selecting high yield genotypes under field conditions is a challenge as the intensity and frequency of rainfall cannot be predicted (Blum et al., 1983a). Therefore, drought simulation by inducing stress treatments on the plants is needed to overcome the drought stress timing (i.e. at which developmental stage drought occurs), intensity and duration unpredictability. A number of artificially stress techniques such as

chemical desiccation (Blum et al., 1983a;Regan et al., 1993;Kamal et al., 2018), rain-out shelter (Kant et al., 2017) and defoliation technique (Dodig et al., 2018) are used to simulate drought stress under different environmental conditions, where drought is unpredictable from season to season.

Chemical desiccation technique was firstly introduced by Blum et al. (1983b) as a reliable technique to simulate drought stress at grain filling phase in wheat. In his study magnesium chlorate Mg $(ClO_4)_2$ was suggested to be used as a desiccant, sprayed to wheat plants 14 days after anthesis. The desiccant disrupts photosynthesis and accelerates leaf senescence forcing the plant to rely on the stem stored assimilates to provide the required carbon for grain filling.

In literature, many studies demonstrated the efficiency of chemical desiccation to mimic post-anthesis drought effect easily, using different types of desiccants in different cereals such as barley, where (Budakli, 2007) did apply 4 % potassium chlorate ($KClO_3$) to estimate reserves contribution to grains. Significant differences between varieties in dry matter translocation and rate of grain weight reduction were shown. The varieties which had lower rate of grain weight reduction were more tolerant to stress, indicating that chemical desiccants can be used for selection of drought tolerance. Nicolas and Turner (1993) reported that chemical desiccation was efficient in revealing wheat genotypes that showed a low reduction in grain weight and a higher remobilization of stem reserves contribution to grain which can be selected as drought tolerant genotypes.

Dogan et al. (2012) studied the contribution of stem reserves to grain filling in triticale cultivars under drought induced by 4 % potassium iodide (KI), showing a significant variation between the cultivars. Ongom et al. (2016), observed that applying KI with 0.6 % or 1 % concentration to sorghum can help in selecting tolerant genotypes. Another study used three different KI concentrations (0.25 %, 0.5 %, and 0.75 %) at the reproductive phase to screen rice germplasm. Tolerant genotypes showed an increase in stem reserve mobilization, confirming that 0.25 % KI can be used as a desiccant for screening drought tolerance in upland rice varieties (Singh et al., 2012).

Several studies associated drought stress imposed by water stress to drought simulated by chemical desiccation, revealed significant correlations between both stresses as shown by Blum et al. (1983a). The reduction in wheat grain weight by field drought stress was significantly correlated with the reduction caused by drought simulated by chemical desiccation (r^2= 0.6) indicating the reliability of this technique.

Nicolas and Turner (1993) investigated the reduction in kernel weight of 82 wheat lines by chemical desiccation using KI in comparison to drought stress, where they found a significant correlation (r^2 = 0.5). As mentioned, in many studies different types of desiccants can be used to simulate post anthesis stress at different concentrations and time points.

Blum (1998) used different types of desiccants applied 10 or 14 days after anthesis in order to select wheat lines with stable kernel weight. Based on the results, using KI as chemical desiccant to simulate drought had less toxic effects and was recommended to screen wheat lines on a large scale. The method was validated by Nezhad et al. (2012) who used KI to screen a worldwide collection of 100 bread wheat accessions and revealed a positive and

significant correlation between water stress under greenhouse conditions and chemical desiccation (KI) under field conditions applied 14 days after anthesis.

Simulation strength of chemical desiccation is dose and time depend. Haley and Quick (1998) reported that using KI as a desiccant in winter wheat genotypes at low concentration (0.15 %) 10 and 15 days post-anthesis did not cause yield reduction while using 0.3 % KI or 2 % $NaClO_3$ 10 days post-anthesis reduced the yield and had a higher efficiency compared to 15 days. Results showed a reduction in the grain filling rate and an increase in stem dry weight, where tolerant cultivars tend to develop greater stem biomass. In another study 0.1 % KI was applied to wheat cultivars at seven days after anthesis, causing a reduction in photosynthesis rate and chlorophyll content but an increase in sucrose and proline (Sawhney and Singh, 2002). Moreover, M. Ezzat Ahmadi (2009) applied 0.4 % KI which was an effective concentration in bread wheat at 12-14 days after anthesis causing significant yield reduction.

Using KI at 10 to 14 days after anthesis was also recommended by Regan et al. (1993) to select for post-anthesis drought tolerant wheat genotypes in a dryland breeding program compared to other desiccants such as $NaClO_3$ and potassium chlorate $KClO_3$ which had a severe effect on yield. The response of two wheat cultivars to the application of the desiccants sodium chloride (NaCl) at 0.1 %, potassium sulphate (K_2SO_4) at 3.5 % and magnesium carbonate ($MgCO_3$) at 0.1 % sprayed at 30 and 60 days after sowing was investigated by El-Ashry and El-Kholy (2005). The study showed that the desiccants affected grain yield per plant, weight of grains per spike and biological yield by inhibiting photosynthesis during grain filling. K_2SO_4 and $MgCO_3$ where more effective than $NaClO_3$. Recently, Kamal et al. (2018), screened wheat cultivars under water stress and chemical desiccation after anthesis, using $KClO_3$ which resulted in a significant reduction of grain yield, aboveground biomass and harvest index, in addition to other physiological traits.

In summary, it is shown that chemical desiccation technique proved its efficiency in simulating post- anthesis drought stress by using different chemicals and has been validated as an effective and useful technique. KI is one of the most used desiccants as it is a simple ionic salt, dissociate into K^+ and I^-. K+ has a role in the osmotic pressure and carbohydrate migration, it enhances the translocation of newly synthesized photosynthates in glycophytic plant species (Marschner, 2012). On the other hand, the chlorate group is considered as a strong oxidizing agent. In addition to its phytotoxic effect to the whole green parts in plants it is reducing the efficiency of photosystem II. When it is dissolved in water K^+ and chlorate (ClO_3^-) will be produced. The chlorate group decreases chlorite and hypochlorite which are rapidly poison cells due to its toxicity (Franco-Navarro et al., 2016).

1.3 Plant genetic resources as a rich source for crop improvement

Plant genetic resources are the raw material for sustainable agriculture and food production, consisting of diverse wild species, landraces and cultivars. Conserving plant genetic resources is crucial to ensure future crop production in presence of the challenges our world is facing nowadays, mainly increasing world population where the production cannot meet the demands and the problems of climate change. Around 10,000 years ago, domestication of plants began, resulting in crops spreading with the humans to different regions on our planet

and thereby developing gene variants capable of adapting to the new climates not found in the wild ancestors. On the other hand, domestication resulted in narrowing down the genetic basis of crops and reducing the genetic variation (Tanksley and McCouch, 1997) as only a portion of wild population diversity was used in this process. In the beginning of the 20thcentury, biologists recognized the importance of genetic diversity, especially the Russian agronomist and botanist Nikolai Vavilov, who realized the danger of extinction of plant genetic resources and the urgent need to conserve them (Harris, 1990).

Genebanks (seed banks or field genebanks) are excellent holders of plant genetic resources in *ex situ* collections (Probert et al., 2009). Nowadays, more than 1,750 genebanks are established worldwide, housing about 7.4 million accessions (Tyagi and Agrawal, 2013). The German *ex situ* genebank, located at the Leibniz Institute for Plant Genetics and Crop Plant Research (IPK) in Gatersleben holds more than 150,000 accessions from 776 genera and 3,212 species. It is the largest and most diverse collection for cultivated crops and wild relatives in Europe contributing in the prevention of extinction (genetic erosion) of plants (Börner et al., 2014). Cereals represent 40 % of all stored accessions at the IPK genebank whereas wheat (*Triticum*) has the largest number among cereals with 28,206 accessions followed by barley *(Hordeum*) with 23,607 samples as shown in the scientific report 2016-2017 of IPK (https://www.ipk-gatersleben.de/fileadmin/content-ipk/content-ipk-forschung/Forschung/Download/Appendix_2016_2017.pdf).

As barley is considered as one of the well adapted cereal crops, it has been used as a model species to understand the genetic background of adaptation to abiotic stresses and to climate change (Dawson et al., 2015). The IPK genebank collection, representing different geographical origins and biological statuses (cultivars, landraces and wild relatives) is considered as a worthy resource for breeders to develop new cultivars adapted to the environmental changes.

The utilization of such genetic resources to understand the natural variation at the phenotypic and genotypic level is important for plant breeding and genetic aspects. Selecting diverse accessions to study traits of interest is a beneficial use of genebanks. Panels of worldwide research collections had been established consisting of around 200 accessions e.g. Genobar (Alqudah et al., 2014), spring barley landraces (Pasam et al., 2014), georeferenced landraces and wild accession (Russell et al., 2016) and EcoSeed (Nagel et al., 2019) populations. The EcoSeed panel is one of these diverse barley collections stored in IPK genebank. It was basically initiated in order to understand the role of the environmental stress on the plant during seed development and seed storage (viability, storability and vigor).

Very recently, 22,626 barley accessions held by IPK genebank were genotyped using Genotyping-By-Sequencing (GBS) technology to understand the natural variation and the population structure of this global barley collection. The study highlighted the future use of genebank genomics in breeding and genetics through discovering beneficial genetic variation in germplasm collections (Milner et al., 2019).

1.4 Barley (*Hordeum* sp.)

1.4.1 Origin, domestication and taxonomy

Barley is one of the first domesticated cereal crops in the world. Since 10,000 years ago barley was growing in the Fertile Crescent and its domestication history began with selections by ancient farmers (Badr et al., 2000). During barley domestication many important traits such as an increase in seed number, change in seed shape and size, increased seed fertility, change in plant and spike architecture and loss of seed shattering were acquired by the natural and artificial selection. The presence of Non-brittle rachis 1 (*btr1*) or Non-brittle rachis 2 (*btr2*), converts the brittle rachis into a non-brittle type (Komatsuda et al., 2004). Based on this barley became more diverse and was adapted to different environments (Pourkheirandish and Komatsuda, 2007).

The cultivated barley (*Hordeum vulgare* L.) is one of the major cereal crops of tribe Triticeae, family Poaceae. The genus *Hordeum* contains 33 annual and perennial species, divided into different subspecies and 45 taxa which are distributed over all continents in the arid and temperate parts, except Australasia (Blattner, 2009).The most economically important species is *Hordeum vulgare*. Barley has the ability to grow in a wide range of climate conditions. It can tolerate different stresses like cold, drought and salinity that made it a prominent model for cereal genetic research (Saisho and Takeda, 2011).

Barley has a basic chromosome number x = 7 with a genome size of 5.1 Gbp. The diploid level is the major feature of barley which facilitate cross-breeding to *Hordeum spontaneum*, the wild relative and ancestor cultivated barley (International Barley Genome Sequencing et al., 2012).

Barley germplasm can be classified into three gene pools that are important for the crossing of related species in plant breeding. The primary gene pool contains *Hordeum vulgare* and *Hordeum spontaneum*. The secondary gene pool consists of *Hordeum bulbosum*, and the tertiary gene pool includes the remaining 30 *Hordeum* species (Harlan and de Wet, 1971).

1.4.2 Utilization and economic importance

As barley grows well under a wide range of climatic conditions and due to its high nutritional value, it is exploited for different purposes. Around 70 % of the world production is used for animal feeding, 20-25 % for malting or other industries and 5 % is consumed by human as a food (Langridge, 2018). The characteristics and properties of grains are important in malting production, for example, hulled barley grains are preferred for malting and brewing due to the impact on beer flavor (Baik and Ullrich, 2008). Above ground parts of barley can also be used for feeding animals (grains and straw) in different forms of forages, such as silage as a source of energy, protein and fiber (Heuzé, 2013). To feed beef cattle and dairy cows is beneficial for meat and milk production because of its high digestibility and nutritional value (Walsh et al., 2008;Wallsten and Martinsson, 2009).

In addition, the grain is rich in starch 65-68 %, protein 10-17 %, betaglucan 4-9 %, free lipids 2-3 % and minerals 1.5-2.5 % (Quinde et al., 2004). The importance of beta-glucan on human health is well known as it lowers blood cholesterol levels and the glycemic index (Pins and

Kaur, 2006). It controls glucose levels, which in turn affect the cardiovascular health and diabetes (Baik and Ullrich, 2008). However, the consumption of barley as food is still very low compared to other cereal grains therefore, the development of new processes for including barley grain in human food is needed.

In terms of production, barley is ranked as the fourth important cereal crop in the world after wheat, rice, and maize. In 2016, the production was more than 141 million tons globally. Russia is the largest producer with 17,992,517 tons, followed by Germany (10,730,500 tons), France (10,306,008 tons), Ukraine (9,435,710 tons) and Australia (8,992,274 tons). The rest was produced in many other countries as shown in Fig. 1 (FAOSTAT, 2016).

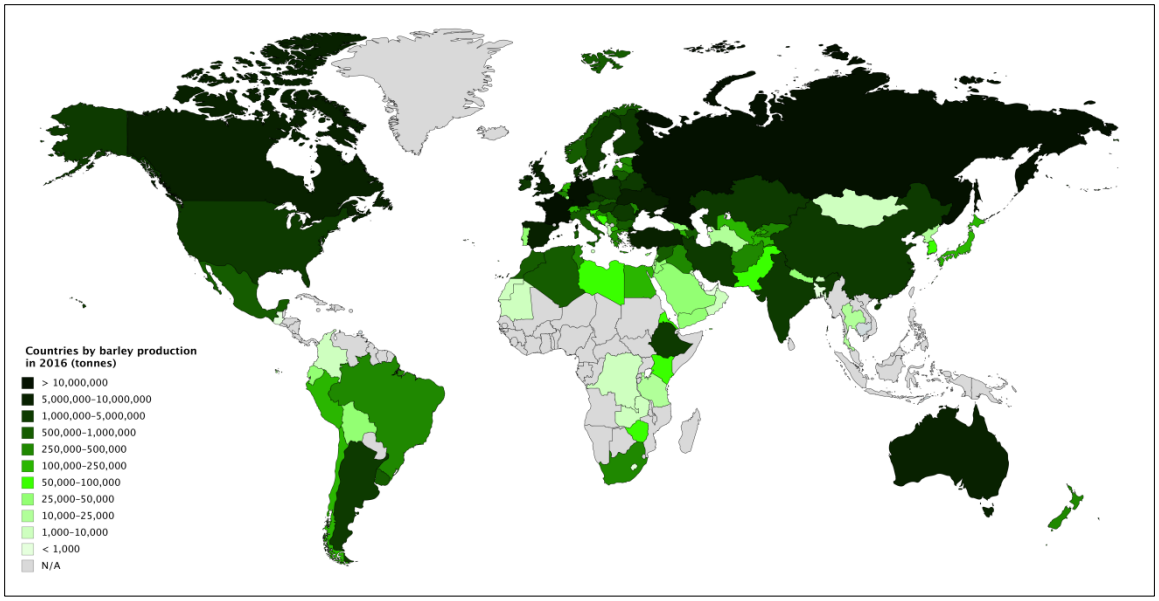

Figure 1. Global map shows the distribution of barley production worldwide (FAO, 2016).

In Germany, barley production was decreased in the period from 1992 to 2012; the reduction was 14.5 % with respective to the amount of harvest. Climate change affected barley production clearly; also increasing the planting area of other crops such as maize can be one of the main reasons for the reduction in barley production in Germany (FAOSTAT, 2016).

Worryingly, climate change including decreasing in water availability, salinity and increasing temperature, threatens crops productivity worldwide and food security, attributed in increasing food demand. Studies and predictions shows that these effects will aggravate in the future. The impact of climate change started to reach southern European countries, where the production of barley and wheat do economically decline (Brisson et al., 2010). With the burgeoning world population, cereal grain yields alone must increase by at least 70 % before 2050.

1.4.3 Morphology and growth stages

Barley morphology can be classified into different types according to many features. Based on spike morphology, it is mainly divided into six-rowed and two-rowed types. In six-rowed types, three spikelets (one central and two lateral) at each rachis are fertile, whereas in the two-rowed barley, only the central spikelet is fertile and the two lateral ones are sterile. *Six-*

rowed spike 1 (*VRS1)* gene is controlling the lateral spikelet fertility/sterility in two-rowed and six-rowed forms (Komatsuda et al., 2007). Irregular barley (row-type mutants) which has fertile central spikelets and different ratio of fertile and sterile lateral spikelets (Zohary and M, 2000) is determined by the loci *VRS2*, *VRS3*, *VRS4* and *VRS5* (Ramsay et al., 2011;Koppolu et al., 2013;Bull et al., 2017;Youssef et al., 2017). Based on the growth habit, barley may be winter, spring or facultative type, depending on the sensitivity to temperature (vernalization), the light (photoperiod) and endogenous factors which are affecting the growth and development of the plant. Exposing to low temperature, enhance flowering as in winter genotypes which are sensitive to vernalization compared to the spring and facultative genotypes. In spring barley *Vrn-H1* is the gene which controlling vernalization, enhancing the transition from the vegetative to the reproductive phase, while *Vrn-H2* (*HvZCCT*) is the responsible gene that delays heading in plants (Hemming et al., 2008).

For example, winter barley is sown in autumn and harvested in the summer, while spring barley needs to be sown in spring and can be harvested in summer too. If the winter barley is planted in spring, it will not flower or the flowering will be too late, and if the spring barley is planted in autumn it will be affected by cold and may be killed by frost. The facultative barley varieties can be planted in spring or fall, as they are cold-tolerant (Wang et al., 2010).

Regarding photoperiod sensitivity, some genotypes need to reach a specific threshold of day length in order to flower. Specific genes are responsible for photoperiod response in barley, the gene *PHOTOPERIOD RESPONSE LOCUS1* (*Ppd-H1*) regulates the response to long day, causing early heading while the recessive allele (*ppd-H1*) reduces the response to long day resulting in a delay of heading time (Turner et al., 2005;Alqudah et al., 2014).

Understanding barley growth and development is essential to ensure crop production. Barley life cycle can be divided into three major phases: vegetative, reproductive and grain-filling phases to reach maturity (Slafer et al., 2002). Each phase includes different stages starting from seed germination, seedling establishment, leaf development, heading, kernel development and maturity. There are several scales that describe the development of cereal crops such as the scale described by Kirby and Appleyard (1987) which is based on the interior morphology of the shoot apical meristem and Zadoks et al. (1974) scale using decimal growth scale. The growth stages are recorded with two digits, the first indicating the primary growth stage and the second the number of plant parts in secondary stages of development. The Zadoks scale is presented in figure 2. This scale divides the plant life into the vegetative phase (Tillering), reproductive phase (Stem extension), the grain-filling (Heading) and the maturity (Ripening).

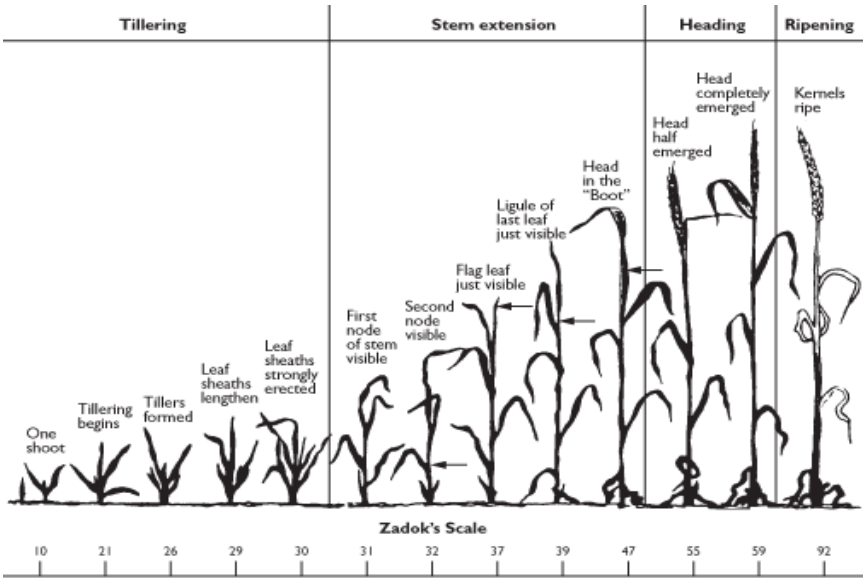

Figure 2. Zadoks scale for cereals growth stages.

The vegetative phase (Z10–Z30) starts at seed germination, plant root and shoot are initiated, roots, leaves, and the tillers are developed and proceed until the collar ('structure at the base of the shoot apical meristem which marks the transition from vegetative to early reproductive phase starting with a double ridge stage, a rudimentary leaf and spikelet initiation') (Kirby and Appleyard, 1987;Sreenivasulu and Schnurbusch, 2012). The reproductive phase (Z31–Z69) is the longest phase in barley life cycle, that starts from spikelets differentiation and initiation, called the early reproductive phase, whereas the appearance of the first awn primordia indicate that plant enter the late reproductive phase where anthesis or fertilization usually happens (in barley awn tipping stage). This phase considers an important phase as the number of survived spikelets and final grain yield are determined (Kirby and Appleyard, 1987). The grain-filling phase and maturity (Z70–Z92) begins 5-10 days after anthesis where cell division and grain filling occur and last until maturity or ripening. During this phase grains are developed and dry matter is accumulated (Alqudah and Schnurbusch, 2017). This phase passes by many stages such as milk stage, dough stage and ripening (Zadoks et al., 1974). During this phase, the final grain yield and its quality parameters are based on assimilates and photosynthesis products (Sanchez-Bragado et al., 2016).

1.5 High-throughput phenotyping

Plant phenotyping started about 10,000 years ago as a tool to select for the best high yielding and stress tolerant plants (Ross-Ibarra et al., 2007). Nowadays it considers a comprehensive estimation of different morphological, physiological, biochemical and molecular traits.

Phenotyping to select high-performance genotypes under diverse environmental conditions is breeders main goal (Kumar et al., 2015a) especially if it is combined with genetic studies. However, phenotyping became to be a bottleneck, limiting the strength of genetic analysis as the progress in the genotyping domain improved more rapidly compared to improving phenotyping facilities.

Phenotyping high numbers of plants using conventional phenotyping procedures (e.g. visually) are time-consuming, costly, labor-intensive and may lead to non-precision outputs. On the other hand, measuring traits such as fresh biomass need plants destruction at a specific stage or time point. To overcome this bottleneck for robust and accurate plant phenotyping the idea of establishing high-throughput platforms became a need (Furbank and Tester, 2011).

During the last years, many efforts have been done in plant phenomics which is the development of phenotyping tools and models to get information about the structure and function of high plant numbers and their performance under different environments and to establish a data base that helps to simulate plant manner under different conditions (Tardieu et al., 2017).

In order to address aforementioned limitations and to answer different biological questions, high-throughput phenotyping technologies were developed to phenotype the large amount of plants under natural climate conditions such as, BreedVision (Busemeyer et al., 2013) drones, phenomobile incorporating hyperspectral scanners for fruit trees and berry bushes (Thorp et al., 2017) and LemnaTec Field Scanalyzer for automated outdoor phenotyping (https://www.lemnatec.com/products/high-throughput-phenotyping-solutions/field-scanalyzer/). Also automated greenhouses or isolated chambers (Hartmann et al., 2011;Hairmansis et al., 2014) as for instance LeafAnalyser (Weight et al., 2008), PHENOPSIS (Fabre et al., 2011), GROWSCREEN (Nagel et al., 2012) were created and used.

One of the phenotyping platforms was developed by LemnaTec company GmbH, Germany (https://www.lemnatec.com/), the so-called High Throughput Phenotyping Solutions or Greenhouse and Growth room Scanalyzers. It is an automated greenhouse–installed system, where the experiment and data collection are carried out automatically. The platform contains automatic watering station that facilitate the application of different water regimes, e.g. drought treatment (Neumann et al., 2015) or salinity (Al-Tamimi et al., 2016) at different time points. The sensor equipment consists of camera systems imaging in three different wavelengths: Near-infrared (NIR), visible (color), and fluorescence (FLUO).

Daily images of plants are analyzed in order to dissect the phenotypic traits (Klukas et al., 2014) and revealing the genetic background for complex traits as drought tolerance and biomass accumulation at different stages based on non-destructive images analysis (Neumann et al., 2015;Rahaman et al., 2017;Ward et al., 2019).

Visible imaging technique was applied to study different traits such as shoot biomass, an important trait in improving grain yield (Fischer and Edmeades, 2010). In a study done by Golzarian et al. (2011), researchers developed a method to estimate the biomass of cereals by imaging the wheat plants which were grown in a hydroponic system under salt stress treatment using a LemnaTec 3D Scanalyzer.

High-throughput phenotyping demonstrated the efficiency of the obtained results to be used in genetic studies to reveal the genetic bases of complex traits. Yang et al. (2014) screened 533 rice lines and cultivars using a rice automatic phenotyping platform. Thirty-two shoot traits

were obtained after image analysis. The data was used in genome wide association study (GWAS) and the analysis revealed 15 loci that were significantly associated with shoot traits.

More recently, Neumann et al. (2017) studied the genetic factors underlying the vegetative biomass from tillering to flowering stages in a set of 99 spring barley genotypes under well-watered conditions, applying non-destructive phenotyping. Seven biomass QTL were detected at different growth stages (early growth and booting stage). Also in maize different QTL underlying vegetative biomass at different growth stages were revealed in a study done by Muraya et al. (2017).

Applying such high-throughput technologies can help in transforming large number of images into valuable data, helping breeders to speed up selection of new, well adapted crops in the presence of climate change.

1.6 Genetic mapping of quantitative trait loci

Quantitative trait loci (QTL) mapping is a statistical method for detecting the genetic basis of variation for complex traits (traits that are controlled by more than one gene and influenced by environmental conditions). QTL analysis showed the allelic variation at a distinct locus controlling the phenotype and revealing the genetic architecture of such traits by linking phenotypic and genotypic data (molecular markers) (Collard et al., 2005). QTL include genomic regions holding allele(s)/gene(s) underlying the genetic determination of a specific complex trait such as yield, quality, drought tolerance and disease resistance. These QTL consider a rich source for breeders to improve selection of high yielding genotypes (Teulat et al., 2003).

Different types of molecular markers have been developed and used for QTL mapping such as simple sequence repeats (SSRs), restriction fragment length polymorphisms (RFLPs), amplified fragment length polymorphisms (AFLPs) and randomly amplified polymorphic DNAs (RAPDs). Nowadays, improved genome sequencing techniques developed stable and efficient DNA markers as Diversity Array Technology (DArT) and Single Nucleotide Polymorphism (SNPs). They provide the opportunity for the characterization of quantitative traits in different crops such as in barley by the 9K iSelect Illumina Infinium array (Comadran et al., 2012) which hold 7,842 gene-based SNPs of which 6,094 have known positions on the pseudomolecules (Mascher et al., 2017) and the newly developed 50K iSelect Illumina Infinium array with accurate physical positions and information of gene annotation using data from the whole exome capture tool (Bayer et al., 2017).

High density markers also derived from Genotyping-by-sequencing (GBS) technology which consider a robust tool for developing markers for genetic studies (Poland et al., 2012).

Phenotypic variation due to genetic factors can be revealed by two main approaches, linkage or bi-parental mapping and association mapping.

1.6.1 Linkage or bi-parental mapping

Linkage mapping considers the classical approach to map QTL associated with desired traits, after establishing a segregating population (e.g. F_2, double haploid, back cross) derived by crossing two parents holding one or more contrasting traits of interest. The principle of

linkage mapping is to identify the allele's polymorphisms between the phenotypic data and polymorphic markers using different software packages.

To detect QTL, several statistical methods are used, e.g. single marker analysis, simple interval mapping (Lander and Botstein, 1989) and composite interval mapping (Zeng, 1993). These techniques can be classified into two categories, one based on marker-by-marker analysis, which is called "single marker analysis", and those that simultaneously take into account two or more markers, which is called interval mapping.

Through this approach low numbers of markers can be used, resulted in low mapping resolution ranging between 10-20 cM, due to low number of recombination. Therefore, large population sizes are essential in order to obtain high-resolution mapping. Other limitations of this approach are the time and resources needed to develop the mapping populations. The last limitation is the limited number of polymorphic (between any two parents) traits (Zhu et al., 2008).

The approach has been widely used to reveal genetic architecture of many traits in different crops. It was applied in *Arabidopsis thaliana* to reveal QTL based on RFLPs for flowering time (Clarke et al., 1995). Börner et al. (2002) applied QTL mapping on a set of 114 RILs using a joint map of RFLPs and microsatellite markers to reveal QTL for important morphological and agronomical traits in hexaploid wheat. In barley Baum et al. (2003) identified trait-marker linkages in a population of RILs genotyped using AFLP and SSR markers. QTL analysis for agronomical and physiological traits under drought conditions was applied by using 167 F_8 RILs (Diab et al., 2004).Fan et al. (2015) carried out a genetic study in a barley double haploid (DH) mapping population using DArT, AFLP and microsatellite markers to reveal QTL under drought and salinity conditions. Rollins et al. (2013a) detected many QTL for yield-related traits and biomass under dryland conditions at different locations for many years using SSR and DArT markers for constructing a genetic linkage map in a RIL barley population. Zhou et al. (2012) identified QTLs for salinity tolerance in a double haploid barley population using a high-density genetic linkage map constructed from SSR and DArT markers, while Mansour et al. (2013) identified QTLs in barley RILs under Mediterranean conditions for days to heading, plant height and thousand grain weight.

Recently, SNPs were used in linkage mapping studies. Huang et al. (2018) applied SNPs to reveal QTL for fusarium head blight correlated with agro-morphological traits in barley. Islamovic et al. (2013) revealed QTL for plant height as well as spike length and angle in a barley mapping population genotyped with SNP, DArT and SSR markers.

Using barley introgression lines genotyped with 4,201 SNPs grown under juvenile drought stress QTL for biomass dry weight and plant height were detected (Honsdorf et al., 2014). Another study on the same barley lines (Honsdorf et al., 2017), evaluated the drought response by applying drought stress ten days after anthesis. QTL analysis revealed loci for TKW, number of grains per ear, days to heading, plant height, grain yield, and plant biomass

1.6.2 Association mapping

While linkage mapping revealed associations within populations derived from bi-parental crosses, association mapping also called linkage disequilibrium (LD) mapping is an approach, given the opportunity to reveal loci by assessing the statistical significance of associations between the natural variation of a phenotype and the genetics of marker polymorphisms in a set of diverse individuals (cultivars, landraces or breeding lines).

Association mapping has overcome the limitations of linkage mapping through increasing the mapping resolution due to many meiotic events, reducing the time required for genetic analysis as there will be no need to cross over several generations and, with this approach multiple alleles per locus can be assessed (Korte and Farlow, 2013). In addition, multi-trial phenotypic data can be used (Zhu et al., 2008).

The LD concept started at the beginning of the twentieth century (Jennings, 1917), defined as the non-random association of alleles at distinct loci, means that when a specific allele at one locus is linked with a specific allele at the second locus more often than expected, i.e. in comparison to alleles at unlinked positions the loci are closely linked and be in LD. The association between alleles at different loci is the concept of LD and identifying QTL, allowing to reveal the highly linked loci or highly significant correlated with the QTL in the genome and help to identify the ones which are close to the candidate genes (Flint-Garcia et al., 2005). It is an important parameter in association genetics. The value of LD determines the required number of markers and the mapping resolution. The level of LD in plants can be measured using different methods, the models can be used depending on different situation as each of them has its advantages and disadvantages (Gupta et al., 2005). The most common used model is r2 providing details of the historic events by reflecting the history of natural selection within the genome, recombination and mutation (Flint-Garcia et al., 2003;Gupta et al., 2005). The model revealed the pattern of LD decay where LD shape is related to many factors resulted in increasing or decreasing the value for instance population size, recombination rate, population admixture, natural or artificial selection and mutation rate (Gupta et al., 2005).

Association mapping started to be applied in plants years after it was first developed to be applied in human genetics (Cockram et al., 2008). It has become a powerful tool to investigate the genetic architecture of complex traits and to identify the genetic basis of phenotypic variation associated with traits of interest (Goddard et al., 2016).

This approach has been used efficiently in plants as *Arabidopsis* (Nordborg et al., 2002;Ehrenreich et al., 2009;Brachi et al., 2010) and other important crops such as maize (Flint-Garcia et al., 2005;Kumar et al., 2014) and wheat (Breseghello and Sorrells, 2006;Neumann et al., 2010;Dodig et al., 2012;Edae et al., 2013;Dong et al., 2016) to identify loci for different traits either under normal or stress conditions.

In barley, association mapping studies have been conducted for flowering time (Cockram et al., 2008;Stracke et al., 2009), grain weight, length and width (Lai et al., 2017b), physiological parameters under drought stress (Wojcik-Jagla et al., 2018), salt tolerance (Long et al., 2013) and spot blotch resistance (Roy et al., 2010).

Association mapping studies can be classified into two approaches: (I) candidate gene approach, where the candidate sequenced genes(s) to be correlated to the phenotypic variation of the studied trait. (II) Genome Wide Association Studies where genome wide distributed polymorphisms will be correlated to the phenotypic traits. The latter approach is implemented in the current study.

1.6.3 Genome Wide Association Studies (GWAS)

Genome Wide Association Studies (GWAS) approach revealed many advantages and success in human and animal genetics as it is not possible to generate a bi-parental mapping population (Brachi et al., 2011). It permits choosing parents for QTL analysis and candidates for mutagenesis and transgenics (Korte and Farlow, 2013).

GWAS is a widespread approach, allowing screening the whole genome through taking the advantage of ancestral recombination events applied in various crops to identify genetic loci underlying traits at a relatively high resolution (Si et al., 2016) besides narrowing down the QTL regions (Comadran et al., 2012). Also, GWAS can be an efficient tool in enhancing the genetic basis of crop breeding material and for identifying candidate genes if it is efficiently utilized (Xu et al., 2018). Nevertheless, to identify the true associations many points need to be considered. The population structure may cause spurious associations or false positives due to the complex genetic relatedness. Correcting population structure is an important step in order to detect true associations (Pritchard et al., 2000a;Flint-Garcia et al., 2003). Several statistical methods are available to account for population structure: Q matrix and principle component analysis (PCA) methods. Using the computationally program STRUCTUR, Q matrix estimates the classes of the individuals within the population and grouped them into subpopulation membership coefficient (Q). These Q(s) are integrated into a general linear model (GLM) to correct the structure (Pritchard et al., 2000b). This method considers computationally intensive efforts especially with large maker numbers. Another used method is PCA (Price et al., 2006) which is less computationally demanding and can handle large number of markers. The PCA showed the variation across the markers and describes the population by clustering the individuals in groups or showing no clear structure.

Correction for population structure using GLM model is not strong and sufficient to decrease the false positives. Another model developed by Price et al. (2006) is the mixed linear model (MLM) that integrate the Q matrix with the kinship relatedness of the population called the kinship matrix (K matrix). Q is considered as a fixed effect and K treated as a random effect.

Significant markers revealed by GWAS analysis can be validated using different tests to address the false positives. Bonferroni correction or false discovery rate (FDR) are the main two tests used. FDR provides an estimate of the number of actual true results among those called significant (Storey and Tibshirani, 2003), while Bonferroni is a more strict test.

Genome wide association mapping is a robust tool aiming to detect QTL of the trait of interest by combining genotypic and phenotypic data (Waugh et al., 2009). Up to now, many QTL were detected using GWAS approach in different crops such as maize (Muraya et al., 2017), soybean (Sonah et al., 2015), rice (Al-Tamimi et al., 2016), wheat (Edae et al., 2014;Qin et

al., 2016;Gahlaut et al., 2017;Mwadzingeni et al., 2017;Qaseem et al., 2018), and barley (Pasam et al., 2012;Wang et al., 2012b;Fan et al., 2016;Jabbari et al., 2018).

Wehner et al. (2015), identified loci involved in drought stress and leaf senescence as electron transport rate at photosystem II, proline and soluble sugars content, osmolality and aboveground biomass in 156 winter barley accessions genotyped with 9 k iSelect SNP-chip. Drought stress was applied at juvenile stage in greenhouse pots experiment. The analysis revealed two main QTL for drought stress and leaf senescence.

In another study Varshney et al. (2012) applied GWAS in order to analyze yield, yield components and developmental, physiological and anatomical traits in a collection of 185 barleys genotyped with different markers (710 DArT, 45 SSR and 61 SNP markers) and grown in two different locations (dry location/drought treatment and the wet location/control treatment). Numerous QTL were detected for different traits distributed on different chromosomes. Loci for plant height, spike length, total above ground biomass yield, grain yield and TKW were found under control condition, while under dry condition QTL for spike length, total above ground biomass yield, grain yield and thousand kernel weight were detected.

GWAS approach proved its capability in finding QTL for drought tolerance traits at different developmental stages in order to develop durable genotypes for the climate change. However, few studies in barley focused in detecting QTL related to yield related traits under drought stress conditions using GWAS approach (Varshney et al., 2012). Therefore, this study was implemented to elucidate the genetic background in barley under drought stress induced by water stress and chemical desiccation to attain candidate genes.

1.7 Research objectives

The main aim of the dissertation is to perform genome-wide association study (GWAS) to map marker trait association (MTAs) related to different, morphological, agronomical and seed quality traits under pre and post-anthesis drought stress using a diverse spring barley panel.

For this purpose, 183 spring barley genotypes (EcoSeed panel) were evaluated under high-throughput phenotyping greenhouse conditions, applying drought at pre-anthesis stage and in the field by applying chemical desiccation (KI) as drought simulator for post-anthesis drought stress. Further, the study aims to evaluate the impact of drought on seed germination and quality. Therefore, the dissertation has specific objectives to address the goal of each part:

- Investigation of the phenotypic variation under drought stress by applying water deficit on high throughput phenotyping platform and chemical desiccation in the field.
- Evaluation of the effect of drought stress applying chemical desiccation on seed germination and quality.
- Studying the genetic variation by applying GWAS for the measured traits.

- Identification marker trait association (MTAs) and putative candidate genes for consistently significant MTAs associated with the measured traits suited to be used for future barley breeding programs.

2 Materials and methods

2.1 Plant material

2.1.1 The EcoSeed panel

The EcoSeed panel used for this study is a diverse collection of spring barley consisting of 184 barley genotypes, selected from the germplasm repository at the Federal *ex situ* Genebank in Gatersleben, Germany and stored in cold storage since 1974. In 2013 the panel was multiplied at IPK experimental fields in order to get fresh seeds for further experiments.

The whole panel consists of 116 two-rowed, 68 six-rowed spring barleys comprising 105 cultivars, 65 landraces, and 14 breeding lines (Table 1), originated from 23 different countries but mainly from Germany (66) and Ethiopia (41) (Table S1).

Table 1. EcoSeed panel information.

	Two-rowed			Six-rowed		
Origin	**Cultivar**	**Breeding Line**	**Landrace**	**Cultivar**	**Breeding Line**	**Landrace**
Africa			3	2	1	36
America				7		
Asia			2			2
Europe	83	11	4	13		7
Others		2	11			

2.1.2 Genotyping

The panel was genotyped by TraitGenetics GmbH, Gatersleben, Germany with Illumina 9K SNP chip. The chip was designed as gene-based SNP and used firstly to understand the natural variation of barley growth habit and the detection of a homologue of the adaptive gene *Antirrhinum CENTRORADIALIS* (Comadran et al., 2012). The chip was extensively used during the last years in the context of natural diversity and haplotype analysis as well as gene identification (Youssef et al., 2017;Alqudah et al., 2018;Nagel et al., 2019).

Quality control had been done for the raw genetic data of 7,865 markers. Finally 4,343 SNP markers were obtained after removing monomorphic SNPs, applying minor allele frequency of (MAF>10%) and excluding SNPs with more than 10 % missing data. The markers were distributed on the seven chromosomes with a total length of 988.5 cM, the largest chromosome was 5H (169.6 cM), while the smallest chromosome was 4H (114.3 cM). The average distance between SNPs was 0.23 cM and the marker coverage was 4 markers per cM (Table 2).

2.1.3 Population structure

The structure was determined by 5,156 polymorphic SNPs using STRUCTURE 2.3.4 software (Pritchard et al., 2000a). PCA was applied as an indicator ordination tool for obtaining clusters using GenStat 18.

Linkage disequilibrium (LD) in the whole panel was estimated using the squared allele frequency correlations (r^2), LD values were plotted to examine the intra-chromosomal LD decay by considering the threshold at r^2= 0.20 using GenStat 18 (VSN International Ltd, UK). Further details about the EcoSeed panel are described by Nagel et al. (2019).

Table 2. The length of each chromosome, number of makers, mean distance of markers and marker coverage per cM across the seven chromosomes of the EcoSeed panel.

Chromosome	Length (cM)	Number of markers	Marker distance	Marker coverage per cM
1H	132.8	433	0.3	3
2H	149.4	726	0.2	5
3H	154.9	730	0.2	5
4H	114.3	437	0.3	4
5H	169.6	770	0.2	5
6H	126.6	640	0.2	5
7H	140.9	607	0.2	4
Genome	**988.5**	**4,343**	**0.23**	**4.4**

2.2 Experiments

2.2.1 Pre-anthesis drought stress experiment based on high-throughput phenotyping

2.2.1.1 Experimental design

The EcoSeed panel was evaluated on the automated phenotyping and imaging platform LemnaTec-Scanalyzer 3D (LemnaTec GmbH, Aachen, Germany) located in a greenhouse at IPK under control and drought treatments. It is a pot based system with maximum capacity of 520 single plants (Fig. 3). Pots are located in carriers that have a RFID chip to store all relevant information. They are placed on ten single lanes (each has 52 pots) on conveyer belts that can move the plants automatically to the imaging and watering units. The system has three imaging chambers (visible, near infrared, fluorescence imaging), each equipped with one top view and one side view camera and a lifter that can rotate the carrier to enable imaging from different angles. For screening the EcoSeed population for pre-anthesis drought tolerance, a modified setup of (Neumann et al., 2015) was chosen.

Figure 3. Automated high throughput phenotyping of EcoSeed panel in the LemnaTec system.

The greenhouse temperature was 18 °C during the day and 16 °C during the night with 15 h light per day. The greenhouse is equipped with 36 lamps; half of them high-pressure sodium vapor lamps and half high-pressure metal halogen vapor lamps with 400 W each. They automatically shut off when the outside light sensor records 65 kLx. The external shading starts when 60 kLx are registered. The used pots are of 2 L volume, 19.5 cm height and the top diameter is 14.5 cm (www.berryplastics.com). Blue-coloured supporters were used to stabilize plants and to prevent any leaf damage during automatic handling of the pots. To guarantee the uniformity within the greenhouse in terms of light and temperature distribution the plants were automatically randomized each night.

Due to the maximum capacity of the platform of 520 plants and having three biological replicates per genotype, a maximum 173 genotypes can be screened within one experiment. Accordingly, from the 184 genotypes of the EcoSeed panel, 173 genotypes were selected based on their germination percentage, where at the end of the experiments 151 genotypes were considered for the analysis due to the death of the rest of plants The two independent experiments were performed in a completely randomized design. The first experiment was implemented in February 2016 for investigating the growth under normal conditions (control), while growth under drought stress conditions was started in December 2017 (Table 3).

Table 3. Schedule of the two experiments on the LemnaTec-platform. DAS: Days after sowing, DS: drought stress.

Treatment	Sowing date	Start of DS DAS 27	Re-watering DAS 45	Last imaging	Imaging duration	End of the experiment
Control	13.02.2016	-	-	31.03.2016	DAS47	DAS58
Drought	29.12.2017	25.01.2018	12.02.2018	25.02.2018	DAS58	DAS58

In both experiments, two seeds from each genotype were placed per pot filled with 800g of soil. Then 200 g of soil was added on top of the seeds to ensure that the seeds are in the same depth. The pots were kept at a field capacity (FC) level of 90 % by using the automated target-weight watering option of the system. After seven days from germination plants were thinned for one plant per pot. In the control experiment plants were kept in the automated phenotyping and imaging platform, receiving a daily watering (90 % FC) for all 58 days that plants were on the platform. In the drought experiment, watering was reduced from day 27 after sowing until day 45 to 10% FC. This low level was chosen to allow a development of severe drought stress without risking plant death. At day 45 plants were re-watered with 300 ml for each plant and the remaining days all plants received watering corresponding to 90 % FC (Fig. 4). In both experiments, after 58 days in the platform, the plants were moved to another greenhouse and kept until maturity under the same temperature and day length conditions to evaluate the influence of pre-anthesis drought stress on final yield parameters.

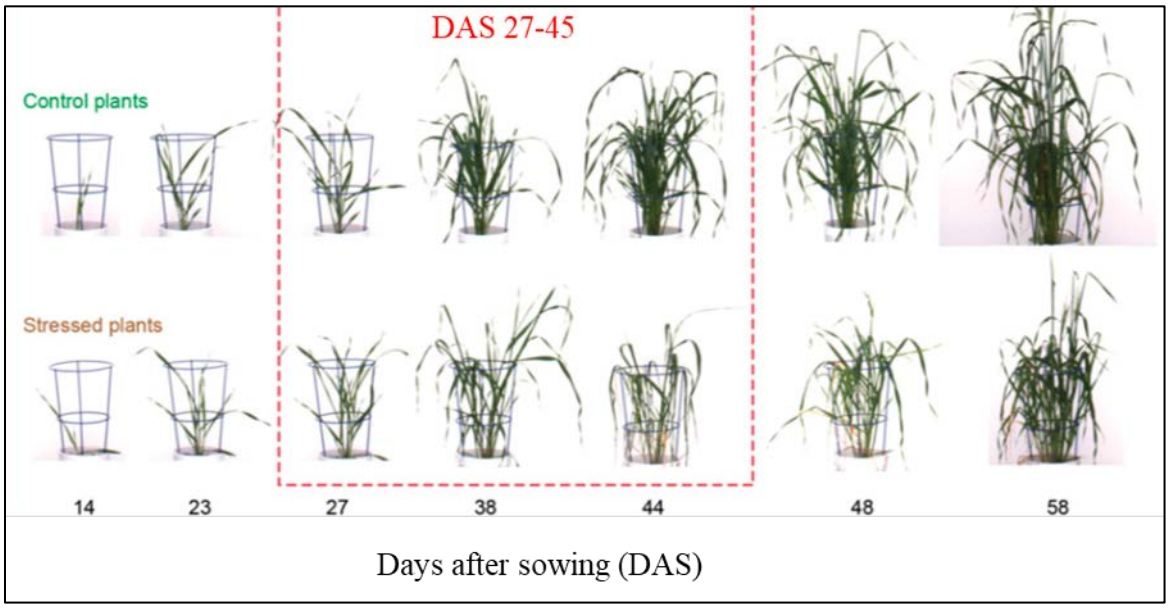

Figure 4. Experimental setup, plants were monitored in a non-invasive way under control and drought stress treatments. Drought stress (in dashed box) was applied from day after sowing DAS27 until (DAS45.

A digital camera (Basler AG, Germany) with high resolution 1628 × 1236 pixels and a pixel size of 4.4 × 4.4 µm was used for daily imaging in three different wavelength: visible (color), near-infrared (NIR) and fluorescence (FLUO) images. During the first ten days, only top view images were taken. After germination and thinning out of one plant per pot, images were taken from top and from three sides view angels at 0°, 45° and 90°. As the platform is automated functioning, unexpected interruptions can be occurred and led to incomplete or missing data for the trait of interest. As a result, the first experiment (control) had missing data in days (20, 35, 36 and 44) and we could only take images until day 47. In the second experiment (drought), an interruption was occurred at days 20 and 31, however the drought experiment ended at day 58 (DAS 58). Each experiment resulted in more than 600 GB of images (from the visible light range) data which had been processed.

2.2.1.2 Images analysis and digital biomass estimation

The software system integrated analysis platform (IAP) http://www.iap.ipk-gatersleben.de. was used for images analysis applying the barley analysis pipeline (Klukas et al., 2014). The most promising traits for genetic studies from the visible light range (Chen et al., 2014;Neumann et al., 2015) were extracted from the resulting image report for further phenotypic analysis. The so called digital biomass (DB) as a proxy for real biomass which was the trait we used in our study and was calculated using side and top view images (Equation. 1).as described in Neumann et al. (2017).

Eq1:

$$\text{Digital biomass} = \sqrt{\text{average pixel side area2} \times \text{top area}}$$

Digital biomass in each experiment was determined independently for each day. The analysis was divided into different parts according to the treatments. The pre-stress phase (PSP) is representing the BLUEs of the control (C) and drought (D) treatment experiments covering the period from DAS9 until DAS26. C treatment experiment was continued from DAS27 until DAS47, where it was terminated. This phase is designated control phase (CP). Drought processing in the D treatment took place from DAS27 until DAS45 (drought phase, DP) whereas the period between DAS46 (re-watering) and DAS58 (end of D treatment experiment) was designated recovery phase (RP).

2.2.1.3 Measurements of traits at maturity

Days to heading (DTH) was recorded for all plants during their time in the stationary greenhouse. At maturity the following agronomic traits were measured per plant: final plant height (PH) from soil surface to the end of the spike without awns, spike length without awns (SPKL), spike number as the final number of spikes counted from each pot, tiller number (TN) as the final tiller number counted from each pot, number of unproductive tiller (UNT) calculated by subtraction of final tiller number from spike number and total biomass (TB). After threshing for all spikes, the total kernel number (KN/plant), kernel weight (KW/plant) and thousand kernel weight (TKW) were measured using Marvin seed analyzer. Straw yield (SY) was calculated by subtraction of kernel weight from total biomass and the harvest index (HI) was calculated as a ratio of grain weight and total biomass.

2.2.2 Post-anhesis drought stress experiment

Two years field experiments were conducted in Gatersleben at IPK (51.8297°N, 11.2717°E, 109 m). Material was sown during March 2016 and 2017 in a randomized complete block design of four replicates per genotype. Each replicate was sown in plot (1x1.5 m) using 30g seeds and each plot was splitted into two rows spaced 0.2 m and 0.4 m between plots (Fig. 5a). The soil type was clay loam and the standard agronomical management practices were applied during the growth period.

2.2.2.1 Chemical desiccation imposing post-anthesis drought stress

Chemical desiccation was used as a technique to simulate post anthesis drought stress by spraying the whole plant canopy with 1 % (w/v) KI (Nicolas and Turner, 1993), over one row

of each plot to desiccate the whole plants while the other row was kept untreated (without spraying) using a plastic cover to prevent contamination of the untreated rows (Fig. 5b). KI was applied ten days after anthesis (Zadoks 49) (Zadoks et al., 1974), which is related to the beginning of grain filling stage. Anthesis with yellow anthers sign of 50 % of plants for each genotype in each plot was recorded separately to define the exact date of spraying. Therefore, the treatment was applied according to the differences in anthesis time. Treated plants with KI showed drought effect as senescence one week after spraying (Fig. 5c).

a)

b)

c)

Figure 5. a) The experimental design in the field, b) spraying one row with 1 % KI by separating the two rows with a plastic barrier, c) visible treatment effect between treated and untreated rows one week after spraying.

2.2.2.2 Morphological and agronomical traits

Growing degree days (GDD) were calculated for both years to measure the required thermal temperature from sowing until applying the treatment. Days to heading (DTH) were recorded in each plot when the spike appeared out of the flag leaf sheath in 50 % of the plants (Z50–Z59). The average plant height (PH) was measured from the ground to the end of the tip of the spike excluding the awn, for three randomly chosen plants from the untreated row in each plot. Spike length (SPKL) without awns was measured for the same three plants.

After maturity twenty tillers with spikes were harvested randomly in each plot from each row (control and treated) in order to measure the total biomass (TB). After spikes threshing kernel number per spike (KN/spike), kernel weight per spike (KW/spike) and thousand kernel weight (TKW) were measured using MARVIN seed analyzer (GTA Sensorik GmbH, Neubrandenburg, Germany). The straw yield (SY) was calculated by subtraction of kernel weight from total biomass. Harvest index (HI) was calculated as the ratio of kernel weight to the total biomass.

2.2.2.3 Drought tolerance indices

Several drought tolerance indices were calculated to determine tolerant genotypes with high yielding potential under drought treatment. TKW was used to calculate drought susceptibility index (DSI, equation 2) across treatments according to Fischer and Maurer (1978) and the extent of injury (injury %, equation 3**)** according to Blum et al. (1983b).

Eq2:

$$DSI = (1 - TKW_{chemical\ desiccation} / TKW_{control}) / (1 - (grand\ means\_TKW_{chemical\ desiccation}) / grand\ means\_TKW_{control})$$

Eq3:

$$injury\% = ((TKW_{chemical\ desiccation} / TKW_{control}) / (TKW_{control})) * 100\%$$

2.2.2.4 Seed quality traits

Seeds from the two years under control and simulated drought treatments were germinated according to ISTA (2014) protocol. Fifty seeds of each replicate were placed between two moistened filter papers and kept in the germination chamber at 20 ºC, 11h light for 7 days. Seeds that had minimum radicle of 1 mm were counted as germinated. Total germination (TG %) was calculated as the ratio between the germinated seeds to the total number of seeds. Normal developed seedlings were recorded to calculate normal seedlings percentage (NS %) which is the ratio between number of normal seedlings to the total number of seeds (Fig. 6).

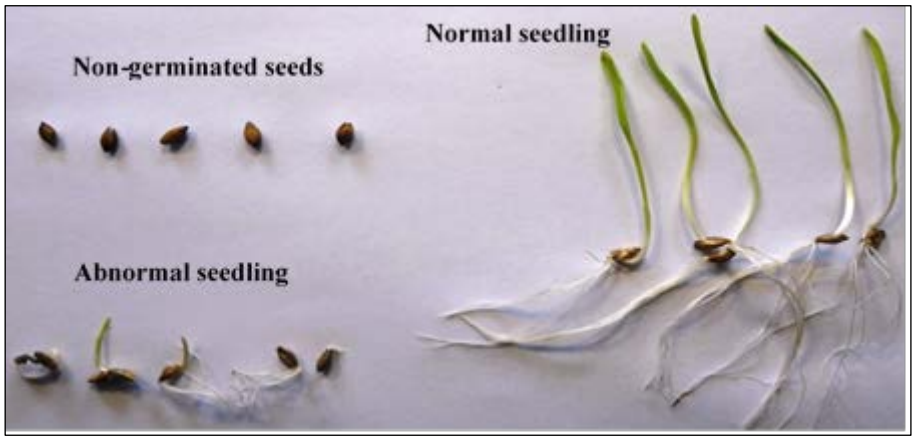

Figure 6. Seedling forms after 7 days of germination, normal seedlings showed normal shoot and root, abnormal seedlings were small or missing the shoot or the root in addition to non-germinated seeds.

2.2.3 Statistical analysis

2.2.3.1 Pre-anthesis drought stress experiment based on high-throughput phenotyping

Statistical analysis and ANOVA were calculated for all measured traits using GenStat18 software (VSN International Ltd, UK). Analysis of variance (ANOVA) was used to compare the differences between genotypes and treatments including their interactions.

The high-throughput data (Digital biomass) was analyzed independently for each day, then BLUEs were calculated for each plant within each experiment and values were used in statistical and variance component analysis.

The repeatability (R^2) was calculated for all measured traits among the replicates within the single experiment according to equation 5.

Eq5:

$$R^2 = \frac{\sigma^2 G}{\sigma^2 G + (\frac{\sigma^2 e}{r})}$$

Where, $\sigma^2 G$ represents the variance of genotype, $\sigma^2 e$ the variance of error and r is the number of replicates.

For digital biomass until the day before applying drought stress, H^2 was calculated across both experiments according to equation 6.

Eq6:

$$H^2 = \frac{\sigma^2 G}{(\sigma^2 G + \sigma^2 G \times E / Num\ of\ experiments)} + (\sigma 2e / r \times Num\ of\ experiments)$$

Where, $\sigma^2 G$ represents the variance of genotype, $\sigma^2 G \times E$ the variance of genotype by enviroment interaction, $\sigma^2 e$ the variance of error and r is the number of replicates.

BLUEs were calculated within each experiment to estimate the mean values of each trait over the replicates and to avoid any discrepancies in phenotypic data which could be a result of environmental influence. Genotypes were considered as a fixed term and replicates as a random term. Calculation was done under a general linear mixed model by residual maximum likelihood (REML) based on mixed linear model (MLM) using GenStat18 software.

2.2.3.2 Post-anhesis drought stress experiment

GenStat18 software (VSN International, 2013) was implemented to analyze phenotypic data for all measured traits. Analysis of variance (ANOVA) was used to compare the differences between genotypes, years and treatments including their interaction. Means separation test for the above-mentioned factors were applied according to the Pearson's least significant difference (LSD) at $P \leq 0.05$ levels of probability.

Broad-sense heritability (H^2) of the studied traits in each treatment was calculated over genotypes and years considering their interactions as the ratio between the genetic variance and the phenotypic variance components according to equation 7.
Eq7:

$$H^2 = \frac{\sigma^2 G}{(\sigma^2 G + \frac{\sigma^2 GY}{Y}) + \frac{\sigma^2 e}{Yr}}$$

where, σ^2G is the variance of genotypes; σ^2G ×Y is the variance component of the interaction genotype (G) × year (Y), σ^2e is the variance of error, r is the number of replicates and Y is number of years
Correlation coefficient was calculated to test the strength of correlation between the two years (2016 *vs* 2017) and BLUEs separately, using GenStat v18 software.

2.2.4 Genome wide association analysis

Genome wide association analysis (GWAS) was performed using the estimated BLUEs values of each treatment for the pre-anthesis drought stress experiment. For the post-anthesis drought stress experiment GWAS was performed by combining the phenotypic data of all measured traits under control and chemical desiccation using the estimated BLUEs values, in addition to each growing season separately.

Associations between measured traits and every single marker (4,343 SNPs) were calculated by applying the mixed linear model (MLM) using GenStat 18 (VSN International Ltd, UK). Kinship was calculated and used to correct for population structure and to control false positive associations. The anlysis was done using single trait association analysis using GenStat 18 (VSN International Ltd, UK). SNPs were considered significant when their P-value passed the threshold of $-\log_{10}(P) \geq 3$ as shown in Manhattan plots.

For further validation, SNPs underwent the false discovery rate (FDR) to exclude false-positive associations at the adjusted P value <0.05 (Storey, 2003). SNPs passed FDR level considered as highly significant markers. An important MTA(s) was defined when the highly associated SNPs ($-\log_{10}$ SNPs ≥ FDR) co-localized on chromosomal segments within the distance of average LD decay (±3cM) and were shown on genetic map using MapChart 2.2 Windows (Voorrips, 2002).

2.2.5 Candidate genes identification

Highly significant associated markers ($-\log_{10}$ SNPs ≥ FDR) were anchored physically using the recently published barley genome sequence (Mascher et al., 2017). The physical map was used to define the candidate genes with their annotation, GO Terms and other information that are available at the BARLEX IPK server http://apex.ipk-gatersleben.de/apex/f?p=284:10. Because of a high number of associated SNPs passing the FDR threshold, in the current study we looked for the candidate genes within 50 Kbp (0.01cM). We used SNPs which were detected under drought and chemical desiccation treatments only. SNPs which are co-located within the physical length of the identified candidate gene interval were considered for further analysis. Such approach empowered us to detect the candidate genes for drought tolerance based on their physical positions on the genome.

2.2.6 SNP-gene based haplotypes

To validate the functionality of the candidate genes, highly confidence genes, including SNPs within their physical position were selected for haplotypes analysis. The selected SNPs were used to obtain the associated trait(s) and then the population was split based on the alleles. Matching the allele with the phenotypic value of associated trait(s) allowed us to reveal the impact of alleles on these traits. The significant differences test between alleles had been calculated using the t-test statistics.

3 Results

3.1 EcoSeed panel structure

The panel structure was divided into four main sub groups (Q groups) as shown in figure 7. Q1 consists of six rowed Ethiopian landraces, Q2 contains the two-rowed German cultivars, Q3 includes the six rowed cultivars and Q4 shows the two rowed cultivars from remaining countries (Nagel et al., 2019). Principal component analysis (PCA) showed four clusters as well (Fig. S1).

The average over all chromosomes LD value (3 cM) was used as a confidence interval to determine associated MTAs (Fig. S2).

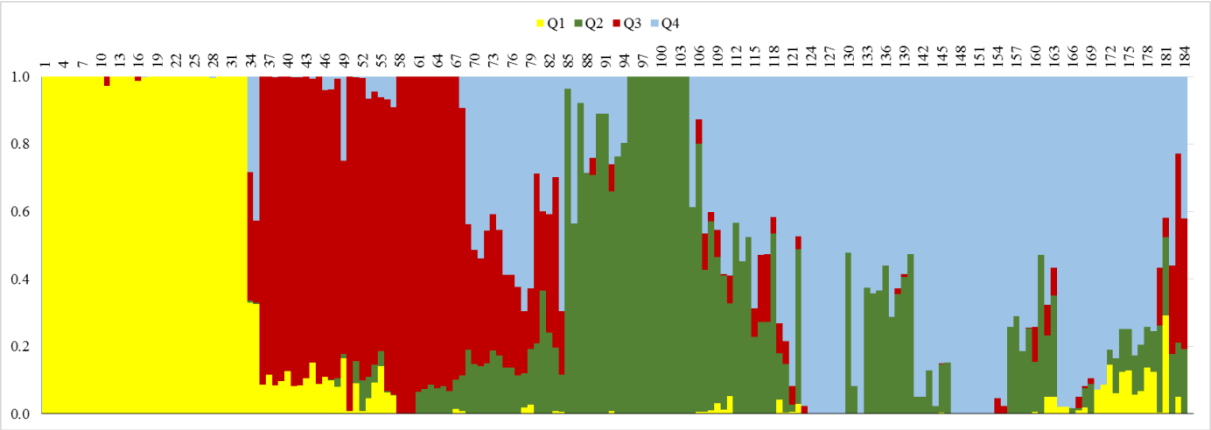

Figure 7. The population structure of the EcoSeed panel shows four main Q groups. In yellow the six-rowed Ethiopian landraces (Q1), in red the six-rowed cultivars (Q3), in green the two-rowed German cultivars (Q2) and in blue the two-rowed cultivars from the remaining countries (Q4).

3.2 Environmental conditions at IPK

For better understanding of the variability of the traits analyzed, temperature and rainfall were recorded for the two growing seasons 2016 and 2017, from March until July. The differences in temperature and rainfall are shown in figure 8. Mean temperatures were 12.9 ^{o}C and 13.4 ^{o}C in 2016 and 2017, respectively. Total rainfall was higher in 2017 (357.6 mm) than in 2016 (180.8 mm). No rainfall was recorded in April 2017 and rainfall amount in June was two times higher in 2016 compared to 2017 which influenced plant growth.

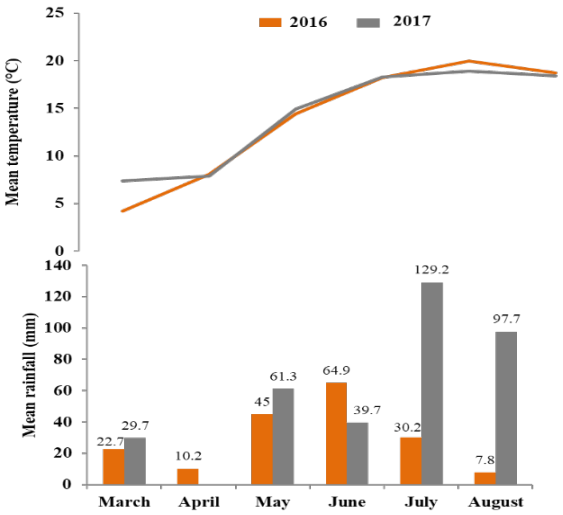

Figure 8. Mean temperature (°C) and monthly rainfall (mm) at IPK during the growing seasons 2016 and 2017.

3.3 Pre-anthesis drought stress experiment

3.3.1 Phenotypic variation

3.3.1.1 Digital biomass

Data of both experiments were image-analyzed with IAP. Digital biomass was determined independently for each day, representing each phase, the pre-stress phase (PSP), the control (C) and drought (D) treatment as shown in figure 9. Histograms showing the distribution of the trait at PSP, C and D treatments were shown in figures (S3, S4 and S5) respectively.

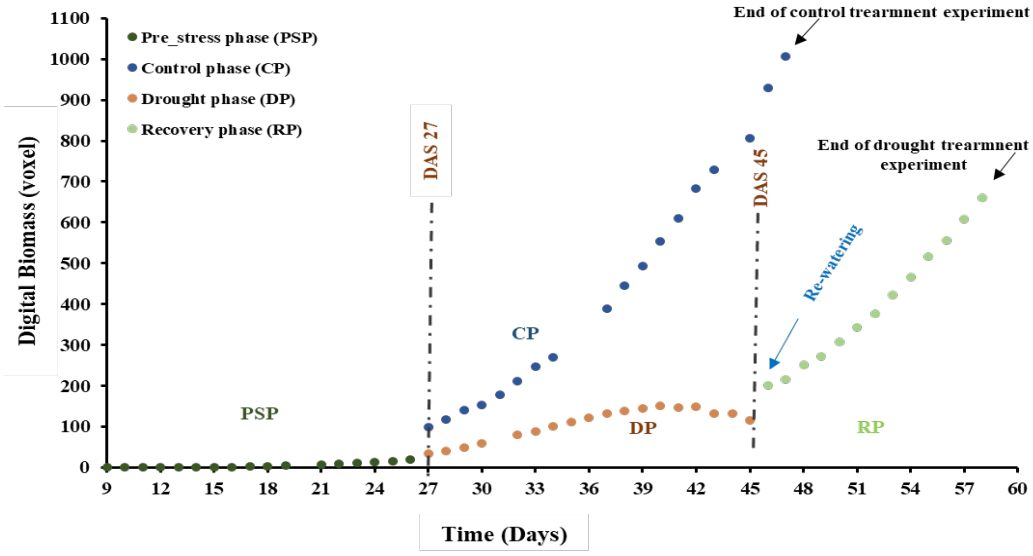

Figure 9. Development of digital biomass over time from the pre-stress phase (PSP) of the control (C) and drought (D) treatment experiments covering the period from DAS9 until DAS26, control phase (CP) from DAS27 until DAS47, drought phase (DP) from DAS27 until DAS45, the period between DAS46 (re-watering) and DAS58 representing the recovery phase (RP). The dashed lines mark the period when drought stress was applied from day after sowing DAS27 to DAS45 and the control and drought stress experiments terminated at DAS47 and DAS58, respectively.

Digital biomass (DB) showed wide phenotypic variation. Coefficient of variation (CV) ranged between 17.7 and 22.9 in PSP, 16.8 and 23.2 in CP, 10.04 and 24.6 in DP and 10.6 and 14.7 in RP (Table S2). For PSP between DAS9 and DAS26 the experimental conditions were the same and, therefore could be compared for the trait biomass over time. A moderate heritability ranging between 0.4 and 0.6 was observed (Fig. 10).

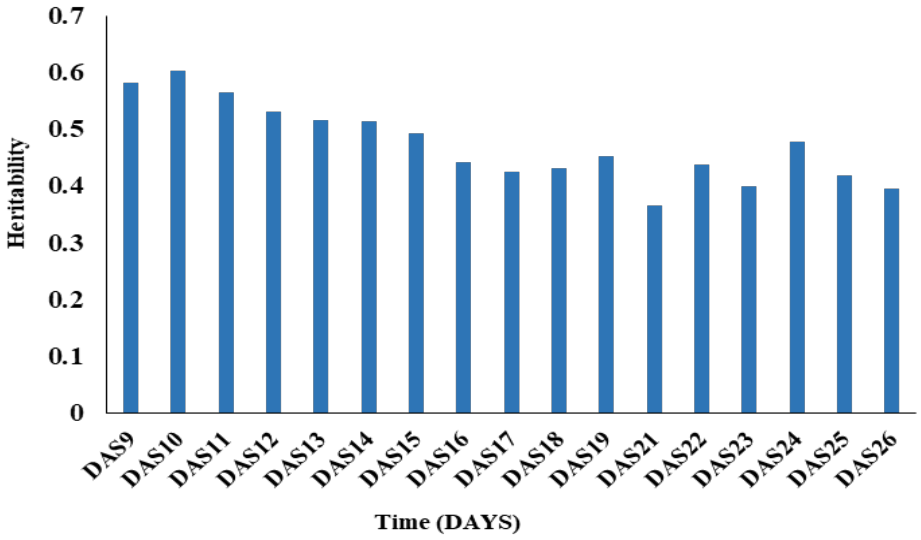

Figure 10. Broad sense heritability values (H^2) of the trait digital biomass. H^2 was calculated based on the best linear unbiased estimates (BLUEs) across control and drought treatment experiments from DAS9 until DAS26, representing the pre-stress phase (PSP).

3.3.1.2 Traits at maturity

The descriptive statistics the analysis of variance (ANOVA) data and histograms showing the distribution under C and D treatments for each trait are shown in table 4, table S3 and figures S6 and S7 respectively.

The trait DTH, showed a high variability ranging from 46 days (HOR5362) to 82 days (HOR2391) under C treatment. Under D treatment the differences ranged from 47 days (HOR5681) to 86 days (HOR4710) (Fig.11a). The drought stress generated a significant ($p<0.001$) increase of about 22 % in DTH compared to the C treatment (Table 4). Furthermore, the *Genotype* × *Treatment* ($G \times T$) interaction was significant ($p<0.001$) (Table S3) due to important variations in response of genotypes to drought stress. The majority of genotypes showed delay in heading under D treatment to around 20 days for instance, HOR4252 and HOR222, other genotypes HOR2174 and HOR2177showed a delay up to 4 days, while HOR2125 showed no difference.

Table 4. Descriptive statistics of the measured traits of EcoSeed panel under control (C) and drought (D) treatments across the best linear unbiased estimates (BLUEs), including the Min: minimum, Max: maximum, standard deviation: SD, coefficient of variation: (CV) and Repeatability: (R^2).

Trait	Treatment	Mean	Median	Min	Max	SD	CV	R^2
Days to heading	C	60.8	60.0	46.0	83.0	5.8	9.5	0.92
	D	74.2	75.0	41.0	89.0	8.9	12.0	0.86
Plant height	C	124.5	125	85.0	165.0	13.9	11.1	0.91
	D	108.3	109.0	79.0	142.0	11.7	10.8	0.75
Spike length	C	9.5	9.7	4.0	13.3	2.1	22.5	0.92
	D	9.5	9.7	3.8	14.8	1.9	19.6	0.92
Spike number	C	12.7	13.0	2.0	27.0	3.1	31.3	0.65
	D	12.0	13.0	5.0	32.0	4.1	30.2	0.67
Tiller number	C	16.0	16.0	6.0	132.0	6.9	43.1	0.72
	D	20.4	20.0	9.0	46.0	5.8	28.5	0.76
Unproductive tiller number	C	3.3	2.0	0.0	21.0	3.1	95.2	0.44
	D	6.9	6.0	0.0	32.0	4.9	70.7	0.61
Total biomass	C	48.3	47.4	11.8	110.2	15.1	31.3	0.81
	D	38.2	37.8	16.3	60.0	7.3	19.2	0.66
Straw yield	C	36.4	34.7	8.0	93.3	12.7	35.0	0.78
	D	27.9	27.6	12.4	53.9	5.6	20.1	0.71
Harvest index	C	0.26	0.30	0.11	0.60	0.04	32.7	0.70
	D	0.27	0.30	0.10	0.50	0.07	31.5	0.83
Kernel weight/plant	C	12.3	11.7	1.0	24.4	4.5	37.9	0.81
	D	10.4	10.1	2.2	23.3	3.6	34.4	0.81
Kernel number/plant	C	304.7	305.5	43.0	635.7	104.5	34.3	0.76
	D	258.9	251.7	62.0	495.5	85.2	32.9	0.77
Thousand kernel weight	C	39.9	39.7	21.5	60.6	7.9	20.3	0.81
	D	40.1	39.7	26.3	54.1	5.8	14.4	0.79

PH ranged from 89 cm (HOR2858) to 162 cm (HOR2130) under C and from 85 cm (HOR6971) to 131 cm (HOR1255) under D treatment (Fig. 11b). Drought provoked a significant reduction (*P<0.001*) in PH. The *G* × *T* interaction was significant (*P<0.001*), indicating important differences in the response of the genotypes (Table S3). Genotypes such as HOR2130, HOR2228 and HOR6658 presented a high reduction ranging between 24 % and 30 %, while genotypes HOR2402, HOR2338 and HOR2215 showed low reduction between 2 % and 5 %. On the other hand, for many genotypes PH were not affected by the treatment such as HOR2764, HOR2441 and HOR2334.

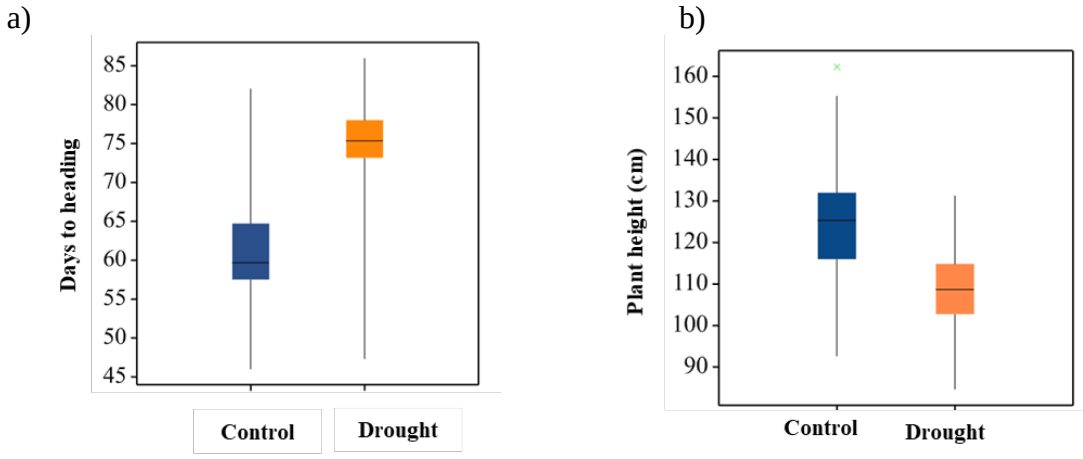

Figure 11. Box plots showing variation in a) days to heading and b) plant height under control and drought treatments.

SPKL ranged from 3 cm (HOR5677) to 13 cm (HOR2198) under C, while under D treatment from 4 cm (HOR5681) to 14 cm (HOR6658) (Fig.12a). No significant difference was found between both treatments while *G* × *T* interaction was significant (*P<0.001*) (Table S3). Some genotypes were positively affected by D resulted in an increase in SPKL between 2 cm and 4 cm, for instance HOR4709, HOR6385, HOR2555 and HOR5677.

SN (representing the number of productive tillers) under C ranged between 3 (HOR2905) and 22 (HOR2101), while under D the difference ranged between 6 (HOR2905) and 23 (HOR2102) (Fig.12b). Drought treatment affected significantly (*P<0.001*) SN. *G* × *T* interaction was not significant (Table S3). Genotype HOR2441 showed high SN while genotype HOR2496 showed low SN under D and HOR4519 showed no difference under both treatments.

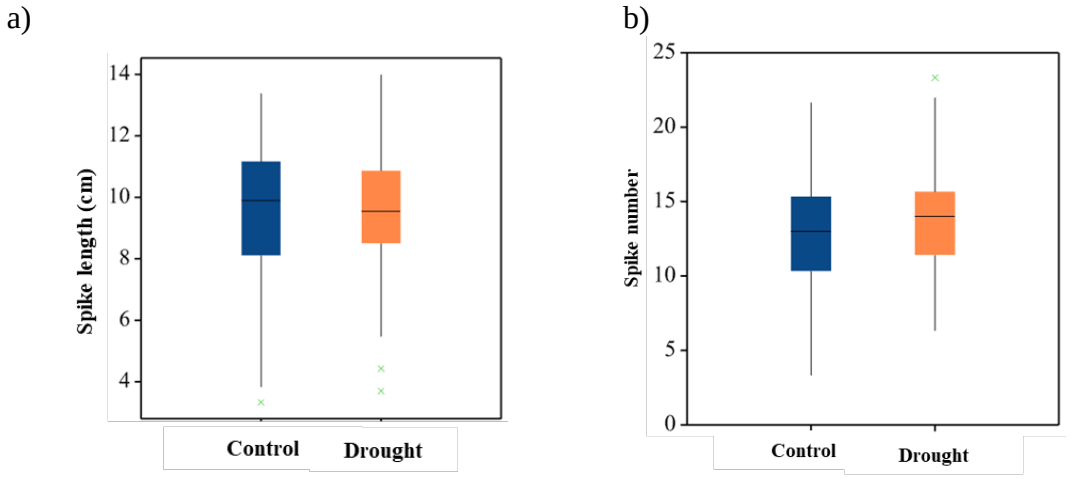

Figure 12. Box plots showing differences in a) spike length and b) spike number under control and drought treatments.

Drought stress resulted in a significant increase (*P<0.001*) in TN (Table S3). TN showed a high variability ranging from 8 (HOR4252) to 26 (HOR2338) under C and from 11 (HOR2749) to 32 (HOR2336) under D (Fig. 13a). The *G* × *T* interaction revealed significant differences (*P<0.001*) (Table S3). Some genotypes HOR2336, HOR2147 and HOR2212

showed high TN under D, while other genotypes did not show significant difference between C and D in TN, for instance HOR2131, HOR2198and HOR2419. Nevertheless, increasing TN under D produced mainly unproductive tillers (UTN). Their number was significantly (*P<0.001*) higher under D compared to the C. UNT ranged between 0 (HOR 2208) and 14 (HOR2905) under C and from 0 (HOR2402) to 22 (HOR2496) under D (Fig. 13b). *G* × *T* interaction was significant (*P<0.001*) (Table S3). Several genotypes showed high number of unproductive tillers such as HOR2212, HOR217, HOR2108 and HOR6974, while other genotypes (HOR2143, HOR2765 and HOR2419) possessed no unproductive tillers.

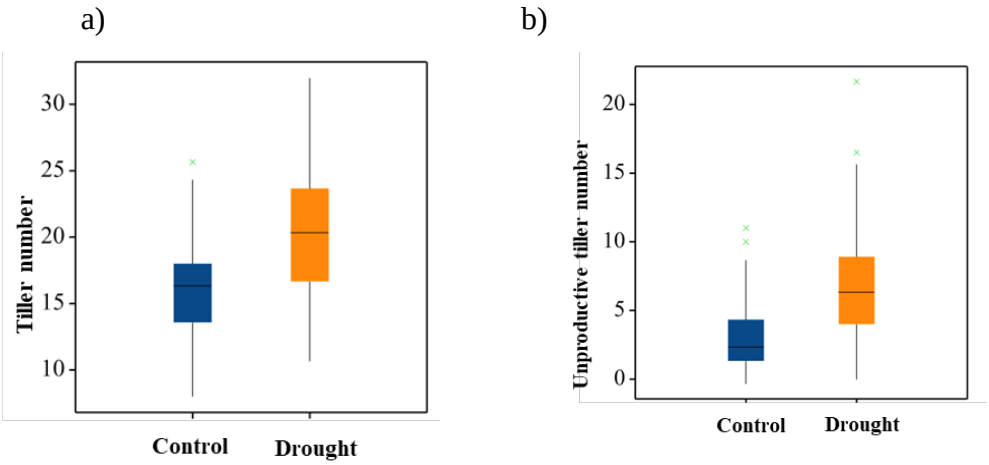

Figure 13. Box plots showing differences in a) tiller number and b) unproductive tiller number under control and drought treatments.

TB ranged between 19 g (HOR5681) and 109.6 g (HOR2071) under C, while under D it ranged from 11.9 g (HOR5681) to 53.7 g (HOR2149) (Fig.14a). D stress significantly (*P<0.001*) reduced TB to about 21 % compared to the C. The *G*× *T* interaction was significant (*P<0.001*) (Table S3), showing important differences between genotypes. Genotypes HOR2441 and HOR2410 had high TB under D, while HOR2071 and HOR2171 were highly negatively affected by drought.

Drought stress generated a significant reduction (*P<0.001*) of 23.5 % in SY, under C compared to D. SY ranged under C between 12.1 g (HOR2183) and 92.0 g (HOR2071) and under D from 8.7 g (HOR5681) to 40.4 g (HOR2157) (Fig.14b). Significant *G*× *T* interaction (*P<0.001*) was shown (Table S3). Genotypes HOR6193 and HOR2100 showed high SY under D, while HOR2120 and HOR2071 showed low SY under drought treatment.

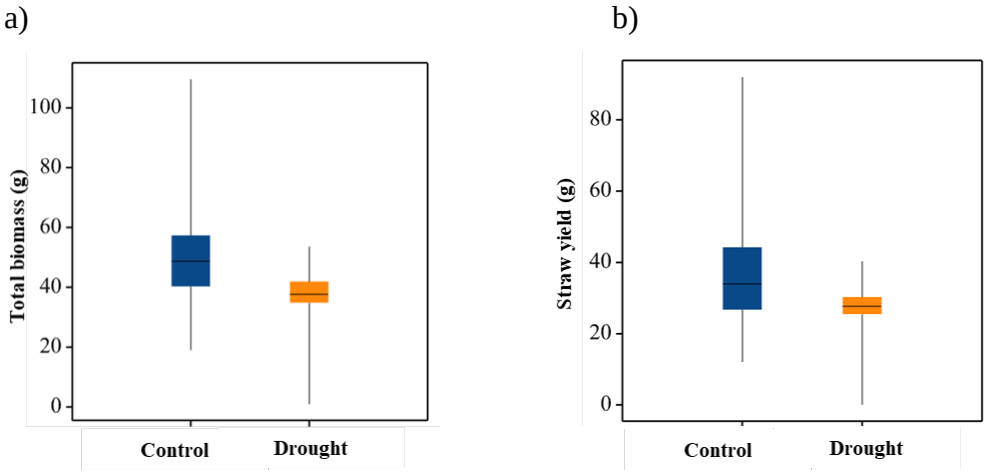

Figure 14. Box plots showing differences in a) total biomass and b) straw yield under control and drought treatments.

HI was significantly different (*P<0.001*) between C and D treatments (Table S3). HI ranged from 0.03 (HOR2905) to 0.48 (HOR2764) under C, while under D it ranged from 0.07 (HOR2496) to 0.48 (HOR2749) (Fig. 15a). Significant *G* × *T* interaction (*P<0.001*) was shown (Table S3). Few genotypes such as HOR22401 and HOR2441 showed high HI under D, while most of the genotypes did not reveal significant changes.

KW/plant showed high variability ranging from 1g (HOR2905) to 24.4g (HOR2183) under C. Under D the differences ranged from 2.2g (HOR2496) to 23.3g (HOR5671) (Fig. 15b). Drought treatment reduced the mean kernel weight significantly (*P<0.001*) compared to C. *G* × *T* interaction was significant (*P<0.001*) (Table S3), showing genotypes with high KW under D such as HOR2441 and HOR6382 but other genotypes, such as HOR1736 and HOR2195 did not show any differences in KW between treatments. Other genotypes as HOR2049 and HOR2171 were negatively affected by drought.

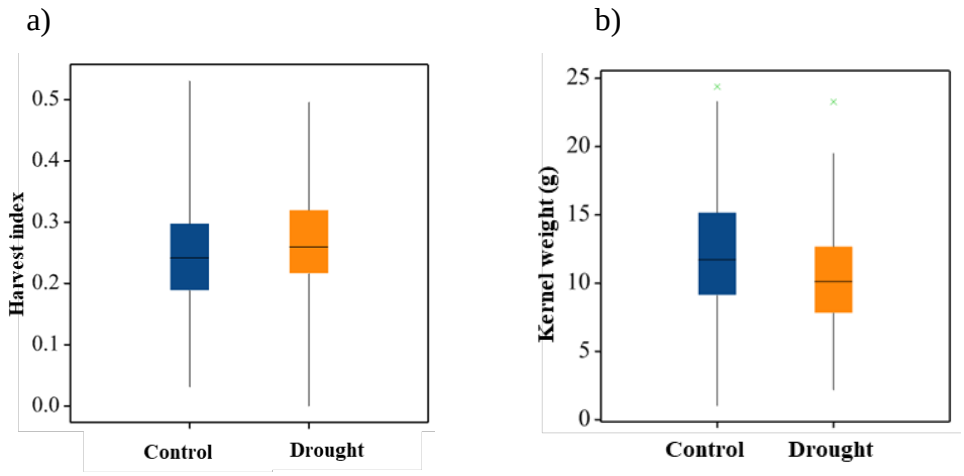

Figure 15. Box plots showing differences in a) harvest index and b) kernel weight/plant under control and drought treatments.

Drought stress exhibited a significant (*P<0.001*) decrease (Table S3) of 15.3 % in KN/plant. The trait showed a high variability ranging from 43 (HOR2905) to 636 (HOR6838) under C treatment (Fig. 16a), whereas under D it ranged from 62 (HOR2496) to 496 (HOR6385). The *G* × *T* interaction was significant (*P<0.001*) (Table S3). Some genotypes were significantly affected by D for instance, HOR6838 and HOR2098, while other genotypes presented significant increases in KN under D such as HOR6382 and HOR2441.

TKW did not show a significant difference under D treatment, compared to C (Table S3). TKW ranged from 21.5 g (HOR2905) to 60.7 g (HOR2160) under C and 26.3 g (HOR6838) to 54.1 g (HOR6313) under D (Fig. 16b). Significant *G* × *T* interaction (*P<0.001*) was shown (Table S3). Some genotypes performed well under D such as HOR1129, HOR2410 and HOR2220 while other had low TKW, for instance, HOR1153 and HOR2157.

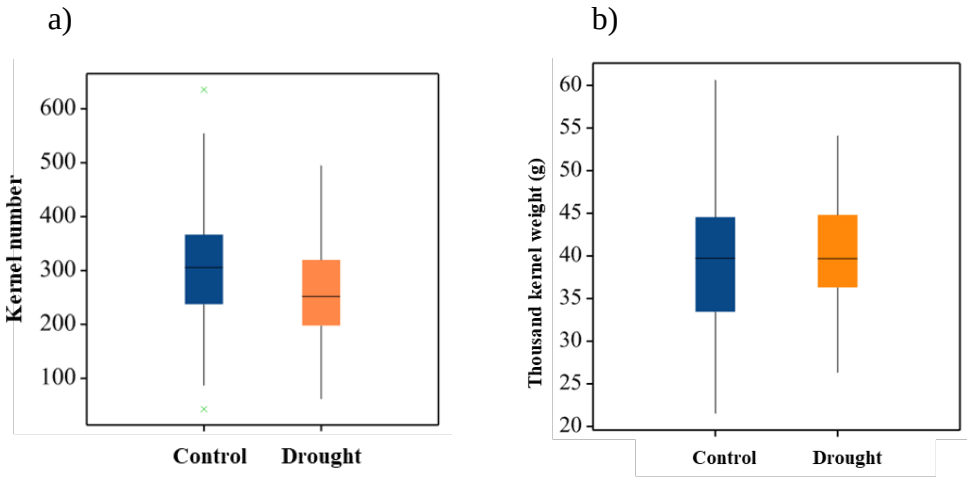

Figure 16. Box plots showing differences in a) kernel number/plant and b) thousand kernel weight under control and drought treatments.

Repeatability of each trait under each treatment was moderate to high, ranging from 0.44 to 0.92 under C and between 0.66 and 0.92 under D treatment (Table 4).

3.3.2 GWAS analysis

3.3.2.1 Digital biomass

GWAS was applied for DB at each time point in PSP, CP, DP and RP. After performing FDR test, in total of 850 MTAs were detected. Among them 217 MTAs at PSP consisting of 33 SNPs, 28 MTAs in CP consisting of seven SNPs, 581 MTAs in DP associated with 93 SNPs and 24 MTAs in RP related to four SNPs were identified. Chromosome 7H held the highest number of MTAs (498) under PSP, CP and DP. After combining the GWAS results at each phase, MTAs were distributed on all chromosomes as shown in figure 17, table S4 and. Manhattan plots in figures S8, S9 and S10 under PSP, CP and DP respectively.

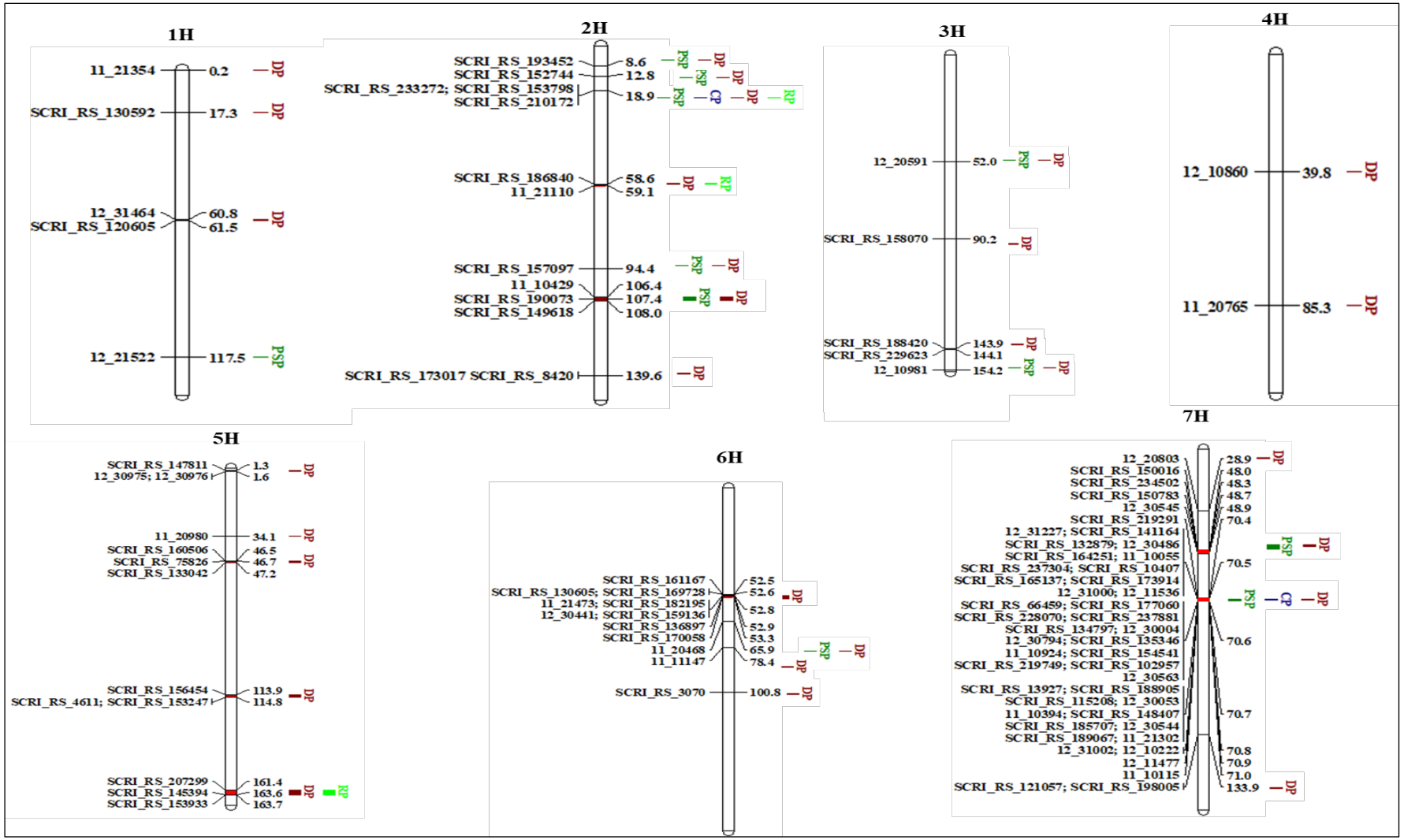
1H
11_21354 0.2 DP
SCRI_RS_130592 17.3 DP
12_31464 SCRI_RS_120605 60.8 61.5 DP
12_21522 117.5 PSP
2H
SCRI_RS_193452 8.6 PSP DP
SCRI_RS_152744 12.8 PSP DP
SCRI_RS_233272; SCRI_RS_153798 SCRI_RS_210172 18.9 PSP CP DP RP
SCRI_RS_186840 58.6 DP RP
11_21110 59.1
SCRI_RS_157097 94.4 PSP DP
11_10429 106.4
SCRI_RS_190073 107.4 PSP DP
SCRI_RS_149618 108.0
SCRI_RS_173017 SCRI_RS_8420 139.6 DP
3H
12_20591 52.0 PSP DP
SCRI_RS_158070 90.2 DP
SCRI_RS_188420 143.9 DP
SCRI_RS_229623 144.1
12_10981 154.2 PSP DP
4H
12_10860 39.8 DP
11_20765 85.3 DP
5H
SCRI_RS_147811 1.3 DP
12_30975; 12_30976 1.6
11_20980 34.1 DP
SCRI_RS_160506 46.5
SCRI_RS_75826 46.7 DP
SCRI_RS_133042 47.2
SCRI_RS_156454 113.9 DP
SCRI_RS_4611; SCRI_RS_153247 114.8
SCRI_RS_207299 161.4
SCRI_RS_145394 163.6 DP RP
SCRI_RS_153933 163.7
6H
SCRI_RS_161167 52.5
SCRI_RS_130605; SCRI_RS_169728 52.6 DP
11_21473; SCRI_RS_182195 52.8
12_30441; SCRI_RS_159136 52.9
SCRI_RS_136897 53.3
SCRI_RS_170058 65.9 PSP DP
11_20468 78.4 DP
11_11147
SCRI_RS_3070 100.8 DP
7H
12_20803 28.9 DP
SCRI_RS_150016 48.0
SCRI_RS_234502 48.3
SCRI_RS_150783 48.7
12_30545 48.9
SCRI_RS_219291 70.4
12_31227; SCRI_RS_141164 PSP DP
SCRI_RS_132879; 12_30486
SCRI_RS_164251; 11_10055 70.5
SCRI_RS_237304; SCRI_RS_10407
SCRI_RS_165137; SCRI_RS_173914 PSP CP DP
12_31000; 12_11536
SCRI_RS_66459; SCRI_RS_177060 70.6
SCRI_RS_228070; SCRI_RS_237881
SCRI_RS_134797; 12_30004
12_30794; SCRI_RS_135346
11_10924; SCRI_RS_154541 70.7
SCRI_RS_219749; SCRI_RS_102957
12_30563
SCRI_RS_13927; SCRI_RS_188905 70.8
SCRI_RS_115208; 12_30053
11_10394; SCRI_RS_148407 70.9
SCRI_RS_185707; 12_30544
SCRI_RS_189067; 11_21302 71.0
12_31002; 12_10222
12_11477 133.9 DP
11_10115
SCRI_RS_121057; SCRI_RS_198005

Figure 17. Genetically anchored position of marker trait associations (MTAs) related to digital biomass (DB) identified at different time point days after sowing (DAS) at pre-stress phase (PSP), control phase (CP), drought phase (DP) and recovery phase (RP). Red chromosomal interval indicates MTAs within interval of ±3 cM.

Twenty-five MTAs for DB at different time points were revealed on chromosome 1H related to five SNPs. Two MTAs were located at 0.21 cM related to one negative effect SNP at DP. Another MTA was located at 17.3 cM with positive effect on DB at DP. Twenty MTAs were located within the genomic interval 60.8-61.5 cM, carrying two SNPs with positive effect on DB at DP. Finally, two MTAs were located at 117.5 cM related to one negative effect SNP detected at PSP. The highest significant SNP was SCRI_RS_120605 located at 61.5 cM with $-\log_{10}(p)= 6.5$ and positive effect (+15.9 voxel) associated with DB (DAS39) at DP.

On chromosome 2H, 145 MTAs were identified for DB at different time points, related to 13 SNPs. 21 MTAs were located at 8.6 cM related to one negative effect SNP of which eight MTAs were related to DB at PSP and 13 MTAs at DP. At 12.8 cM, 13 MTAs were identified associated with one SNP affected DB negatively, where one MTA was identified at PSP and 12 MTAs were detected at DP. High number of MTAs (74) related to three SNPs with negative effect were detected at 18.9 cM where seven MTAs associated with DB at all phases, 24 MTAs at PSP, 22 MTAs at CP, 21 MTAs at DP and four MTAs at RP were identified within the genomic interval (58.6-59.1 cM) related to two SNPs with positive and negative effect on DB at DP and RP. At 94.4 cM, 19 MTAs were associated with one negative effect SNP, where 11 MTAs were identified at PSP and eight MTAs at DP. Within the genomic region (106.4-108 cM) 12 MTAs carrying three positive effect SNPs were identified, 10 MTAs were identified at PSP and two MTAs at DP. At 139.6 cM, two MTAs related to two negative effect SNPs were associated with DB at DP. The SNP SCRI_RS_210172 was the highest significant SNP located at 18.9 cM with $-\log_{10}(p)=6.9$ with negative effect (-119.2 voxel) on DB at CP.

On chromosome 3H, 36 MTAs related to five SNPs were identified. Two MTAs were located at 52.0 cM associated with one positive effect SNP at PSP and DP. Another MTA with negative effect was identified at 90.2 cM related to DB at DP. At the genomic region 143.9-144.1 cM six MTAs were associated with 2 SNPs at DP. 27 MTAs were identified at 154.2 cM related to one negative effect SNP, of which 12 MTAs were detected at PSP and 15 MTAs at DP. The highest significant SNP was 12_10981, located at 154.2 cM with $-\log_{10}(p)=9.4$ affected DB negatively (-21.6 voxel) at DP.

The lowest number of MTAs (2) were identified on chromosome 4H at DP. One MTA was located at 39.8 cM, where SNP 12_10860 had the highest $-\log_{10}(p)= 3.8$ and associated positively (+6.0 voxel) on DB at DP. The other MTA was identified at 85.3 cM and had a positive effect on DB at DP.

Regarding to chromosome 5H, 41 MTAs related to 13 SNPs were identified. 40 MTAs at DP and one MTA at RP. Within the genomic region 1.32-1.6 cM, 22 MTAs related to three negative and positive effects SNPs were identified at DP. One MTA was located at 34.1 cM with positive effect on DB at DP. At the interval 46.5 -47.2 cM, five MTAs related to three positive effect SNPs were identified at DP at different time points. Six MTAs were located within the genomic interval 113.8-114.7 cM related to three positive and negative effect SNPs at DP. Within the genomic interval 161.4-163.7 cM, seven MTAs related to three positive and negative effect SNPs were identified, one SNP is associated with DB at RP and six MTAs at

DP at different time points. The most significant SNP on chromosome 5H was SCRI_RS_145394 with $-\log_{10}(p)=5.6$ with positive effect (+10.1 voxel) on DB at RP.

On chromosome 6H, 103 MTAs were identified at different time points related to 12 SNPs. 94 MTAs carrying nine negative effect SNPs were located at (52.5-53.3 cM) identified at DP. At 65.9 cM, seven MTAs related to one negative effect SNP were detected, where five MTAs were identified at PSP and two MTAs at DP. Another two MTAs were located at 78.4 cM and at 100.8 cM, associated positively with DB at DP. The SNP with highest $-\log_{10}(p)=4.6$ was 12_30441, located at 52.8 cM which showed negative effect (-11.1 voxel) on DB at DP.

The highest number of MTAs (498) related to 47 SNPs were identified on chromosome 7H. One MTA with negative effect was located at 28.9 cM associated with DB at DP. Within the genomic region 48-48.9 cM, 30 MTAs related to four negative effect SNPs of which three MTAs are detected at PSP and 27 at DP at different time points. 463 MTAs were found at 70.4-71 cM, related to 40 SNPs of which 157 MTAs associated with 20 negative and positive effect SNPs respectively, were detected at PSP, four MTAs related to four negative effect SNPs were detected at CP and 302 MTAs related to 40 negative and positive effect SNPs were identified at DP at different time points. At 133.9 cM, four MTAs carrying two negative effect SNPs were associated with DB at DP. With the high number of MTAs, SNP 12_11536 located at 70.9 cM had the highest $-\log_{10}(p)=8.3$ and showed negative effect (-20.3voxel) on DB at DP.

3.3.2.2 Traits at maturity

GWAS was performed for 12 traits under C and D experiments. The analysis was based on the estimated means (BLUEs). Results showed high number of significant associations passed FDR level $P \leq 0.05$. We were able to detect 201 significant MTAs for nine studied traits (DTH, PH, SPKL, SN, TN, UTN, TB, SY and KW/plant) under C (47) and D treatment (154) (Table S5). All MTAs were distributed on all chromosomes clarified on the map (Fig. 18) and Manhattan plots are shown in figures S11 under C and S12 under D. Chromosome 3H held the highest number of MTAs (59).

On chromosome 1H, 15 MTAs related to 12 SNPs were detected. One MTA is located at 12.5 cM associated with PH under C treatment. Two MTAs were detected within the genomic interval 49.9-50.8 cM carrying two negative effect SNPs associated with DTH and SN under D treatment. Another MTA was located at 55.5 cM associated negatively with DTH under D. Within the genomic interval 59.1-62.8 cM, two MTAs were related to DTH under D, carrying two SNPs with negative effect on the trait. At the genomic interval 81.7-82.6 cM, five MTAs related to three SNPs were negatively associated with SPKL, SY and DTH under D. Three MTAs were located at 86.5 cM associated with SPKL, SY and SN under D related to two negative effect SNPs. One MTA was located at 117.5 cM associated positively with TN under C. The highest significant SNP was 12_21522 located at 117.5 cM with $-\log_{10}(p)=6.1$ affected TN positively (+5.5) under C treatment.

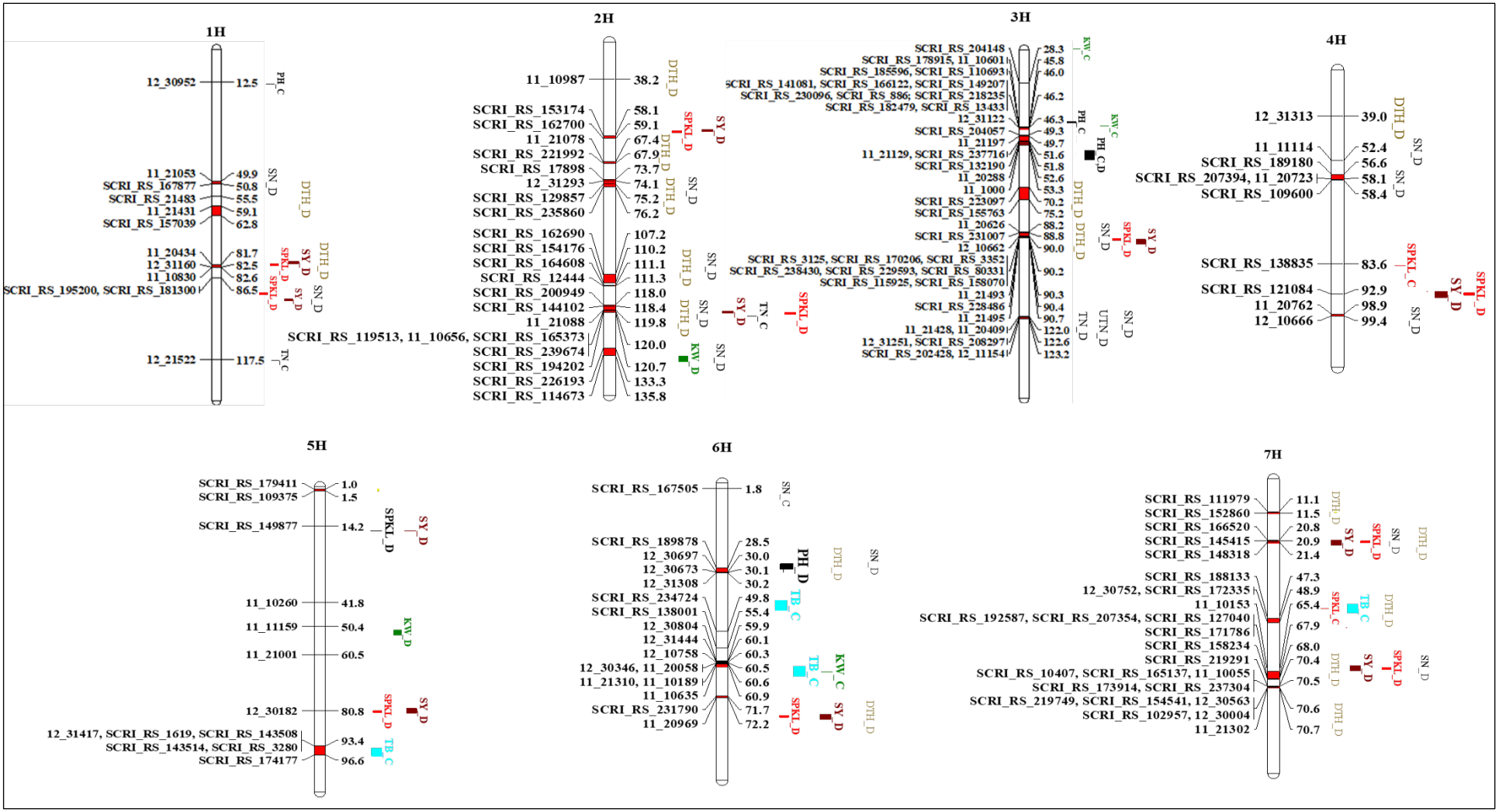

Figure 18. Genetically anchored positions of marker trait associations (MTAs), related to traits at maturity detected under control (C) and drought (D) treatment experiments. Red chromosomal interval indicates MTAs (within the interval of ±3 cM), each color is showing different traits.

Thirty-two MTAs related to 23 SNPs were identified at chromosome 2H, 32 MTAs under D treatment and one MTA under C treatment distributed as follow. One MTA was located at 38.2 cM associated positively with DTH under D treatment. Four MTAs were located within the genomic interval 58.1-59.1 cM carrying two negative effect SNPs associated with SPKL and SY under D. At genomic interval 67.4-67.9 cM, two MTAs were identified related to two SNPs affected DTH negatively under D treatment. Within the genomic intervals 73.7-76.2 cM and 107.2-111.3 cM, four MTAs for each interval were identified, related to four SNPs with negative effect on DTH and SN under D. The genomic interval 118.0-120.7 cM harboured 15 MTAs related to eight negative effect SNPs were associated with DTH, SN, SY and TN under D and SPKL under both treatments. Two MTAs were located within the interval 133.3-135.8 cM associated with KW and SN under D with two SNPs, one with positive effect on KW and the other with negative effect on SN. Among all SNPs, SCRI_RS_144102 which was located at 118.4 cM had the highest $-\log_{10}(p)=8.8$ and was associated negatively (-1.4) with SN under D treatment.

The highest number of MTAs (59) related to 43 SNPs were detected on chromosome 3H all with negative effect on the associated traits. One MTA was located at 28.3 cM affecting negatively KW under C. Within the genomic interval 45.8-46.3 cM 15 MTAs were identified related to 13 SNPs associated with PH and KW under C. Nine MTAs were identified within the genomic interval 49.3-53.3 cM related to seven SNPs associated with PH under C and D treatments. Another two MTAs related to two SNPs were located within the interval 70.2-75.2 cM associated with DTH under D treatment. 26 MTAs were detected within the interval 88.2-90.7 cM related to 14 SNPs associated with DTH, SN, SPKL and SY under D treatment. Seven MTAs were located at 122-123.2 cM related to six SNPs associated with TN, UTN and SN under D treatment. The SNP 11_21197 was the most significant SNP located at 49.7 cM with $-\log_{10}(p)=11.1$ and negative effect (-7.0 cM) on PH under D.

The lowest number of MTAs (11) related to 10 SNPs was detected on chromosome 4H. One MTA was located at 39.0 cM associated with DTH under D treatment. At 52.4 cM one MTA was detected associated with SN under D treatment. Within the genomic interval 56.6-58.4 cM, four MTAs were identified related to four SNPs associated with SN under D. One MTA was located at 83.6 cM associated with SPKL under C treatment. Two MTAs were located at 92.9 cM related to one SNP associated with SY and SPKL under D treatment. Within the genomic interval 98.9-99.4 cM, two MTAs were identified related to two SNPs associated with SN under D treatment. All MTAs showed negative effects on the associated traits and the most significant SNP with highest $-\log_{10}(p)=4.9$ was SCRI_RS_207394 located at 58.1 cM and associated with SN under D treatment with negative effect (-1.4).

On chromosome 5H, 20 MTAs related to 13 SNPs were revealed. Two MTAs were located within the genomic interval 1-1.5 cM related to two negative effect SNPs associated with DTH under D. At 14.2 cM, two MTAs were identified related to one SNP associated negatively with SPKL and SY under D treatment. Another MTA was located at 41.8 cM associated negatively with DTH under D. Two MTA were identified under D treatment one at 50.4 cM associated positively with KW and another at 60.5 associated negatively with KN. At 80.8 cM, two MTAs were identified carrying one SNP associated negatively with SPKL and

SY under D treatment. Within the genomic region 93.4-96.6 cM, 11 MTAs were identified related to six positive effect SNPs associated with TB, SY under C and SN under C and D treatments. The highest significant SNP was SCRI_RS_143508 located at 93.4 cM with $-\log_{10}(p)=5.2$ and positive effect (+1.5) on SN under C.

Twenty-three MTAs related to 17 SNPs were detected on chromosome 6H. One MTA was located at 1.8 cM associated positively with SN under C treatment. Within the genomic interval 28.5-30.2 cM, four MTAs were identified related to four SNPs associated negatively with PH, DTH and SN under D treatment. Two MTAs associated with TB under C treatment were identified at 49.8 cM with negative effect and another two at 55.4 cM with positive effect. Within the genomic interval 59.9-60.9 cM 11 MTAs were identified related to eight SNPs with positive and negative effect on TB and KW under C treatment. Five MTAs were detected within the genomic interval 71.7-72.2 cM related to two SNPs with negative effect on SPKL, SY and DTH under D treatment. The most significant SNP with highest $-\log_{10}(p)=6.2$ was 12_30673 located at 30.1 cM associated negatively (-1.5) with SN under C treatment.

On chromosome 7H, 41 MTAs related to 26 SNPs were detected all with negative effect on the associated traits. Two MTAs related to two SNPs are located within the interval 11.1-11.5 cM associated with DTH under D treatment. Within the genomic interval 20.8-21.4 cM, five MTAs were identified related to three SNPs associated with DTH, SY, SPKL and SN under D. Four MTAs were detected within the genomic region 47.3-48.9 cM carrying three SNPs associated with SPKL and TB under C and DTH under D treatment. In addition, 18 MTAs were detected within the genomic interval 65.4-68.0 cM related to six SNPs, associated with DTH, SY, SPKL and SN negatively under D treatment. Within the genomic region 70.4-70.7 cM, 12 MTAs were identified related to 12 SNPs associated with DTH under D treatment. The most significant SNP was 11_10153 with $-\log_{10}(p)=7.2$ located at 65.4 cM showing negative effect (-0.9) on SY and SPKL under D treatment.

High number of MTAs associated with digital biomass and maturity traits were identified under pre-anthesis drought stress. We could detect MTAs co-located between DB and maturity traits at different chromosomes. At chromosome 1H, MTAs located at 60.8 cM associated with DTH, and DB at DP. At 117.5 cM a common MTA is associated with DB at PSP and TN under C treatment. MTAs were located within the genomic interval (58.6-59.1 cM) on chromosome 2H, associated with DB at DP and RP and SPKL and SY under D. At 107.2 cM a common MTA associated with DB at PSP and DTH under D was revealed. On chromosome 3H, one MTA was located at 90.2 cM common between DB at DP and different maturity traits (SPKL, DTH, SY and SN) under D treatment. At chromosome 4H one MTA was co-located at 39.0 cM associated with DB at DP and DTH under D treatment. On chromosome 5H, one MTA was located at 1.5 cM common between DB at DP and DTH under D. Chromosome 7H harboured common MTAs, one at 48.9 cM associated with DB at DP and TB under C. Other MTAs were located within the genomic region 70.4-70.7 cM associated with DB at PSP, CP, DP and DTH under D trait.

3.3.3 Identification of candidate genes

3.3.3.1 Digital biomass

Based on the highly significant genomic regions, highly significant SNPs associated with DB at D treatment were co-localized according to their physical position as stated in the latest barley reference genome sequence in order to identify potential candidate genes.

Biomass development under D treatment showed high number of MTAs at different time points. We could identify a number of candidate genes alongside with the highly significant associations related to drought (DSP) (Table S6).

On chromosome 1H, two candidate genes were characterized, the first candidate gene *HORVU1Hr1G064200.1* was related to BOPA2_12_31464, encoding RNA-binding KH domain-containing protein, which has a key role in regulating stress-response. The second candidate gene was *HORVU1Hr1G064020.1* detected via SCRI_RS_120605, found to be responsible for GDSL esterase/lipase.

On chromosome 3H one candidate gene *HORVU3Hr1G085290.1* was identified through SCRI_RS_158070 and annotates ARID/BRIGHT DNA-binding domain, a ELM2 domain protein.

Three candidate genes were detected on chromosome 5H The first gene *HORVU5Hr1G111120.2* was identified by BOPA2_12_30976 and encodes Remorin family protein. The second candidate gene *HORVU5Hr1G050160.1* was detected alongside SCRI_RS_75826, annotating Asparagine-tRNA ligase. The third candidate gene on 5H, *HORVU5Hr1G050570.2* was identified by SCRI_RS_133042 which annotates Cystathionine beta-synthase family protein.

On chromosome 6H the candidate gene *HORVU6Hr1G079150.1* was identified by the SNP BOPA1_ABC06682-1-1-311, annotating Adenine nucleotide alpha hydrolases-like superfamily.

Two candidate genes were recognised on chromosome 7H. The first one, *HORVU7Hr1G107760.1* was identified by BOPA2_12_30486 encoding Pentatricopeptide repeat protein and the second gene *HORVU7Hr1G056490.1* was detected through SCRI_RS_134797 encoding basic-leucine zipper (bZIP) transcription family protein.

3.3.3.2 Traits at maturity

According to the highly significant SNPs, 19 candidate genes were identified under D treatment related to different traits. The candidate genes were distributed on the seven chromosomes. Six candidate genes were identified on chromosome 1H, three on chromosome 2H, four on chromosome 3H, one candidate gene each on 4H and 5H and two candidate genes each on chromosome 6H and 7H. All the candidate genes were located within the interval of the physical gene position (Table S7) where many of them are involved in drought stress tolerance.

On chromosome 1H, the candidate gene *HORVU1Hr1G052890.4* was associated with SN by SCRI_RS_167877. The gene encodes sterol C4-methyl oxidase 1-2. Other candidate genes,

HORVU1Hr1G058500.1, *HORVU1Hr1G064950.1* and *HORVU1Hr1G072810.4* were associated with DTH by SCRI_RS_21483, SCRI_RS_157039 and BOPA1_6250-1056, respectively. The first candidate gene encodes Histone H2B.1. The second candidate gene encodes signal sensing machinery two-component response regulator ORR21 and the third putative gene annotated transcription factor ILR3. Further candidate genes on chromosome 1H were associated with SY and SPKL. *HORVU1Hr1G072490.2* was identified by BOPA1_2881-935, encoding ATP-dependent zinc metalloprotease FtsH and *HORVU1Hr1G074410.4* by SCRI_RS_195200 SNP is encoding a protein of unknown function (DUF668).

Three candidate genes were detected on chromosome 2H, two of them were associated with DTH, *HORVU2Hr1G089970.3* related to SCRI_RS_17898, annotates Aquaporin-like superfamily protein. The second candidate gene, *HORVU2Hr1G090010.1* related to BOPA2_12_31293 annotates Defensin-2 peptides whereas the third one, *HORVU2Hr1G111050.1* is related to SPKL and SY by SCRI_RS_119513, encoding a Protein kinase superfamily.

On chromosome 3H, four candidate genes were revealed. The candidate gene *HORVU3Hr1G051000.1* was related to BOPA1_2027-1307 annotating for HSP20-like chaperones superfamily protein. The second gene, *HORVU3Hr1G053760.3* is associated by SCRI_RS_132190 annotating GDSL esterase/lipase. Both candidate genes were associated with PH. Another candidate gene *HORVU3Hr1G085270.8* related to SN, SY and SPKL by SCRI_RS_80331 annotating Fructose-1,6-bisphosphatase class 1. The candidate gene *HORVU3Hr1G085290.1* was associated with SN by SCRI_RS_158070 annotating ARID/BRIGHT DNA-binding domain, ELM2 domain protein.

The candidate gene on chromosome 4H *HORVU3Hr1G096830.4* was related to TN by BOPA2_12_11154 and annotates Carboxypeptidase Y homolog A.

On chromosome 5H, one candidate gene *HORVU4Hr1G063980.6* was identified related to SN by SCRI_RS_189180 which annotates Senescence/dehydration-associated protein.

Two candidate genes were identified on chromosome 6H. One candidate gene *HORVU6Hr1G012040.1* was related to SN via BOPA2_12_31308 and annotated Pentatricopeptide proteins. The second candidate gene *HORVU4Hr1G081670.1* was identified alongside with BOPA2_12_10666 annotating respiratory burst oxidase homologue D.

On chromosome 7H, two candidate genes were revealed. *HORVU5Hr1G000590.2* was associated with DTH by SCRI_RS_179411 and annotates for Ethylene receptor 1. The candidate gene *HORVU7Hr1G018230.3* was associated with SY, SN and SPKL through SCRI_RS_148318. The gene encodes for proteins of unknown function (DUF630 and DUF632).

3.3.4 SNP-gene based haplotypes

3.3.4.1 Digital biomass

To validate the function of the candidate genes, haplotype SNP-gene based analysis was applied for highly significant SNPs (co-located within the physical position of the candidate gene) detected under DP at one or two time points, where most of the significant SNPs did appear (Fig. 19).

On chromosome 3H significant SNP SCRI_RS_158070 was located at 611854023 bp within the *HORVU3Hr1G085290.1* interval associated with DB at DAS28. The SNP carries C and T alleles. Genotypes carrying C allele showed significantly ($p<0.001$) lower DB compared to the genotypes carrying T allele. The genotypes with C allele were mainly 2-rowed cultivars.

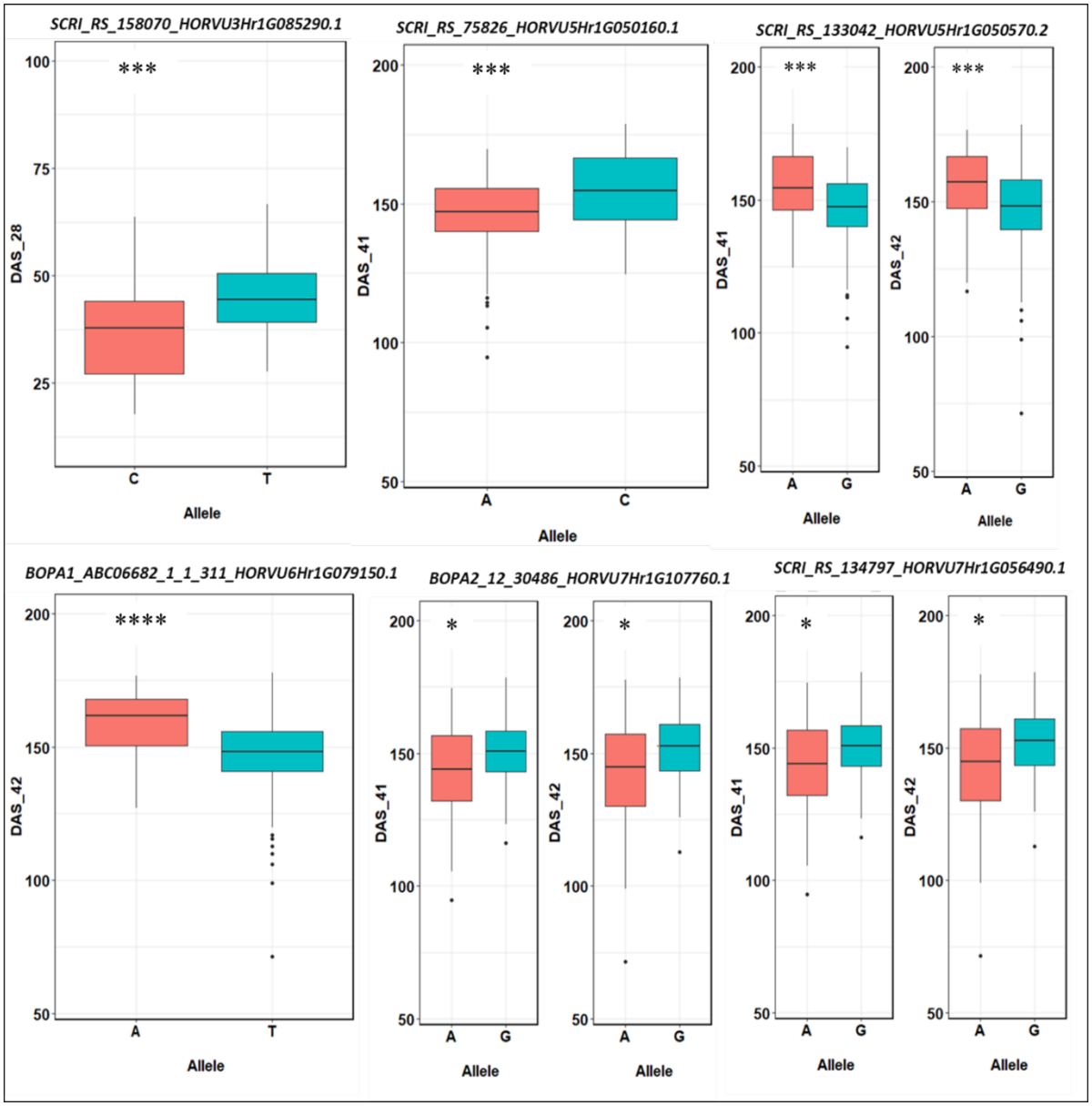

Figure 19. SNP-gene based haplotypes for the most significant SNPs located within the candidate gene interval, showing the allelic effect on the digital biomass at different time points during pre-anthesis drought stress. *** p<0.001, ** p<0.01, * p<0.05 and ns: not significant.

On chromosome 5H, one identified significant SNP was. SCRI_RS_75826 located at 388731481 bp, within the candidate gene *HORVU5Hr1G050160.1* interval and related to DB at DAS41. The SNP carries A and C alleles. The genotypes representing different row types and origins, carrying allele A showed significantly (*p<0.001*) lower DB compared to the ones carrying allele C. The second SNP SCRI_RS_133042 located at 394033818 bp within *HORVU5Hr1G050570.2* interval was related to two time points DAS41 and DAS42. The SNP carries A and G alleles. Genotypes carrying allele A showed significantly (*p<0.001*) higher DB and represent different origins and row types.

On chromosome 6H, one SNP BOPA1_ABC06682-1-1-311l located at 536786820 bp within the interval of the candidate gene *HORVU6Hr1G079150.1* carrying A and T alleles, was related to DB at DAS42. The analysis showed that the genotypes carrying allele A showed significantly (*p<0.001*) higher DB at that time point compared to the genotypes carrying allele T.

Two significant SNPs were detected on chromosome 7H, representing DB at the two time point DAS41 and DAS42. The first SNP (BOPA2_12_30486) was located at 235388310 bp within the interval of *HORVU7Hr1G107760.1* and the second one (SCRI_RS_134797) was located at 236134087 bp, within *HORVU7Hr1G056490.1* interval. Both SNPs carry A and G alleles and these genotypes representing different row types of cultivars and landraces. Genotypes carrying allele A showed significantly (*p<0.05*) lower DB compared to the ones carrying allele G.

3.3.4.2 Traits at maturity

Haplotypes SNP-gene based analysis was applied for highly significant SNPs detected under D treatment experiment Fig. 20.

Six significant SNPs were located on chromosome 1H. The first SNP SCRI_RS_167877 was located at 391319382 bp within the interval of the candidate gene *HORVU1Hr1G052890.4*. The allelic variation (A, G) at this SNP was associated with SN. Genotypes carrying allele A which were mainly 2-rowed cultivars from European countries showed significantly (*p<0.001*) higher SN compared to genotypes carrying allele G. Two significant SNPs were associated with DTH. SCRI_RS_21483 (427145216 bp) located within the candidate gene *HORVU1Hr1G058500.1* interval carrying A and C alleles. Genotypes carrying allele A which were mainly 6-rowed type barleys with high number of Ethiopian landraces showed significantly (*p<0.001*) earlier heading compared to the genotypes carrying allele C. SNP SCRI_RS_157039 at 464421881 bp located within the candidate gene *HORVU1Hr1G064950.1* interval carrying A and G alleles. Allele A genotypes were highly significant *(p<0.001)* different compared to genotypes carrying the G allele (2-rowed European cultivars) being late in heading. SNP BOPA1_6250-1056 was identified at 499157309 bp co- localized within the interval of the candidate gene *HORVU1Hr1G072810.2* and associated with DTH trait. This SNP carries A and T alleles. The difference was highly

significant (*p<0.001*) and the genotypes (2-rowed European cultivars) carrying allele A showed late heading compared to the ones carrying T allele. SNP (BOPA1_2881_935) carrying A and T alleles located at 497940358 bp within gene *HORVU1Hr1G072490.2* interval was associated with SY and SPKL. The genotypes carrying allele A showed significantly (*p<0.001*) lower SPKL compared to the ones carrying allele T. For SY no significant difference between both alleles was found. Results showed that most of the genotypes carrying A allele are European cultivars. Further, SNP SCRI_RS_195200 on chromosome 1H was located at 507977141 bp within the interval of the candidate gene *HORVU1Hr1G074410.4* position. The SNP was associated with SPKL and SY, carrying C and T alleles. The analysis showed that presence of allele C (2-rowed European cultivars) significantly (*p<0.001*) increased the SPKL compared to the genotypes carrying allele T, while no significant difference between both alleles was found in SY.

Chromosome 2H showed three significant SNPs of which two were associated with DTH. One SNP (SCRI_RS_17898) at 640849650 bp was located within *HORVU2Hr1G089970.3* interval and having C and T alleles. Genotypes carrying allele C were significantly (*p<0.001*) earlier in heading compared to the ones carrying allele T. The genotypes carrying C allele were mainly European cultivars. The second SNP (BOPA2_12_31293) located at 641328117 bp carrying A and T alleles was detected within *HORVU2Hr1G090010.1*. Genotypes which were mainly 6-rowed Ethiopian landraces carrying allele A showed significantly (*p<0.001*) earlier heading compared to the genotypes carrying allele T. The third SNP (SCRI_RS_119513) at 721944874 bp was found within the interval of *HORVU2Hr1G111050.1.* This SNP was linked to SPKL and SY and carrying C and T alleles. Genotypes which were mainly 2-rowed German cultivars carrying allele C had significantly (*p<0.001*) lower SPKL than the ones carrying allele T. No significant difference was detected between both alleles related to SY.

Four significant SNPs were revealed on chromosome 3H of which two were associated with PH. SNP (BOPA1_2027_1307) located at 367111723 bp and related to *HORVU3Hr1G051000.1* carries alleles A and G. Allele A resulted in a significant (*p<0.001*) decrease in PH in the genotypes (2-rowed cultivars) carrying this allele. SNP (SCRI_RS_132190) was located at 396190351 bp within the interval of *HORVU3Hr1G053760.3.* The SNP carries C and T alleles. Genotypes carrying allele C were significantly (*p<0.001*) shorter compared to genotypes carrying allele T. Another SNP SCRI_RS_80331 carrying C and T alleles was located at 611856132 bp and co-localized within the interval of *HORVU3Hr1G085270.8* related to SPKL, SN and SY. Genotypes carrying allele C had significantly (*p<0.001*) higher SPKL and SN and were representing mainly the 6-rowed Ethiopian landraces. No significant differences were detected between the two alleles for SY.

The SNP (SCRI_RS_158070) carrying C and T, located at 611854023 bp and related to *HORVU3Hr1G085290.1,* was associated with SN. Genotypes carrying allele C significantly (*p<0.001*) decreased SN compared to the ones carrying allele T.

On chromosome 4H one SNP (BOPA2_12_11154) was identified at 654554805 bp within *HORVU3Hr1G096830.4* interval, related to TN. This SNP carries A and G alleles. Genotypes carrying allele A (European cultivars) had significantly ($p<0.001$) higher TN than the ones carrying allele G.

Chromosome 5H had one SNP SCRI_RS_189180 associated with SN and situated at 535568894 bp within *HORVU4Hr1G063980.6* interval. The SNP carries C and T alleles where genotypes (mainly 2-rowed European cultivars) carrying allele C had significantly ($p<0.001$) higher SN compared to the ones carrying allele T.

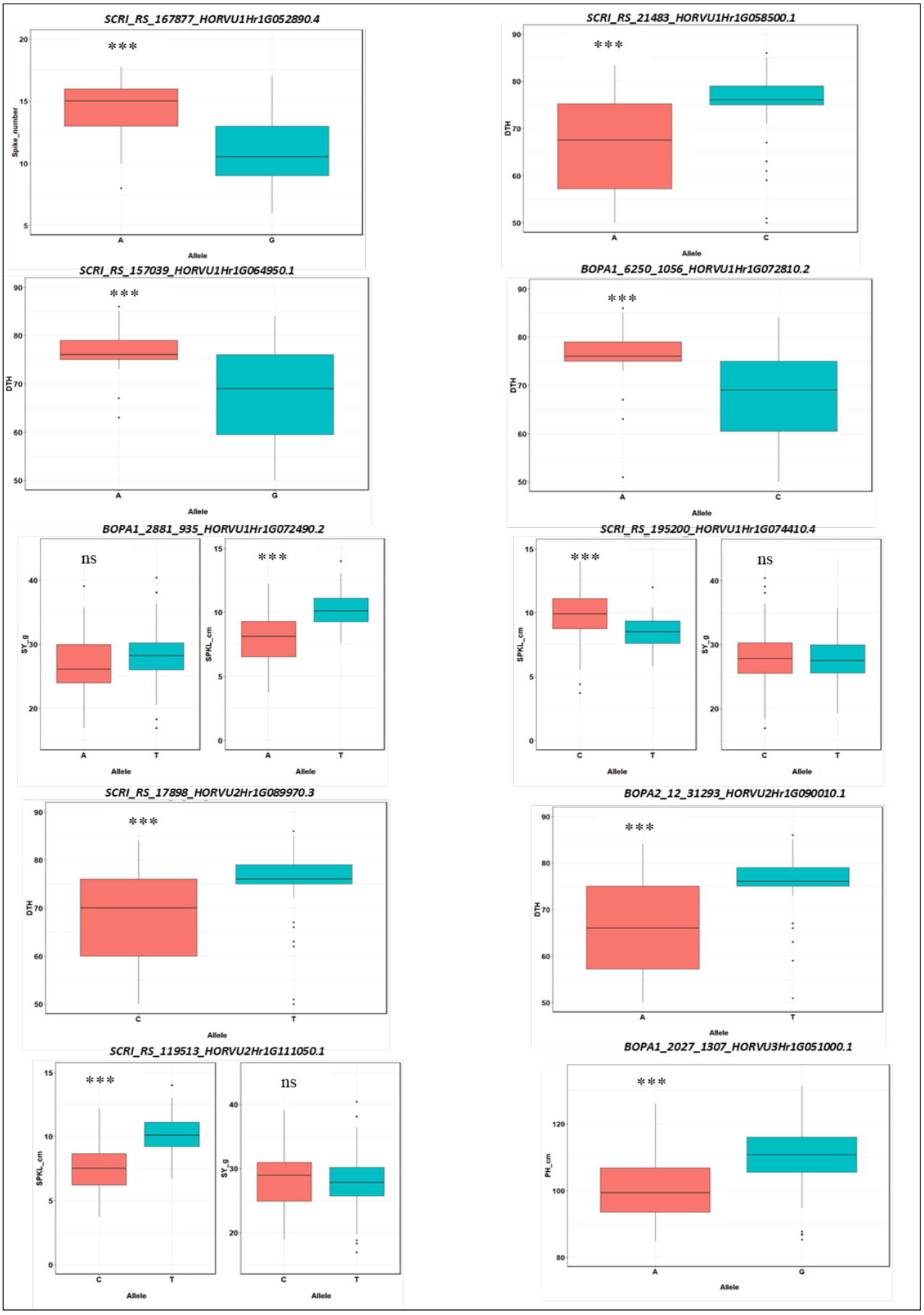
SCRI_RS_167877_HORVU1Hr1G052890.4
***
Spike_number
Allele
A
G
SCRI_RS_21483_HORVU1Hr1G058500.1
***
DTH
Allele
A
C
SCRI_RS_157039_HORVU1Hr1G064950.1
***
DTH
Allele
A
G
BOPA1_6250_1056_HORVU1Hr1G072810.2
***
DTH
Allele
A
C
BOPA1_2881_935_HORVU1Hr1G072490.2
ns
SY_g
***
SPKL_cm
Allele
A
T
SCRI_RS_195200_HORVU1Hr1G074410.4
***
SPKL_cm
ns
SY_g
Allele
C
T
SCRI_RS_17898_HORVU2Hr1G089970.3
***
DTH
Allele
C
T
BOPA2_12_31293_HORVU2Hr1G090010.1
***
DTH
Allele
A
T
SCRI_RS_119513_HORVU2Hr1G111050.1
***
SPKL_cm
ns
SY_g
Allele
C
T
BOPA1_2027_1307_HORVU3Hr1G051000.1
***
PH_cm
Allele
A
G

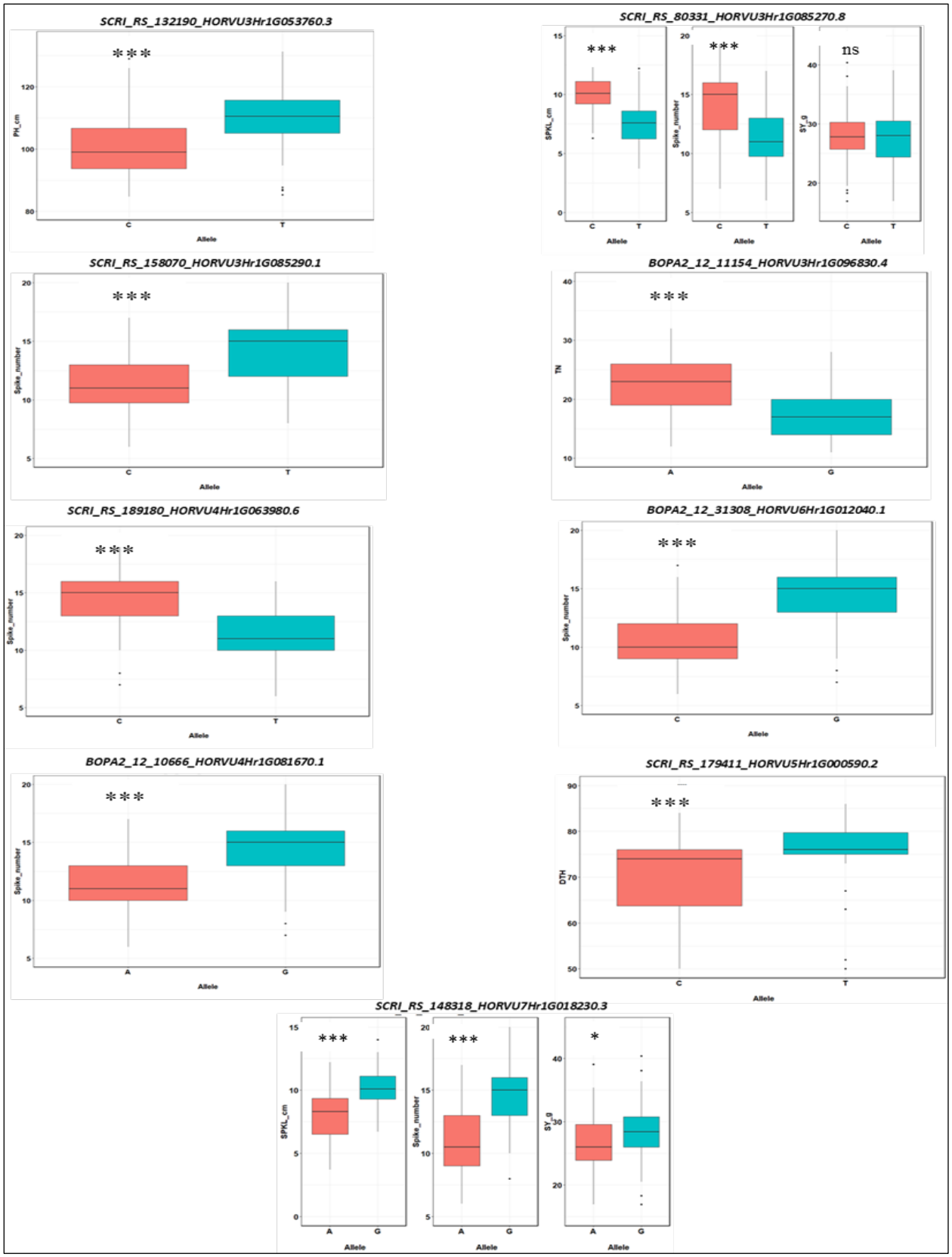

Figure 20. SNP-gene based haplotypes for the most significant SNPs located within the candidate gene interval, showing the allelic effect on the associated maturity traits during pre-anthesis drought stress. *** p<0.001, ** p<0.01, * p<0.05 and ns: not significant.

On chromosome 6H SNP (BOPA2_12_31308) located at 22810044 bp within the interval of *HORVU6Hr1G012040.1* was associated with SN. The allelic variation (C and G) showed that genotypes carrying allele C had significantly (*p<0.001*) lower SN compared to the genotypes carrying allele G. SNP (BOPA2_12_10666) located at 620025304 bp within the gene *HORVU4Hr1G081670.1* interval, carries A and G alleles. Genotypes of different row type carrying allele A had significantly (*p<0.001*) lower SN compared to the ones (2-rowed cultivars) carrying allele G.

Chromosome 7H is carrying two relevant SNPs. SCRI_RS_179411 existed at 2261856 bp within the interval of *HORVU5Hr1G000590.2* and is associated with DTH. The SNP holds C and T alleles. The allelic variation showed that genotypes which were mainly 2-rowed cultivars and holding allele C showed significantly (*p<0.001*) earlier heading compared to the genotypes carrying allele T. The second SNP (SCRI_RS_148318) located at 23795915 bp and was identified within the interval of *HORVU7Hr1G018230.3*. This SNP carries A and G alleles associated with SPKL, SN and SY traits. Genotypes of different row type carrying allele A showed significantly (*p<0.001*) lower SPKL and SN compared to the genotypes carrying allele G and a significant difference (*p<0.05)* in SY compared to the genotypes carrying allele G.

3.4 Post-anthesis drought stress experiment

3.4.1 Phenotypic variation in morphological, agronomical and seed quality traits

The descriptive statistics, analysis of variance (ANOVA) data and histograms showing the distribution under C and D treatments for each trait are shown in table 5 table S8 and figures S13 and S14, respectively.

DTH, PH and SPKL were measured under control treatment as they will be determined before applying the desiccant. The traits were significantly different (*P<0.001*) in both growing seasons (Table S8). Genotypes in 2016 reached heading earlier (65.4±3.2 days) compared to 2017 (78.5±4.3 days). PH mean was higher in 2016 (102.8±10.1 cm), reaching 97.8±10.0 cm in 2017. SPKL was also higher in 2016 (9.3±1.9 cm) compared to 2017 (8.3±1.7 cm) (Table 5). Significant differences (*P<0.001*) between genotypes related to the aforementioned traits were shown (Table S8).

Table 5. Morphological, agronomical and seed quality traits of EcoSeed panel under control (C) and chemical desiccation (CD) treatments across the two growing seasons 2016 and 2017 and the best linear unbiased estimates (BLUEs). Min: minimum, Max: maximum, SD: standard deviation, CV: coefficient of variation.

Trait	Treatment	Year	Mean	Median	Min	Max	SD	CV
Days to heading	C	2016	65.4	65	56	73	3.2	4.9
		2017	78.5	78	66	86	4.3	5.4
		BLUES	72	72.1	62.5	77.6	3.1	4.3
Plant height	C	2016	102.8	103.3	76.7	130.3	10.1	9.9
		2017	97.8	99	64	130.3	10	10.2
		BLUES	100.2	102.2	74.9	118	8.5	8.5
Spike length	C	2016	9.3	9.3	4	14	1.9	20.7
		2017	8.3	8.5	4	14.3	1.7	20.2
		BLUES	8.8	9.1	4.1	11.5	1.5	17.3
Growing degree days	C	2016	995.9	1006	865	1277	66.2	6.7
		2017	1137	1130	918.4	1312	79.6	7
		BLUES	1066	1073	896	1160	53.4	5
Total biomass	C	2016	55.1	53	20	100	15.2	27.5
		2017	46.6	44.9	20	79	11	23.6
		BLUES	51.7	49.4	26.3	84.1	11.3	21.8
	CD	2016	48.4	45	18	100	15.1	31.1
		2017	45.4	42.2	14.8	106	14.1	31.7
		BLUES	46.2	44.9	31.6	65.4	6.9	15
Straw yield	C	2016	30.9	29.1	4.2	63.8	11	35.7
		2017	24.6	23.9	7.6	42.5	6.6	26.8
		BLUES	28.3	27.4	13.7	51.8	7	24.6
	CD	2016	29.8	27.6	2.2	64	10.8	36.1
		2017	26.6	24.7	2.4	87	9.9	37.2
		BLUES	27.6	14.2	41.5	24.7	3.4	0.1
Harvest index	C	2016	0.44	0.44	0.23	0.65	0.07	16.4
		2017	0.47	0.47	0.24	1.1	0.07	15
		BLUES	0.45	0.45	0.19	0.56	0.05	10.9
	CD	2016	0.38	0.38	0.2	0.6	0.07	19.5
		2017	0.42	0.42	0.13	0.92	0.07	17.4
		BLUES	0.4	0.4	0.28	0.5	0.04	9.9
Kernel weight/spike	C	2016	1.4	1.3	0.4	2.5	0.4	27.4
		2017	1.3	1.2	0.7	2.3	0.4	26.8
		BLUES	1.4	1.3	0.7	2.3	0.3	23.1
	CD	2016	1.1	1	0.4	2.2	0.3	31.9
		2017	1.2	1.1	0.2	3.9	0.4	34.7
		BLUES	1.1	1.1	0.8	1.6	0.2	15.7
Kernel number/spike	C	2016	27.8	25.2	12.6	49	7.5	26.9
		2017	28.3	24.8	11.6	55.4	8.4	29.8
		BLUES	28.4	24.9	13.4	49.5	7.7	27
	CD	2016	26.7	24.4	11	49.4	7.5	28

		2017	28.6	24.8	12.2	67.8	9.5	32.9
		BLUES	27.7	26.9	17.5	39.9	4.3	15.6
Thousand kernel weight	C	2016	49.3	49.9	31.6	64.9	6.3	12.8
		2017	47	47.4	32.7	60.6	5.3	11.2
		BLUES	48.1	48.8	33.9	58.1	4.8	10
	CD	2016	40.2	40	25	62.7	6.9	17.3
		2017	40.3	41.2	15.9	58.9	6.7	16.8
		BLUES	40	40.3	24.6	51.7	4.8	12
Total germination%	C	2016	96.8	98	33.3	100	6.2	6.4
		2017	96.5	98	58.3	100	5.2	5.4
		BLUES	96.7	98	76.7	100	3.4	3.6
	CD	2016	94.6	97	20.4	100	8.3	8.8
		2017	95.9	98	44.9	100	6.1	6.3
		BLUES	95.2	96.8	69.1	99.8	4.5	4.7
Normal seedling %	C	2016	92	94	29.2	100	8.8	9.6
		2017	92.5	95.9	52.1	100	8	8.6
		BLUES	92.3	94	70.6	99.8	5.2	5.6
	CD	2016	87.2	90	20.4	100	11.3	13
		2017	88.6	92	34.7	100	10.3	11.6
		BLUES	87.9	89.2	59.8	96.3	6.1	6.9
Drought susceptibility index		2016	0.97	0.99	-1.9	2.8	0.7	69.9
		2017	0.98	0.95	-3.6	4.5	0.9	89.4
		BLUES	0.98	0.96	0.05	2.2	0.4	36.2
Injury%		2016	18.4	18.8	-37.7	52.3	12.9	69.9
		2017	16	15.3	-10.7	44.3	9.8	61.1
		BLUES	16.3	16.2	-0.8	32.9	5.7	34.9

GDD from sowing until spraying for both growing seasons were significantly different (*P<0.001*) (Table S8). In 2016 the mean of GDD was 995.9±66.22 while in 2017 it was 1,137±79.61. However, high correlation coefficient (r = 0.74) between 2016 and 2017 was found (Fig. 21) and proved by high heritability (H^2= 0.87) across the two growing seasons showing that the treatment was applied in the right stage.

TB was significantly (*P<0.001*) affected by CD treatment. TB showed high variability ranging from 26.3 g (HOR2858) to 84.1 g (HOR2571) under C and from 31.6 g (HOR2858) to 65.4 g (HOR6313) (Fig. 22a). Significant differences (*P<0.001*) between the growing seasons were obtained (Table S8). CD effect was higher in 2016 (12.0 %) compared to 2017 (2.6 %). The *G* × *T* interaction was significant (*P<0.001*) (Table S8). Genotypes such as HOR6735 and HOR2571 were affected by CD treatment, while other genotypes had high TB under CD but were not significant different to C, such as HOR2490 and HOR2099.

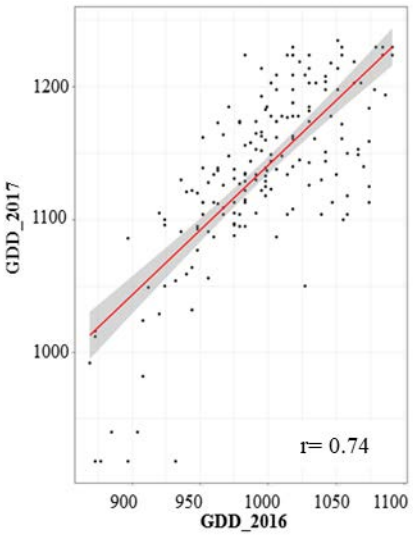

Figure 21. Correlation coefficient of growing degree days (GDD) from sowing until spraying between the growing seasons 2016 and 2017.

CD treatment did not show a significant effect on SY (Table S8). SY ranged from 13.7g (HOR2858) to 51.8g (HOR5851) under C, while under CD it ranged from 14.2g (HOR6974) to 41.5 g (HOR5410) (Fig. 22b). The growing seasons 2016 and 2017 were significantly different (*P<0.001*) (Table S8). CD effect in 2016 was 3.4 % compared to 8.2 % in 2017. *G* × *T* interaction was significantly different (*P<0.001*) (Table S8). Some genotypes were highly affected by CD, for instance, HOR6125 and HOR6735, while other genotypes were not affected such as HOR2094 and HOR2131.

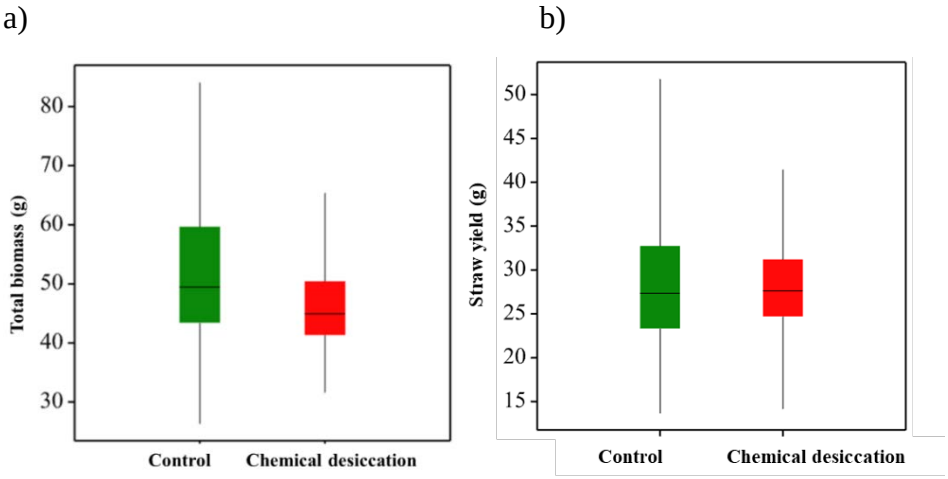

Figure 22. Box plots showing differences in a) total biomass and b) straw yield under control and chemical desiccation treatments.

Harvest index (HI) was affected significantly (*P<0.001*) by CD (Table S8), HI ranged from 0.19 (HOR5584) to 0.55 (HOR2091) under C, while under CD it ranged from 0.28 (HOR5681) to 0.49 (HOR2496) (Fig. 23a). Significant difference (*P<0.001*) between both growing seasons was shown (Table S8). In general, CD treatment caused a reduction in HI of 13 % in 2016, while the effect was lower in 2017 (10 %). The *G* × *T* interaction was

significant (*P<0.001*). Genotypes HOR2571 and HOR5584 had high HI under CD, while other genotypes such as HOR2130 showed low HI after treatment.

KW/spike decreased significantly (*P<0.001*) under CD treatment. No significant differences were detected between 2016 and 2017 (Table S8). KW/spike showed high variability ranging from 0.69 g (HOR2858) to 2.3 g (HOR5584) under C treatment and from 0.75 g (HOR2858) to 1.6 g (HOR6489) under CD (Fig. 23b). *G* × *T* interaction was significant (*P<0.001*) (Table S8). Most of the genotypes were affected by CD such as HOR2555, HOR786 and HOR2754, while few genotypes were more tolerant such as HOR2838, HOR6974 and HOR2490, showing a high KW/spike under CD.

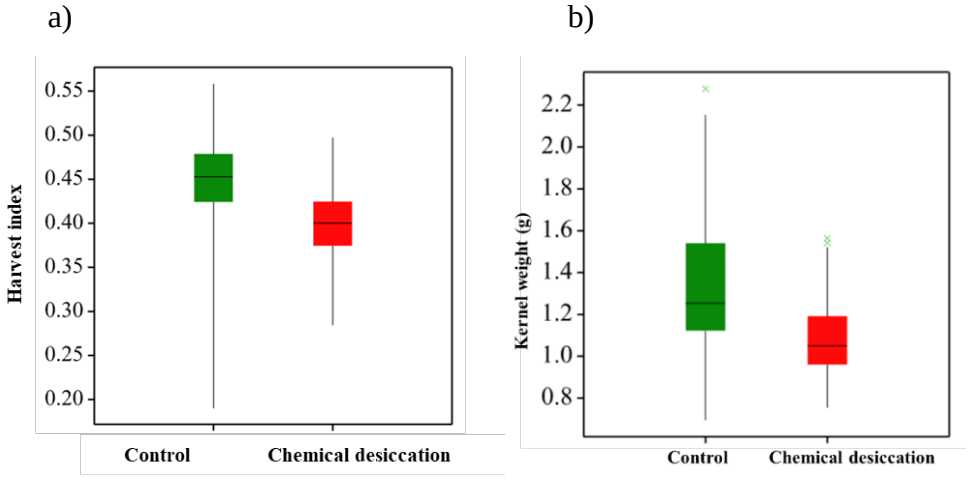

Figure 23. Box plots showing differences in a) harvest index and b) kernel weight/spike under control and chemical desiccation treatments.

KN/spike was affected significantly (*P<0.001*) by CD treatment. Significant differences (*P<0.001*) between both growing seasons were shown (Table S8). In 2016, the reduction under CD reached 3.9 % while in 2017 the effect of the treatment was low (0.24 %). High variability in KN/spike ranged from 13.4 g (HOR2858) to 49.5 g (HOR2215) under C and from 17.5 g (HOR2858) to 39.9 g (HOR5664) under CD (Fig. 24a). The *G* × *T* interaction was not significant (Table S8).

TKW decreased significantly (*P<0.001*) due to CD treatment compared to the control (C) and a significant difference (*P<0.001*) between both growing seasons was obtained (Table S8). In 2016, the reduction in TKW due to CD reached 14.5 % while in 2017 the effect of the treatment was higher (18.5 %). TKW showed high variability ranging from 33.9 g (HOR2177) to 58.1 g (HOR2226) under C, but from 24.6 g (HOR255) to 51.7 g (HOR5879) under CD (Fig. 24b). Significant *G* × *T* interaction (*P<0.001*) was found (Table S8). Few genotypes such as HOR6382 showed better performance under CD.

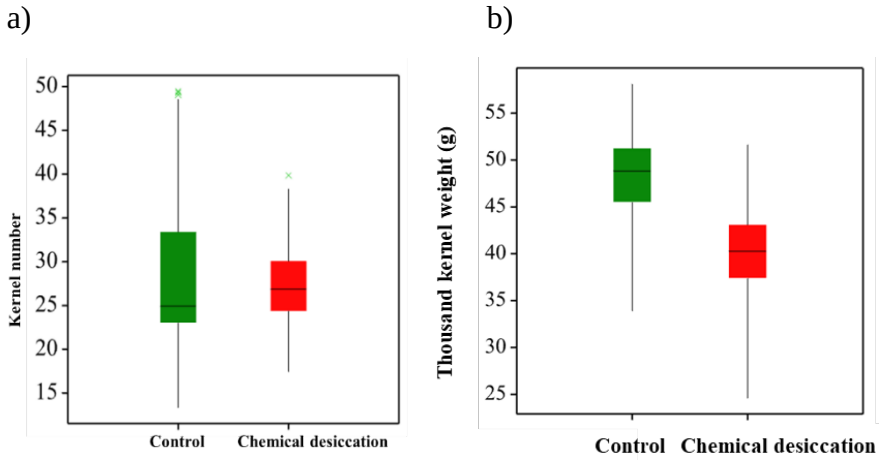

Figure 24. Box plots showing differences in a) kernel number/spike and b) thousand kernel weight under control and chemical desiccation treatments.

Results for TG % and NS % showed significant differences between treatments (*P<0.001*) (Table S8). TG % ranged from 77 % (HOR6674) to 100 % for 16 genotypes such as HOR6560 under C. Under CD the difference ranged from 69 % (HOR6735) to 100 % for five genotypes such as HOR4707 (Fig. 25a). Generally, CD affected significantly (*P<0.001*) TG % causing a reduction of 1.5 %. No significant differences were found between both growing seasons and *G* × *T* interaction (Table S8). Genotypes such as HOR6735 and HOR2555 were affected by CD, while other genotypes showed stable TG % under both treatments such as HOR4705 and HOR2496. A few genotypes performed well under CD for instance, HOR2401 and HOR5970.

NS % showed a high variability ranging from 71 % (HOR6674) to 100 % (HOR2138) under C and between 60 % (HOR6735) and 96 % (HOR2094) under CD treatment (Fig. 25b). CD affected significantly (*P<0.001*) NS % but no significant differences between both growing seasons and *G* × *T* interaction were shown (Table S8). Most genotypes were affected by the treatment, such as HOR6735 and HOR255. Few genotypes performed well under CD, e.g. HOR2149 and HOR2185. Other genotypes showed high NS % under CD compared to C such as HOR2905 and HOR2164.

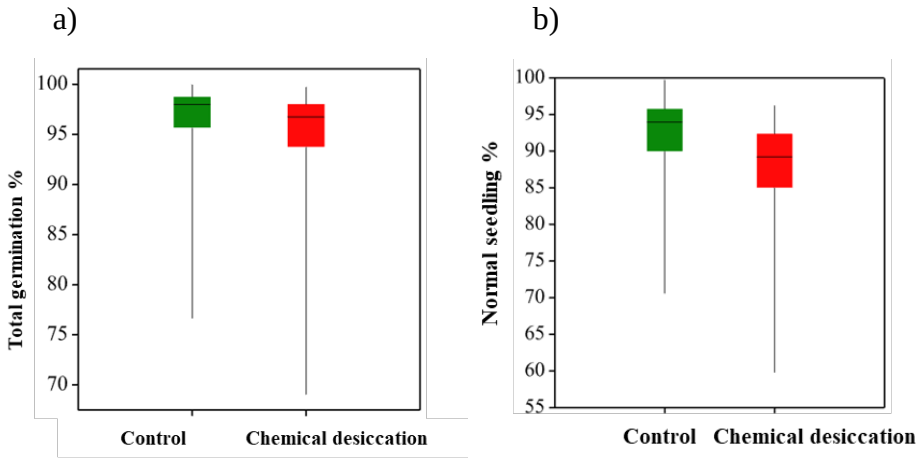

Figure 25. Box plots showing differences in a) total germination % (TG %) and b) normal seedling % (NS %) under control (C) and chemical desiccation (CD).

Genotypes performance under CD was evaluated by DSI and Injury % based on TKW. DSI showed high variability ranging from 2.2 to -0.05. Low DSI values (DSI<1) were detected for several genotypes like HOR6974 and HOR257. High DSI values (DSI>1) were observed in other genotypes, for instance HOR2555 and HOR2130 indicating poor tolerance to CD. In general, genotypes did not show a specific cluster regarding to DSI. No significant difference between both growing seasons was found (Table S8).

Injury % due to CD ranged between -0.8 % (HOR2571) to 32.9 % (HOR2555). A significant difference (*P<0.001*) between both growing seasons was observed (Table S8). Few number of genotypes were not affected by CD such as HOR6974 and HOR2571.

3.4.2 Correlation between 2016 and 2017 growing seasons

Significant correlation between the growing seasons 2016 and 2017 for the traits under C and CD treatments are shown in figure 26. Correlation coefficients (r) ranged from 0.34 for HI to 0.90 for KN/spike under C, while under CD. r ranged from 0.08 for DSI and injury % to 0.57 for TG %. High correlation coefficients indicated that the measured triats were relatively stable in both growig seasons.

a)

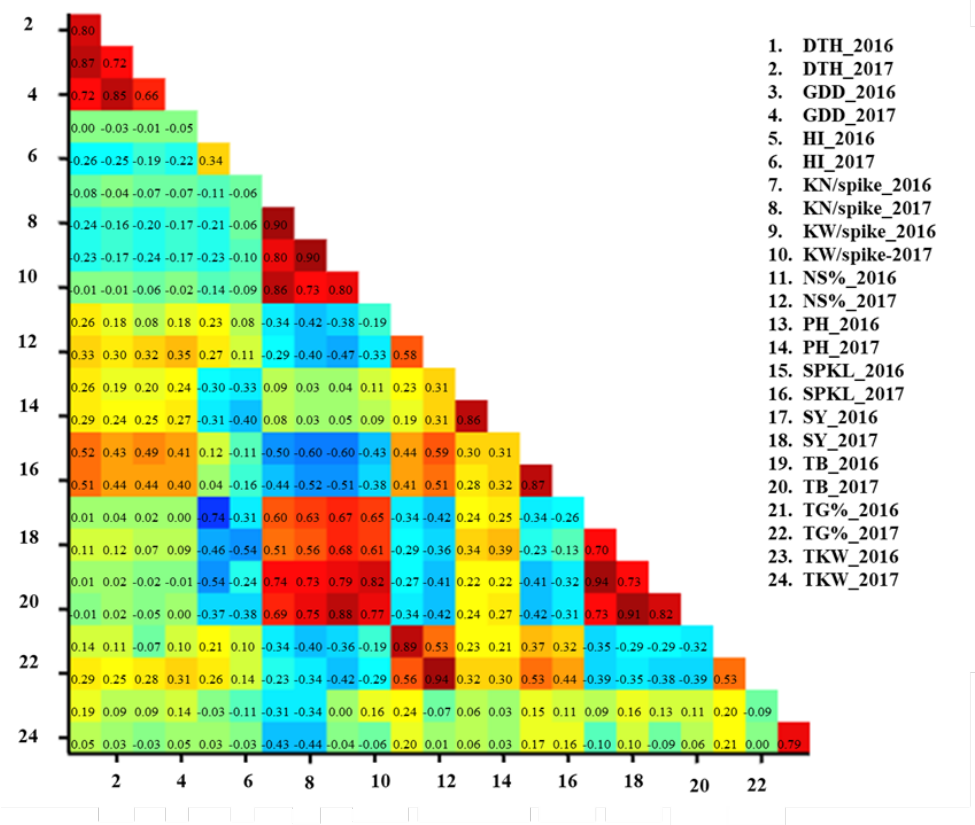

b)

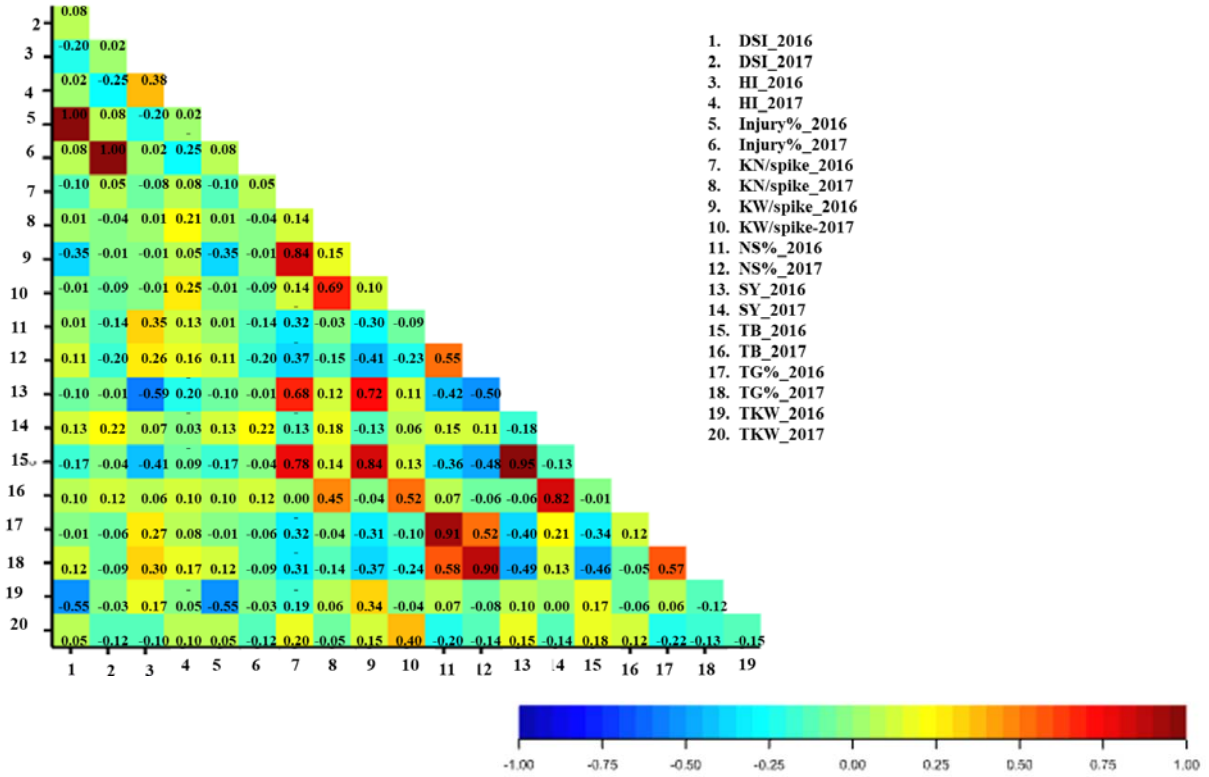

Figure 26. Correlation coefficients between the growing seasons 2016 and 2017 under a) control and b) chemical desiccation treatments.

3.4.3 Broad sense heritability under control and chemical desiccation treatments

The broad sense heritability values of the measured traits under C and CD are shown in figure 27. Most of the traits had high heritabilities of ≥0.6 but up to 0.93.

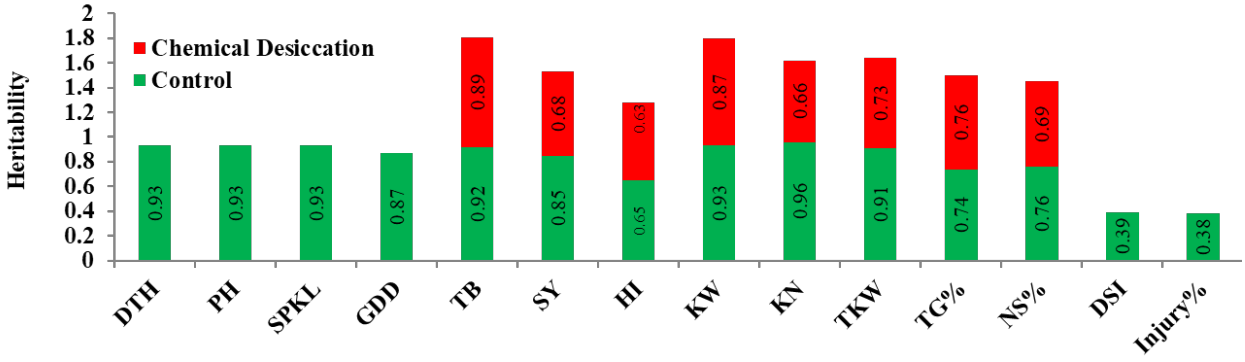

Figure 27. Broad sense heritability (H^2) values of the studied traits. H^2 was calculated under control and chemical desiccation treatments.

3.4.4 GWAS analysis

Genome wide association analysis was performed under C and CD treatments. The analysis was made for the two growing seasons 2016 and 2017 separately. The results are shown in figures S15 and S16, respectively. Analysis of the BLUEs are shown in Manhattan plots in figures S17 under C treatment and S18 under CD and described in details below.

GWAS analysis of BLUEs revealed 412 MTAs, distributed over the seven chromosomes, where chromosome 2H held the highest number of MTAs (116). The detected MTAs were associated with TB, KW/spike, KN/spike TKW, TG % and NS % under C and CD treatments but with HI under CD and. DTH, SPKL, GDD and PH under C treatments only. KN/spike under C revealed the highest number of MTAs (114). All significant associations are shown in figure 28 and table S9.

On chromosome 1H, 54 MTAs related to 34 SNP were revealed. One MTA was located at 42.1 cM associated negatively with PH under C treatment. Within the genomic region 46.5-50.8 cM, 14 MTAs were identified related to eight SNPs associated with KN/spike under C and CD and KW/spike under C positively as well as TG %, SPKL under C and NS % under CD negatively. Nine MTAs were detected at interval 54.4-55.9 cM carrying seven SNPs related to KN/spike under C with positive effect and TG % under C and CD with negative effect. At 62.3 cM, four MTAs were identified, carrying one SNP associated positively with KN/spike under both treatments and negatively with NS % and TG % under CD. Within the interval 66.2-67.1 cM 10 MTAs were detected carrying four SNPs associated negatively with TG % under C and CD, NS% under CD and positively with KN/spike under C treatment. Two MTAs were identified within the interval 81.7-82.5 cM carrying two SNPs associated negatively with TG % under C treatment. One MTA was located at 86.5 cM associated negatively with TG % under C. Within the interval 92.2-97.9 cM, nine MTAs were identified by seven SNPs associated positively with KN/spike and negatively with NS % under C and CD as well as TG % under C treatment. At 122.2 cM, two MTAs by one negative effect SNP were identified related to TG % and NS % under C. Two MTAs associated with two SNPs were located within the interval 128.2-132.5 cM and positively associated with KN/spike under C treatment. SNP 11_10686 located at 67.14 cM with $-\log_{10}(p)=11.1$ was the most significant marker associated negatively (-2.8) with TG % under CD.

In total 116 MTAs related to 77 SNPs were identified on chromosome 2H, where 85 and 31 MTAs were detected under C and CD, respectively. Within the genomic interval 18.9-19.9 cM 10 MTAs were identified associated with TB, DTH, KN/ spike, KW/spike and TKW under C, carrying seven positive effect SNPs. Thirty MTAs were identified within the interval 56.2-59.6 cM related to 20 SNPs negatively associated with TG % under C and CD, NS %, DTH, GDD and SPKL under C treatment but with positive effect on TKW and KN/spike under C. At 67.4-67.9 cM five MTAs were identified associated with four SNPs, one with negative effect on NS % under CD and three with positive effect on KN/spike and KW/spike under C treatment. Within the genomic interval 73.7-76.6 cM 28 MTAs were identified

associated with KN/spike and TB under both treatments, TKW and KW/spike under C and TG %, NS % under CD. The interval consists of 12 SNPs with negative effect on TKW, TG % and NS % but a positive effect on the other traits. Eleven MTAs were identified within the genomic interval 79.4-80.2 cM carrying eight SNPs associated positively with KN/spike under C and CD and KW/spike under C. Within the genomic interval 91-94.7 cM, eight MTAs were identified carrying six SNPs affected positively KN/spike under C and CD treatments. One MTA was located at 98.7 cM associated positively with KN/spike under C treatment. Within the interval 108-111.3 cM three MTAs were detected carrying three positive effect SNPs associated with KN/spike under C treatment. At 119.8-120.7 cM interval five MTAs were identified under C treatment, related to five SNPs positively associated with KN/spike but negatively with TG % and NS %. Seven MTAs carrying seven SNPs under C treatment were detected within the interval 130.3-133.3 cM. Six were positively associated with KN/spike but one negatively with TKW. Within the interval 135-136.4 cM two MTAs carrying two SNPs were detected, associated negatively with TG % and positively with KN/spike under C treatment. Seven MTAs were located within the genomic region 147.3-148.2 cM carrying three SNPs, where one SNP affected TG % under C and NS % under both treatments negatively. The other two SNPs affected TG % and NS % under CD and KN/spike under C. The highest significant SNP among all MTAs was SCRI_RS_2961 located at 74.4 cM with $-\log_{10}(p)=17.7$ and a positive effect (+8.5) on KN/spike under C treatment.

On chromosome 3H, 53 MTAs related to 27 SNPs were identified. At 3.3 cM two MTAs related to one SNP were detected to be negatively associated with TB and KN/spike under C treatment. Within the genomic region 50.7-51.8 cM, seven MTAs were detected carrying four SNPs. Three were negatively associated with TG % under C and CD as well as NS % under C and TKW under CD. One SNP was positively associated with HI under CD and KN/spike under C. One MTA was located at 62.3 cM associated positively with KN/spike under CD. At 75.2 cM, three MTAs related to one SNP were located, negatively associated with NS % and TG % under CD but positively with KN/spike under C treatment. Eleven MTAs carrying four SNPs were identified within the interval 86.2-88.2 cM and associated negatively with NS %, TG % and KW/spike under C and CD as well as TKW under C treatments. Within the genomic region 90-90.7 cM 19 MTAs related to nine negative effect SNPs were detected, associated with TG % and NS % under both treatments. One MTA was located at 123.2 cM associated positively with KN/spike under C treatment. At 132.7 cM two MTAs were identified related to one SNP associated negatively with TG % and NS % under C treatment. Four MTAs were identified within the interval 142.6-143.9 cM related to four SNPs of which three affected KW/spike under C and CD negatively and one showed a positive effect on the same trait under CD. At 154.2 cM three MTAs were identified related to one SNP positively associated with TB under C and KW/spike under C and CD treatments. The highest significant SNP was SCRI_RS_3125 located at 90.2 cM with $-\log_{10}(p)=19.9$ and negatively (-3.3) associated with TG % under CD treatment.

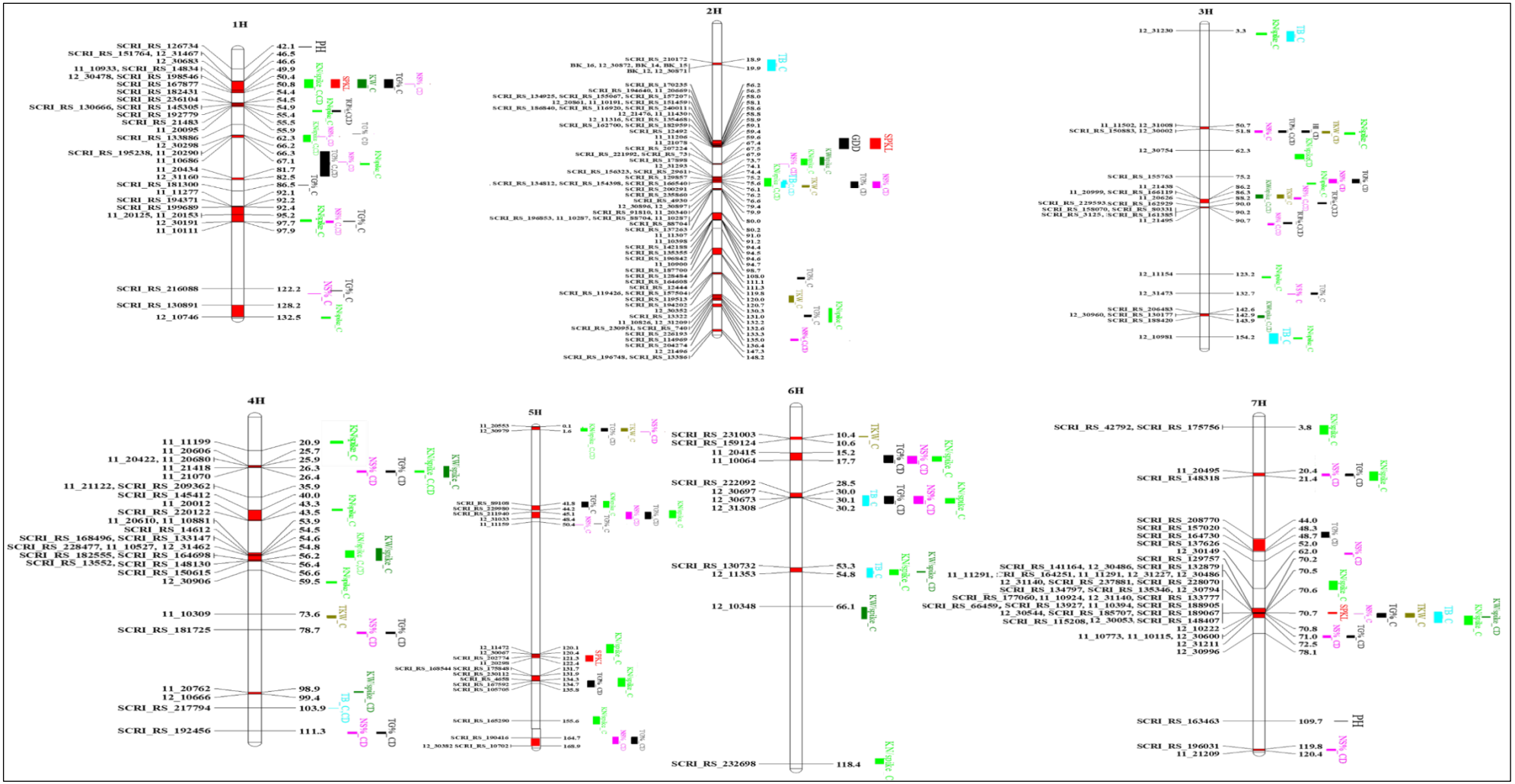

Figure 28. Genetically anchored position of highly associated MTAs distributed on the seven chromosomes and identified under field condition for BLUEs under control (C) and chemical desiccation (CD) of each genotype. Red chromosomal interval indicates MTAs (within confidence interval of ±3 cM). Each trait was given different color.

On chromosome 4H, 47 MTAs related to 31 SNPs were revealed. At 20.9 cM, one MTA was identified, positively associated with KN/spike under C. Sixteen MTAs were identified within the region 25.7-26.4 cM related to five SNPs associated negatively with TG % and NS % under CD but positively with KN/spike under C and CD as well as KW/spike under C treatments. Two MTAs were identified at 35.9 cM related to two SNPs negatively associated with KN/spike under C treatment. Within the genomic region 40.0-43.5 cM three MTAs related to three SNPs were identified associated positively with KN/spike under C. Fifteen MTAs were identified within the genomic region 53.9-56.6 cM carrying 13 SNPs associated positively with KN/spike under C and CD treatments and KW/spike under C treatment. One MTA was located at 59.5 cM negatively associated with KN/spike under C. At 73.6 cM, one MTA was identified associated positively with TKW under C treatment. Two MTAs related to one SNP were detected at 78.7 cM. They were negatively associated with TG % and NS % under CD treatment. Within the genomic interval 98.9-99.4 cM, two MTAs related to two SNPs were detected to be positively associated with KW/spike under CD. At 103.9 cM, two MTAs were identified, related to one SNP and positively associated with TB under both treatments. Two MTAs were detected at 111.3 cM related to one SNP showing a negative effect on NS % and TG % under CD treatment. The most significant SNP was 11_20606 located at 25.7 cM with $-\log_{10}(p)=12.9$ affecting KN/spike positively (+7.5) under C treatment.

Thirty-three significant MTAs related to 23 SNPs were identified on chromosome 5H. Within the genomic region 0.1-1.6 cM, seven MTAs related to three SNPs were detected associated positively with KN/spike under C and CD but negatively with TG % and NS% under CD but TKW under C treatments. Two MTAs were detected within the interval 41.8-44.2 cM related to two SNPs negatively associated with TG % but positively with KN/spike under C treatment. Within the genomic interval 45.1-48.4 cM, three MTAs were identified carrying three SNPs of which three SNPs were negatively associated with TG % and NS % under CD but one had a positive effect on KW/spike under C treatment. Two MTAs related to one SNP were detected at 50.4 cM. They were negatively associated with NS % and TG % under C treatment. Within the genomic region 120.1-122.4 cM four MTAs related to four SNPs were detected, associated negatively with SPKL but positively with KN/spike under C treatment. Seven MTAs related to seven SNPs were identified within the genomic region 131.7-135.8 cM. They were negatively associated with TG % under CD and positively with KN/spike under C treatment. One MTA was located at 155.6 cM associated positively with KN/spike under C treatment. Within the genomic region 164.7-168.9 cM, seven MTAs related to three positive and three negative effect SNPs were identified. They were associated with TG % and NS % under both treatments. The highest significant SNP was 11_20553 located at 0.1 cM with $-\log_{10}(p)= 6.0$ and showing an increment effect (+4.2) on KN/spike under C treatment.

The lowest number of MTAs (20) were identified on chromosome 6H. At the 10.4-10.6 cM interval, two MTAs were located, related to two negative effect SNPs associated with TKW under C treatment. Within the interval 15.2-17.7 cM, three MTAs were detected related to two SNPs. One with negative effect on TG % and NS % under CD and one showing a positive effect on KN/spike under C. Six MTAs were detected within the interval 28.5-30.2

cM related to four SNPs associated negatively with TG % and NS % under CD but positively with KN/spike and TB under C. Within the genomic interval 53.3-54.8 cM seven MTAs were detected, related to two SNPs positively associated with KN/spike and TB under C but negatively with KW/spike under C and CD treatments. One MTA was located at 66.1 cM associated positively with KW/spike under C treatment. Finally, one MTA was located at 118.4 cM positively associated with KN/spike under C treatment. Within all identified MTAs on chromosome 6H, SNP 11_10064 was the most significant SNP located at 17.7 cM with $-\log_{10}(p)=7.1$ affecting KN/spike (+4.5) positively under C treatment.

On chromosome 7H, 89 MTAs were identified. Two MTAs were located at 3.8 cM related to two SNPs and positively associated with KN/spike under C treatment. Within the interval 20.4-21.4 cM, four MTAs related to two SNPs were identified. They were negatively associated with TG % and NS % under CD and positively with KN/spike under C treatment. Three MTAs related to three SNPs were identified within the genomic interval 44.0-48.7 cM and were negatively associated with TG % under CD. One MTA was located at 52.0 cM, associated negatively with NS % under CD. Another MTA was located at 62.0 cM associated positively with KN/spike under C treatment. Within the genomic region 70.2-72.5 cM, high number of MTAs (73) was identified related to 42 SNPs. They had negative effect on SPKL, NS %, TG %. And positive effect on KN/spike, TKW, TB under C as well as KW/spike under both treatments. Two MTAs were located at 78.1 cM carrying one SNP associated with TG % and NS % under CD treatment. Another MTA was located at 109.7 cM having a negative effect on PH under C treatment. Within the genomic region 119.8-120.4 cM, two MTAs related to two SNPs were detected. They were negatively associated with NS % under CD treatment. Among all SNPs, 12_30996 located at 78.1 cM was the highest significant marker with $-\log_{10}(p)=6.8$ and negatively (-3.2) associated with TG % under CD.

In summary, the GWAS analysis revealed 412 MTAs, distributed on the seven chromosomes. The detected MTAs were associated with traits under C (269 MTAs) and under CD (143 MTAs) treatments. Our results elucidated vast phenotypic/genetic variation of the traits under study. TG % appeared with the highest number of MTAs (55), all with negative effects under both treatments. The SNP SCRI_RS_3125 located on chromosome 3H at 90.2 cM had the highest $-\log_{10}(p)=19.9$ and was associated with TG % under CD treatment. Among all the revealed MTAs, 212 and 200 MTAs affected the traits negatively and positively, respectively.

Comparing the results of this post-anthesis drought stress experiment with those of the pre-anthesis drought stress experiment (chapter 3.3.2) a number of common MTAs could be detected (Table 6) mostly for KN/spike, TG % and NS % traits under C and CD as well as DTH and SN under D.

Table 6. Marker trait associations (MTAs) co-located between pre-anthesis and post-anthesis drought stress experiments distributed at the seven chromosomes.

Chromosome	Position	Pre-anthesis drought experiment	Post-anthesis drought experiment
1H	50.8	SN_D	KN/spike_C
1H	55.5	DTH_D	KN/spike_C, TG %_C, CD
1H	62.8	DTH_D	KN/spike_C, CD, TG %, NS %_CD
1H	81.7-82.5	SPKL, SY, DTH_D	TG %_C
2H	18.9	DB (PSP, CP, DP, RP)	TB, KN/spike, DTH, KW/spike_C
2H	58.1-59.1	SPKL, SY_ D	TKW, DTH, KN/spike, SPKL, GDD, NS %_C, TG %_C, CD
2H	67.4-67.9	DTH_D	KN/spike, KW/spike_C, NS %_CD
2H	73.6-76.2	DTH, SN_D	TKW, KW/spike_C, TG %, NS %_CD, TB, KN/spike_C,CD
2H	94.4	DB (PSP, DP)	KN/spike_C,CD
3H	75.2	DTH_D	KN/spike_C, TG %, NS %_CD
3H	88.2	DTH_D	TKW_C, TG %, NS %_CD , KW/spike_C, CD
3H	90-90.7	SN, DTH, SPKL, SY_D	NS %, TG %_C,CD
3H	123.2	UTN_D	KN/spike_C
4H	56.6	SN_D	KN/spike_C
5H	41.8	DTH_D	TG %_C
6H	30.1-30.2	DTH, SN_D	TB, KN/spike_C
7H	70.5-70.7	DTH_D, DB (PSP, DP)	TB, TKW, NS %; TG %_C, KW/spike_C,CD

3.4.5 Identification of candidate genes

Among the aforementioned highly significant associated SNPs identified under CD or detected under both treatments, we were able to identify 10 candidate genes distributed on chromosomes 1H and 2H with five genes for each where the SNPs were located within the gene physical position interval (Table S10).

On chromosome 1H the candidate genes were involved in the genetic variation of different traits under both C and CD. The first candidate gene *HORVU1Hr1G051470.3* was associated with TG % and KN/spike under both treatments by BOPA1_7800_594. The gene annotates an S-adenosyl-L-methionine-dependent methyltransferases superfamily protein. The second candidate *HORVU1Hr1G051660.8*, was associated with TG % and KN/spike under C and CD too through SCRI_RS_198546 which encodes the MADS-box transcription factor 56. The candidate genes *HORVU1Hr1G058500.1* and *HORVU1Hr1G076110.4* were associated with TG % under C and CD through SCRI_RS_21483 and SCRI_RS_199689, respectively. The candidate gene *HORVU1Hr1G058500.1* encodes Histone H2B.1 and the second candidate gene encodes protein kinase superfamily protein. The fifth candidate gene on chromosome 1H was *HORVU1Hr1G067110.1* which was associated with TG % under C and CD and in addition, NS % under CD only through BOPA1_4665_882. It encodes for Ethylene-responsive transcription factor 8.

Chromosome 2H, revealed two candidate genes identified under CD treatment. Both genes were associated with TG % and NS %. The first candidate gene *HORVU2Hr1G041320.2* was associated with TG % under CD alongside SCRI_RS_141874 and encodes 3'(2'),5'-bisphosphate nucleotidase. The second putative gene *HORVU2Hr1G084790.1* has unknown function until now and was associated with NS % under CD treatment by SCRI_RS_59851. The third candidate gene *HORVU2Hr1G013400.32* referred to BK_16 SNP was associated with TKW under both treatments and annotates for the pseudo-response regulator 7. Another candidate gene *HORVU2Hr1G091010.1*, was associated with TG %, NS % and TB under CD and with KN/spike under both treatments by SCRI_RS_2961. This putative gene encodes WD repeat-containing protein 44. Further, the candidate gene *HORVU2Hr1G091030.9* was associated with KN/spike under both treatments through SCRI_RS_166540. It annotates RNA polymerase II C-terminal domain phosphatase-like 1.

3.4.6 SNP-gene based haplotypes

Haplotypes analysis of SNP-gene alleles was applied to show the allelic effect on the associated traits (Fig. 29).

Five candidate genes were identified on chromosome 1H. The first one was associated with SNP BOPA1_7800_594 and located at 69960449 bp within *HORVU1Hr1G051470.3* interval. This SNP was associated with TG % and KN/spike carrying C and G alleles. Genotypes carrying C allele showed significantly *($p<0.001$*) higher TG % and lower KN/spike than the ones carrying G allele. Results showed that most of the genotypes carrying allele C were mainly 2-rowed cultivars originated from Germany. The significant SNP SCRI_RS_198546 located at 383207519 bp was co-localized within the interval of *HORVU1Hr1G051660.8* gene. The allelic variation A and C is highly related to TG % and KN/spike. Genotypes carrying allele A showed significantly (*$p<0.001$*) lower TG % and higher KN/spike. These genotypes were mainly 6-rowed Ethiopian landraces. SNPs SCRI_RS_21483 located at 427145216 bp and SCRI_RS_199689 located at 513210386 bp were associated with TG %. Both SNPs were co-located within the interval of *HORVU1Hr1G058500.1* and *HORVU1Hr1G076110.4* respectively. The first SNP carries A and C alleles. Allele A caused highly significant (*$p<0.0001$*) reduction in TG % compared to C allele. The second SNP carries C and T alleles. Genotypes containing allele C showed significantly (*$p<0.001$*) lower TG % compared to allele T. Most of the genotypes carrying allele A related to both SNPs were 6-rowed Ethiopian landraces. SNP BOPA1_4665_882 was located at 476365129 bp within the vicinity of *HORVU1Hr1G067110.1* and associated with TG % and NS %. The SNP holds A and G alleles, where allele A is responsible for a highly significant (*$p<0.001$*) increase in TG % and NS %. Genotypes carrying this allele were mainly 2-rowed European cultivars.

Chromosome 2H carried several significant SNPs related to different traits showing significant allelic variation. SNP SCRI_RS_141874 was located at 203352775 bp and co-located within the interval of *HORVU2Hr1G041320.2*. This SNP carries A and G alleles where allele A showed highly significant (*$p<0.001$*) increment effect on TG %. Genotypes carrying this allele were mainly 2-rowed cultivars originated from Germany. SNP

SCRI_RS_59851 was identified at 613854115 bp within the interval of *HORVU2Hr1G084790.1*. This SNP was associated with NS % and carries A and G alleles where genotypes with allele A showed a highly significant (*p<0.001*) positive effect on the trait. Genotypes carrying this allele were again mainly 2-rowed German cultivars. SNP BK_16 was located within the gene *HORVU2Hr1G013400.32* at 29124351 bp, co-located within gene interval associated with TKW. BK_16 carries C and G alleles. Allele C had highly significant (*p<0.001*) positive effect on TKW under C, while under CD no significant difference between both alleles was shown. Genotypes holding allele C were mainly 6-rowed landraces originated from Ethiopia and Greece. Another highly significant SNP SCRI_RS_2961 located at 646873475 bp was identified within the interval of *HORVU2Hr1G091010.1*. It carries C and T alleles. Genotypes containing the C allele showed significantly *(p<0.001*) lower KN/spike under both treatments and higher TG %, NS % and TB under CD compared to the genotypes carrying allele T. These genotypes carrying allele C were mainly 2-rowed type from different European countries. Finally, SNP SCRI_RS_1665408 was detected at 646934425 bp within the interval of the candidate gene *HORVU2Hr1G091030.9*. This SNP carries A and G alleles. Genotypes carrying allele A showed significantly (*p<0.0001*) higher KN/spike under both treatments and were mainly 6-rowed type originated from Africa and Europe.

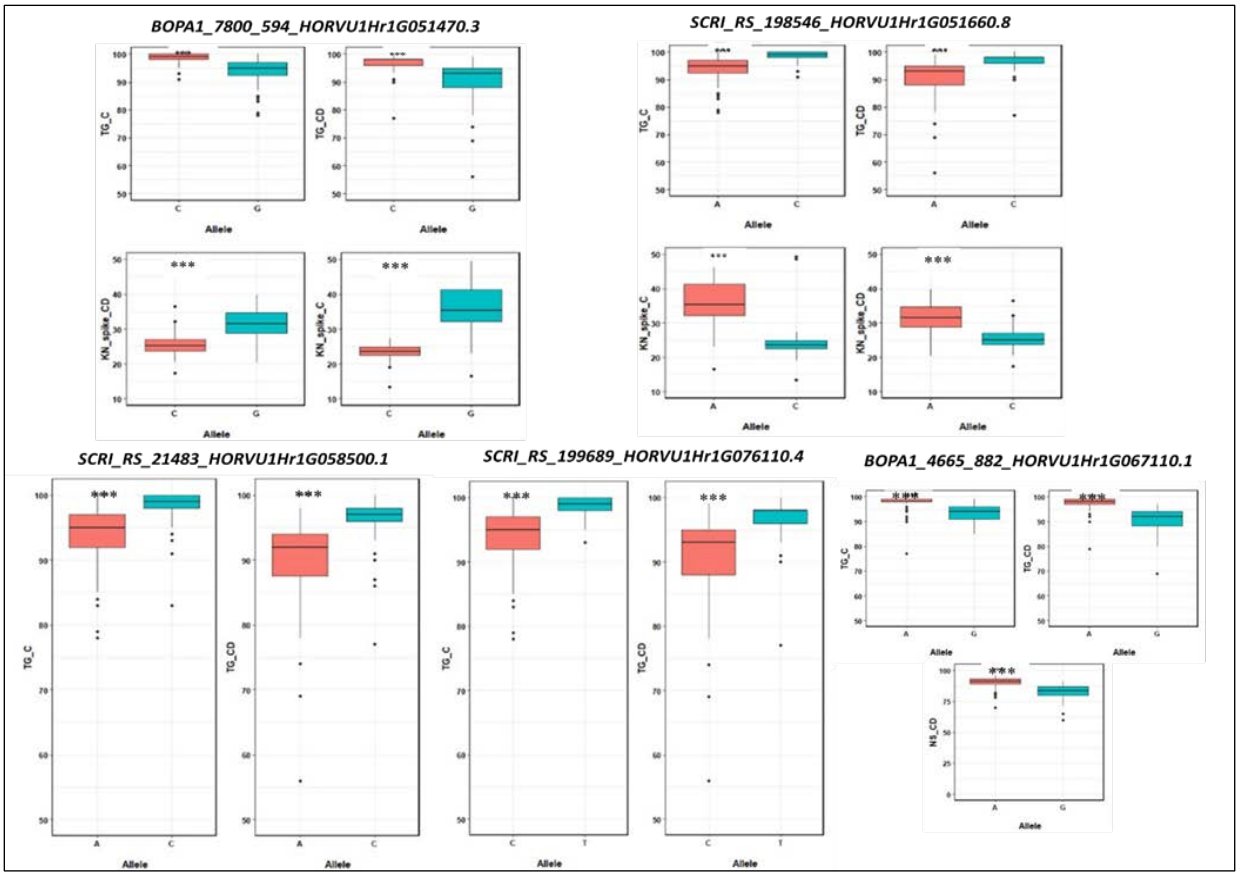

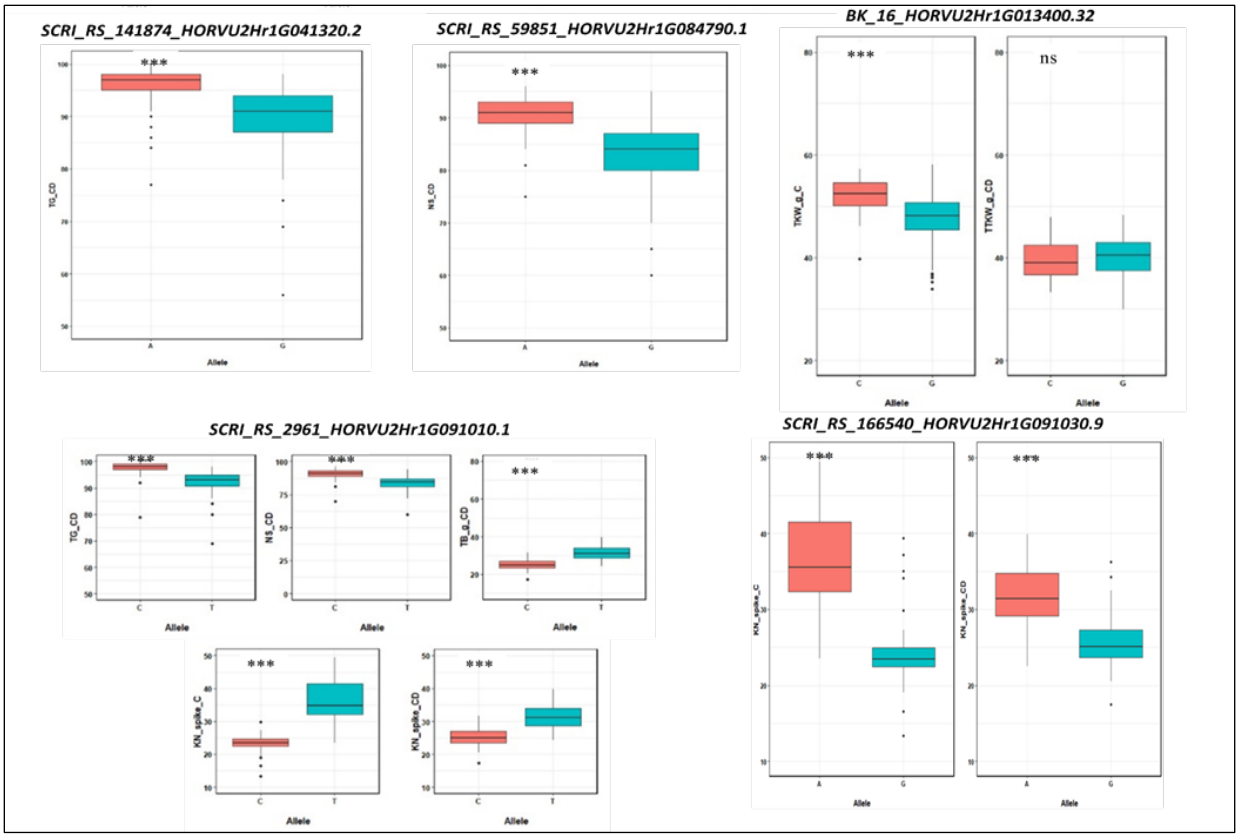

Figure 29. SNP-gene based haplotype for the most significant SNPs located within the candidate gene interval, showing the allelic effect on the associated traits during post-anthesis drought stress. *** p<0.001, ** p<0.01, * p<0.05 and ns: not significant.

4 Discussion

4.1 Pre- and post- anthesis drought stress experiments

Drought is a major constraint limiting barley world production. Drought effect depends on plant developmental stages at which stress occurs, drought intensity as well as the interaction with other stresses such as high temperature and the complex genetic and environment (*G* × *E*) interaction of drought tolerance factors (Gahlaut et al., 2017;Mwadzingeni et al., 2017) limited the usefulness of breeding drought tolerance varieties (Fleury et al., 2010).

In the current study, drought stress was applied at two different phases (Fig. 30): (**I**) Pre-anthesis drought application by withholding water exploiting high throughput phenotyping platform. Using such platform facilitates us to get more insights into biomass development over time and its association with yield related traits after maturity. (**II**) Post-anthesis stress, imposed by chemical desiccation under filed conditions. Both experiments were conducted in order to identify the genetic bases of drought tolerance traits and their potential contribution to improve yield related traits under such conditions.

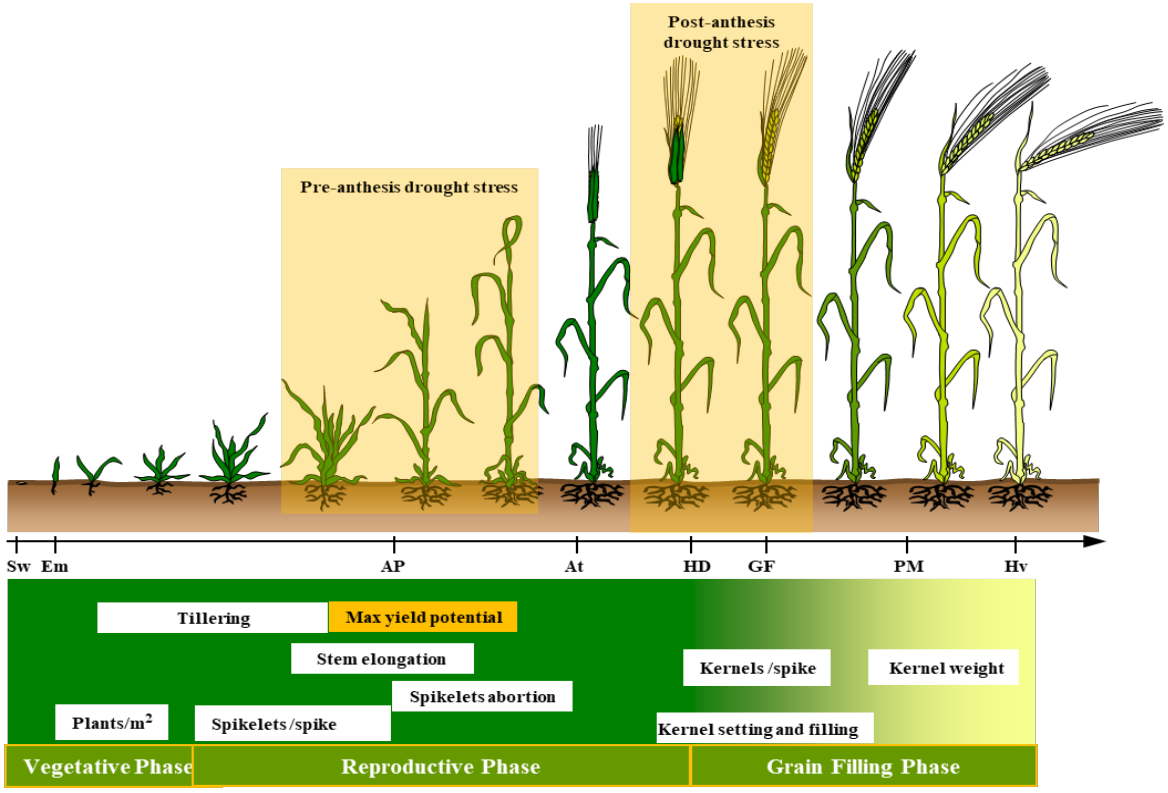

Figure 30. Diagram illustrating the developmental phases and stages of barley at which drought stress was applied and the influence on yield related traits (Sw: sawing, Em: emergence, AP: Awn primordium, At: Awn tipping, HD: Heading, GF: Grain Filling, PM: Physiological maturity, Hv: Harvesting) adapted from (Alqudah and Schnurbusch, 2014).

Pre-anthesis drought stress (during tillering and spikelets development) is considered as a critical phase for tillering, total biomass, spikelets development, maximum yield potential and spikelets abortion and therefore affecting final yield related traits (Alqudah and Schnurbusch, 2014). In the current study drought stress during pre-anthesis phase influenced spikelets development and increased spikelet abortion that led to reduction of KN/plant and KW/plant.

This coincides with the results of (Honsdorf et al., 2017). Water stress is known to affect the source (carbohydrate production) and sink (grain filling) in the plant resulting in competition among plant organs where high number of unproductive tillers (as a result of drought, followed by re-watering after drought stress phase) and unfertile spikes can also attribute to kernel number and weight reduction (Ugarte et al., 2007). In our results, TB was higher under control treatment which is consistent with other results on barley (Wehner et al., 2015;Al-Ajlouni et al., 2016). In wheat biomass decreased under water stress due to the reduction in photosynthesis Senapati et al. (2019). In this connection, a number of studies indicated that photosynthesis-related processes are the most sensitive ones to water deficit of many biological processes activated when plants encounter environmental stresses (Huo et al., 2015). Pre-anthesis drought stress also caused a delay in heading time of the plants, which was in agreement with (Al-Ajlouni et al., 2016), who concluded that delay in heading under pre-anthesis water stress at high temperature in barley reduced seed number and resulted in small grains due to reduced carbohydrate translocation in plants.

Post-anthesis drought (applied at the beginning of grain filling) influenced yield related traits. Imposing drought by 1 % KI successfully simulated post-anthesis drought stress and led to a major reduction in TKW. In addition, it was slightly reducing KN/spike and KW/spike. Similar results were reported in barley (Budakli, 2007) and wheat (Nicolas and Turner, 1993;M. Ezzat Ahmadi, 2009;Tarawneh et al., 2019). The effect of desiccation is to accelerate leaf senescence, forcing the plant to rely on the stored assimilates in the stem to provide the carbon required for grain filling (Blum, 1998;Haley and Quick, 1998). It has been reported that post-anthesis drought reduced plant photosynthetic rate, stomatal conductance and leaf chlorophyll that may lead to a decrease of late formed tillers fertility which contribute to reducing grain number and yield reduction (Sawhney and Singh, 2002;Samarah et al., 2009).

The low rainfall amount in 2016 resulted in an earlier heading compared to 2017. Plants headed earlier as a mechanism to escape drought. Although TKW was not significantly different between the two years, the reduction of KW/spike due to CD was higher in 2016 (21.9 %) compared to 2017 (8.2 %). The low rainfall has probably induced differences in physiological aspects of the plants at the point of the desiccant application and these likely caused the differences in KW between both growing seasons (Nicolas and Turner, 1993). Although the total rainfall amount was lower, PH, SPKL TB and SY were higher in 2016 compared to 2017. This may be due to the distribution of rainfall in the raining season as in April 2017 no rainfall was recorded which maybe the cause of reduction in the mentioned traits. Chemical desiccation affected seed germination and resulted in low NS %, especially in seeds harvested in 2016. The low soil moisture amount in addition to the variation in KW and size (Yamasaki et al., 2017) after applying the desiccant (the seeds became smaller and shrivelled), contributed to an increased in reduction of TG % and NS %. In general, drought stress in combination with high temperature results in a decrease of seed vigour (Samarah and Alqudah, 2011). In summary, both water stress and chemical desiccation treatments significantly influenced plant growth and productivity, mainly by affecting the photosynthetic systems and yield related traits.

The experimental design used in the current study showed high phenotypic variation among genotypes in both experiments as basis for selecting genotypes with minimum yield loss (i.e. KW, KN and DSI values) under drought stress in comparison to control. From this point of view, drought tolerance could be attributed to low susceptibility to stress (less yield reduction) (Shakhatreh et al., 2001). In the current study yield component traits showed significant $G \times T$ interaction indicating that, tested genotypes responded to stress treatments differently. Under pre-anthesis drought genotypes (HOR632) a 6-rowed landrace and (HOR2441), a 2-rowed cultivar showed very good performance under water stress, while under post-anthesis drought HOR6974 and HOR2490, a 2-rowed breeding line and a 2-rowed cultivar, respectively, were the genotypes that had high KW and KN. It was difficult to find genotypes that have lower yield losses or the same ranking pattern in response to stress in both experiments. These results are in line with the results of other studies. Gonzalez et al. (2008) and Szira et al. (2008) concluded that drought tolerance in barley is stage specific, as in one stage genotypes will be highly adapted to drought while in other stages the same genotypes will show poor performance. The study done by Szira et al. (2008) confirmed that drought tolerance in barley is stage specific by finding genotypes (e.g. REC) showing high performance under drought stress in germination stage, while under late drought application the same genotype at the adult stage had low yield (TKW).

High heritability was observed for post-anthesis drought experiment traits. For example, H^2 of KN/spike and KW/spike were 0.66 and 0.87, respectively. Also in the pre-anthesis drought experiment H^2 of DB was ranging between 0.4 to 0.6 and repeatability of maturity traits for each treatment varied between 0.61 to 0.92. This clearly indicates that these traits are genetically controlled, i.e. highly influenced by genetic factors. The results of the current study showed rather high heritability values, giving some hint that experimental design is suited for phenotyping of a diverse collection. In combination with the high number of SNP markers used material is a good source to perform GWAS and to detect MTAs for the traits of interest.

4.2 EcoSeed population

The EcoSeed population is a worldwide panel representing different geographical regions (23 countries), and is composed of 116 two and 68 six-rowed spring barley genotypes. The accessions consist of a broad range of 105 cultivars, 65 landraces and 14 breeding lines. In the pre-anthesis stress experiment, the structure of this population could not explain clearly the phenotypic variation. There was no clear relationship between the spike row type and the geographical origin (Fig. S19). This is in agreement with the finding of Alqudah et al. (2016), who found that row type and the geographical origin did not show clear differences neither with respect to the developmental stages nor to the yield related traits such as plant height under controlled condition.

Under post-anthesis drought stress phenotypic variation maybe explained by population structure (clear separation according to row type) (Fig. S20). Interestingly, yield related traits (TB, SY and KN/spike) were among the group of 6-rowed type genotypes mainly the Ethiopian landraces, while seed quality traits (TG % and NS %) were within the 2-rowed type, at most the German cultivars. These results are in accordance with previous studies

(Samarah et al., 2009;Alqudah and Schnurbusch, 2014) reporting that row-type can explain the variation for some yield related traits under filed conditions. In the present study, under late drought stress. 6-rowed genotypes showed higher TB, SY and KN/spike values in comparison with the 2-rowed genotypes. However, 2-rowed genotypes showed higher TG % and NS % compared to 6-rowed ones. Significant negative correlation (r= -0.4) was found between the mentioned yield related traits and seed quality traits, indicating that increasing yield related traits in the 6-rowed type negatively affected seed quality by reducing seed vigour.

In order to identify MTAs, a sufficient population size is required to get accurate results (Wang et al., 2012a). In this study 183 barely genotypes were used, showing a clear structure which was expected due to the composition of the panel. It was clustered into four majors Q groups. Thereby, MLM model with kinship matrix was used to control for false positives. Kinship is considered as a powerful and efficient model in controlling population structure compared to other models (Kang et al., 2008;Pasam et al., 2012). In addition of using the high resolution Infnium iSelect 9k SNP chip and implementing FDR ($p<0.05$) to handle the false positive associations, it is increasing the analysis robustness and association accuracy. More and more GWAS studies have been done to identify loci associated with different morphological and agronomical traits under control conditions. However, few studies were done under drought stress. In this study, applying GWAS empowered us to dissect the genetic background and efficiently detect novel associations for natural variation of drought tolerance related traits.

4.3 GWAS analysis of pre-anthesis drought stress experiment

4.3.1 Digital biomass

Biomass accumulation as a dynamic trait scored on a daily basis became achievable by analysing non-destructive plant imaging over time under control and drought treatments. It enables the detection of important novel MTAs at different time points.

Unique MTAs for DB under control or drought stress treatments were identified in this study that had not been reported before. On chromosome 1H many MTAs were found at DP. One MTA is located at 17.2 cM and appeared only at DAS37 another MTA is located at 0.21 cM appearing at DAS41-42, closely to the end of the drought stress period. Within the interval 60.8-61.4 cM MTAs were strongly appeared from the beginning of the DP (DAS27) and persisted closely to the end of the stress period (DAS42). These MTAs were close to genomic region (60.0 cM) of flowering time gene *HvCO9/Hv CMF11* that has a role in delay flowering in barley (Kikuchi and Handa, 2009). The digital biomass analysis revealed that many of DB MTAs were overlapped with DTH MTAs under drought in the same experiment. It seems that the delay in heading under drought stress in the examined population can be attributed to the allelic variation around the genes determining the heading date. The presence of GA genes within the interval can also elucidate the biomass accumulation since GA, is involved in growth and developmental processes in plants (Pearce et al., 2013). MTAs located at 117.5 cM associated with DB at PSP were overlapped with MTAs associated with TN under drought showing the importance of this genomic region in yield related traits.

On chromosome 2H we identified novel MTAs located at 8.5 cM and 12.5 cM appearing at PSP, persisting during DP until DAS40 and reducing biomass accumulation. Remarkably, an important genomic region (18.9 cM) consisting of significant associations appeared at PSP, CP, DP and RP. The variation in biomass accumulation in our population may be due to allelic variation of *PpdH1* gene located in this region. It may harbour biomass MTAs detected at all phases and has been reported to be associated with many other traits, e.g. grain number and weight/spike but also heading time (Honsdorf et al., 2017) confirming its importance in barley development and yield under drought stress. MTAs identified at 58.6-59.1 cM were appeared shortly at the beginning of DP and once more at end of RP. This region is bearing three genes, *FRIZZLE PANICLE (FZP)* that influence floral meristem and suppress panicle in rice (Bai et al., 2016) and genes *HvKNOX1* and *HD6-2H* responsible for the formation of supernumerary spikelets in wheat (Dobrovolskaya et al., 2015). These MTAs are also associated with SY and SPKL under D treatment. Further MTAs were detected at 94.4 cM during PSP and DP. The comparable region was reported by Honsdorf et al. (2017) to have an effect on grain number/spike under drought condition. The genomic interval 106.4-108 cM at PSP and DP is harbouring the heading time gene *BFL/HvAPO2* and was associated with DTH under D in our results.

On chromosome 3H MTAs revealed at 52.0 cM at PSP and DP were located very close to the gene *HvFT* genes which enhance floral transition in barley (Kikuchi and Handa, 2009). The allelic diversity at this gene has clearly impact on DB and PH as this region was overlapped with MTAs associated with PH under C and D treatments. At 90.2 cM one MTA is detected that appeared only at the very beginning of DP (DAS28), co-located with *LOW NUMBER OF TILLERS* gene (*HvLNT*) that may play a role in biomass accumulation in addition to DTH, SN, SY and SPKL under D. MTAs located at 143.9-144.1 cM at the late period of DP had been previously detected for SPKL (Varshney et al., 2012). The most significant SNP with $-\log_{10}(p)= 9.4$ was located at 154.2 cM and detected at PSP and DP. In this region we were not able to identify known candidate genes.

On chromosome 4H we could detect 2 MTAs appeared at 39.8 cM and 85.3 cM at DP. MTA at 39.8 cM is co-located with previously reported gene (*HvTID1/HvTUA2)* which have a major role in cell division and elongation in rice (Sunohara et al., 2009). This MTA is overlapped with DTH trait under D treatment. This result shows the crucial role of this gene in biomass accumulation in spring barley genotypes as SNP 12_10860 showed a positive effect on DB. Moreover, the second MTA showed also high positive effect on DB but without known candidate genes.

Only one MTA on chromosome 5H was identified under RP whereas all others were identified at DP. Within the genomic region of 46.5-47.2 cM MTAs are co-localized with 3 different known genes. *Hv CMF13*.that has an impact on flowering time in barley, *ASPARAGINE SYNTHASE1 (HvAS1)* having an effect in amino acid and nitrogen metabolism under different abiotic and biotic stresses and *BRITTLE CULM12/ GIBBERELLIN-DEFICIENT DWARF 1 (HvBC12/GGD1),* that was described in rice (Li et al., 2011) and has a role in cell elongation through GA biosynthesis pathway. SNPs in this region had an increment effect on biomass accumulation, which may indicate that such region carrying the

mentioned known genes improving biomass accumulation under drought stress. No more known candidate genes were identified within the regions of the other MTAs.

On chromosome 6H no known candidate genes were identified within the region of the detected MTAs.

MTAs identified on chromosome 7H at 28.9 and 133.9 cM at DP were not detected before. Other MTAs within the genomic region of 48.0-48.9 cM were detected at PSP and DP and overlapping with the trait TB trait under C treatment show the importance of this region in biomass accumulation. Within the genomic region 70.4-71 cM at PSP and DP the highest number of MTAs (463) related to 40 SNPs are co-located with the the circadian clock-related genes, *HvCO15, (HvWFP1/HvIPA1/HvSPL14* and *HvLHY/ HvCCA1*. At the same genomic region MTAs related to DTH were detected suggesting the potential role of these genes in biomass accumulation associated with heading time.

GWAS analysis showed that MTAs associated with biomass accumulation appeared in a temporal way. MTAs were mainly identified at DP, likewise a high number also appeared under PSP in combination with D. In contrast, only a few MTAs were detected under CP and RP. Some MTAs tended to persist for a short period only, while others appeared over longer periods. Interestingly, the genomic region at 18.9 cM on chromosome 2H was harbouring MTAs appearing at all phases from DAS15-DAS58. Many MTAs were co-located with known genes, notably heading time genes *(HVCO, HV CMF, BFL)* or with MTAs associated with yield related traits.

4.3.2 Traits at maturity

Most of the MTAs were detected under drought stress and distributed over all chromosomes. On chromosome 1H, the genomic region 49.9-62.8 cM was associated with KN/plant and DTH under D treatment and co-located with *GIBBERELLIN INSENSITIVE DWARF1*and *SEMIDWARF 1(HvGID1, HvSD1)* as well as *GIBBERELLIN 20 OXIDASE 2 (HvGA20ox2)* genes. GA, is involved in various growth and developmental processes in plants. It has a role in the development of spikelets and the floral organs during the reproductive phase in wheat (Pearce et al., 2013). In spring barley, Boden et al. (2014) showed the importance of (GA) in enhancing heading and it is highly involved in adaptation and improvement of yield as well as quality traits. In addition, Huang et al. (2015) reported the major role of *HvGA20ox2* in the regulation of bioactive GA levels which are changeable according to the developmental and environmental signs. Presence of GA related genes under drought confirmed its role in drought tolerance. Other MTAs were detected for SPKL, SY DTH and SN under drought treatment at the genomic region 81.7-86.5 cM. This region corresponds with the heading time gene *HvCMF5*. At 82.6 cM, Honsdorf et al. (2017) identified QTL related to heading date under drought matching the association we detected at the same position for the same trait. GWAS analysis revealed novel MTAs within the genomic region (117.5 cM) on chromosome 1H associated with TN. which were not reported before.

On chromosome 2H, MTAs within the genomic region 58.1-59.1 cM were associated with SPKL and SY. Within this region several genes are located. One of them is *HvHOX2,* which has a major role in plant biotic and abiotic stress tolerance mechanism (Chew et al., 2013).

Others are *HEADING DATE6 (HD6-2H)* the barley ortholog of *RICE FLORICAULA/LEAFY (BFL)* and the gene *KNOTTED1-LIKE HOMEOBOX1 (HvKNOX1)* that has a pivotal function in shoot apical meristem development and in different morphological processes through development (Kuijt et al., 2014). On the same chromosome, MTAs located within the genomic region 67.4-67.9 cM associated with DTH and at 73.7-76.2 cM associated with DTH and KN/plant under drought were not previously reported. Highly associated SNPs were identified around *Barley FLORICAULA/LEAFY/ABERRANT PANICLE ORGANIZATION (BFL/HvAPO2*) genes, which show the impact of these genes on heading time in barley. Many novel MTAs were identified at 111.1-111.3 cM, 118.0-120.7 cM and 133.3-135.8 cM for many traits under drought which were not detected earlier.

MTAs within the genomic region 45.8-46.3 cM on chromosome 3H were associated with KW/plant and PH under C. Within the same interval three genes are located. One is *Gigantea-like protein (HvGI)* that has a main role in different physiological processes including drought tolerance, transpiration and flowering time regulation (Mishra and Panigrahi, 2015). In addition it plays a role in plant height and phase transition in maize (Bendix et al., 2013), which is in consistence with the results reported here. Another two, *HvGA3ox2* and *DWARF 18 (HvD189)* are known to affect plant height (Chono et al., 2003). In the same region (Pasam et al., 2012) detected associations related to plant height under control conditions which are in agreement with our findings. Moreover, MTAs were located within the genomic region 49.3-53.3 cM associated with PH under control and drought treatments. This genomic region is harbouring the *(BR) BRASSINOSTEROID INSENSITIVE 1* and *SEMIBRACHYTIC/ Dwarf61 (HvBRI1/ uzu1HvD61)* genes which were detected in the meristem, root, shoot and seedlings hypocotyl (Friedrichsen et al., 2000). This region also contains the gene *FT-like homolog (HvFT2)* which enhance floral transition and responsible for flowering in barley (Kikuchi and Handa, 2009). Our results show the importance of this region in plant height under control and drought treatments. MTAs related to DTH under drought were detected within the genomic region 70.2-75.2 cM which is in accordance with findings of Honsdorf et al. (2017). The genomic region 88.2-90.7 cM is carrying MTAs for different traits e.g. DTH, SPKL, SY and SN co-localized with the gene *LOW NUMBER OF TILLERS-1 (HvLNT-1).* MTAs within the genomic region 122.0-123.2 cM and associated with TN and UTN cannot be related to candidate genes or previous reported associations.

The lowest number of MTAs were detected on chromosome 4H. They are related to SN, SY and SPKL under drought but were not mentioned before in other studies.

On chromosome 5H several MTAs have been revealed at 80.8 cM related to SPKL and SY. In the same region the *DWARF RICE WITH OVEREXPRESSION OF GIBBERELLIN-INDUCED GENE* (*HvDOG*) is located, which is known to be involved in seed dormancy (Nagel et al., 2019). The current findings indicate a potential role of this gene in yield related traits under drought.

At 60.6 cM on chromosome 6H MTAs related to SY and TB were found. In the same region, the *MANY-NODED DWARF 6* (*HvMND6*) gene is present. Mascher et al. (2014) showed that the presence of *mnd* mutant is increasing tiller number but resulted in spikes shortening. An

increased tiller number may affect SY and TB. Further significant associations were observed close to putative heading time genes at 49.22 cM *CCT MOTIF FAMILY3* (*Hv CMF3*) at 59.06 cM, *ARABIDOPSIS PSEUDO-RESPONSE REGULATOR1/ TIMING OF CAB EXPRESSION1* (*HvPRR1/HvTOC1)* and at 67.91 cM *CRYPTOCHROMES1b* (*HvCry1b*) confirming their pivotal role of heading date under drought stress.

On chromosome 7H MTAs related to different traits were detected. MTAs within the genomic region 65.4-68.0 cM were associated with yield related traits in co-location with the three genes *HvCO12*, *HvCO13/HvM* and *HvCO1*. These genes are known to be associated with heading time and other developmental and yield traits in spring barley (Maurer et al., 2016;Neumann et al., 2017). The presence of heading time related genes within this interval explain the variation in DTH and hence yield related traits in the current study. Other important MTAs were identified for DTH under drought stress within the genomic region 70.5-70.82 cM including also many developmental genes e.g. *WEALTHY FARMERS PANICLE1/ IDEAL PLANT ARCHITECTURE1/SQUAMOSA PROMOTER BINDING PROTEIN-LIKE14* (*HvWFP1/HvIPA1/HvSPL14*) and *HvCO15* which play a role in heading time pathway in barley (Cockram et al., 2012), in addition to the circadian clock-related genes *HvLHY/HvCCA1* are known to be located there. The allelic variation at this region is promising for improving adaptation under drought stress conditions. There are other genomic regions on 7H that were not identified previously or co-locate with known candidate genes.

GWAS analysis of pre-anthesis drought stress provided explanations for the genetic architecture of drought stress tolerance in barley. Many MTAs with medium to high effects related to nine different traits were found. High number of associations was detected for DTH and SN under control and drought treatments. In addition, there were numerous known genes which were closely linked to the traits identified in this study.

4.4 GWAS analysis of post-anthesis drought stress experiment

GWAS analysis revealed high number of MTAs on all chromosomes, at each growing season 2016 and 2017 and the BLUEs. Most of these MTAs were relatively stable in both growing seasons and BLUEs indicating consistent associations, hence, they have been considered in further genetic analysis for candidate genes and SNP-gene based haplotypes. Many MTAs have been found to be associated with studied traits under both treatments (C and CD) of which many of them are putatively novel MTAs.

On chromosome 1H, MTAs were mainly detected for KN/spike, TG % and NS% under both treatments. One genomic region at 46.5-50.8 cM showed pleiotropic effect MTAs associated with the mentioned traits and in addition, to SPKL. MTAs located at 54.4-55.9 cM were co-localized with known heading time gene *GIBBERELLIN INSENSITIVE DWARF1 (HvGID1)*. This region has conflicting effect by reducing TG % under both treatments and increasing KN/spike under C. Very recently, Abdel-Ghani et al. (2019) identified QTL located in this region associated with root to shoot ratio. In our study, KN/spike was negatively correlated with TG % under both treatments (Fig. S21), suggesting that *HvGID1* is increasing KN/spike but resulted finally in low percentage of germination as seeds were small and shrivelled especially under CD treatment. MTAs located at 62.3 cM and associated with TG % under

CD were close to a QTL reported by Wang et al. (2012b) also related to seed germination. The gene encodes a late embryogenesis abundant (LEA) protein which is known to be involved in desiccation tolerance of seeds under water stress (Goyal et al., 2005). MTAs within the genomic region 92.1-95.2 cM are associated in our study with TG % under C and KN/spike under C and CD. The region is known to carry the gene *Ppd-H2/HvFT3* (*PHOTOPERIOD RESPONSE LOCUS 2/ FLOWERING TIME LOCUS 3*). The gene promotes flowering under short days and have an important role in barley plant development e.g. enhancing spikelet primordia initiation and early reproductive development of spring barley (Mulki et al., 2018). Another MTA was identified at 132.5 cM, related to KN/spike under C treatment which is in agreement with previous QTL reported for grain number but under drought stress in barley (Varshney et al., 2012).

Chromosome 2H showed highest number of consistent MTAs. MTAs within the genomic region 18.9-19.9 cM are associated with KN/spike, KW/spike, TKW, TB and DTH under C. They are located within the *Ppd-H1* (*PHOTOPERIOD RESPONSE LOCUS1*) gene interval (Comadran et al., 2012). The allelic variation at this gene showed different response to long day conditions that clearly influence development and yield production (Maurer et al., 2015) e.g. late heading genotypes mainly from Europe are carrying less responsive allele (*ppd-H1*), produced higher number of tillers and grains which in turn improve yield (Alqudah et al., 2014). Our findings are also in consistence with Honsdorf et al. (2017) who detected associations in the same region with KN, KW and DTH under terminal drought stress, indicating the potential role of photoperiod response gene in drought tolerance in barley. At 56.2-59.6 cM, MTAs related to KN/spike, TKW, DTH, SPKL, GDD, NS % under C and TG % under C and CD were detected. The region was also described carrying associations to KN/spike and DTH under drought stress (Honsdorf et al., 2017). Also (Thabet et al., 2018) found four SNPs within the similar genomic region associated with germination %. Many associations related to TG % under CD were identified in the same region, suggesting that this region is important for early germination and seedling development for seeds developed under drought stress. The genomic region at 58.0-59.6 cM consists of many SNPs associated with different traits under both treatments. This centromeric region includes also many genes e.g. the flowering time gene, *CENTRORADIALIS* (*HvCEN/eps2S/eam6*), which promotes early heading in spring barley (Alqudah et al., 2014) and affects vernalisation requirement (Comadran et al., 2012). Here MTAs associated with DTH and TKW were found. This region is also harbouring developmental related genes responsible for tillering like *HvGID1* and *KNOTTED1-LIKEHOMEOBOX1* (*HvKNOX1*) which may explain the effects on yield related traits like TKW under C. Another gene located within the same region may be related specifically to TG % and NS % under C and CD. It is the *HOMEODOMAIN LEUCINE ZIPPER BOX* (*HvHOX2*) gene that has a role in plant development and cell differentiation e.g. during embryo development. It also plays a defence mechanism role in plants affected by biotic and abiotic stresses through cuticle formation (Chew et al., 2013). MTAs within the genomic interval 79.4-80.2 cM are close to the major row type gene *SIX-ROWED SPIKE 1* (*Vrs1*) splitting barley into two and six-rowed type (Komatsuda et al., 2007).

On chromosome 3H, MTAs at the genomic region 90-90.7 cM related to TG % and NS % under both treatments were detected. In the same region, (Thabet et al., 2018) identified significant association for germination % under drought stress. At 142.6-143.9 cM MTAs associated with KW/spike under both treatments were detected. Varshney et al. (2012) found in the comparable region QTL for spike length under drought conditions. In our study there was a negative correlation between KW/spike and SPKL which may be can the explanation for the occurrence of the effects on both traits in the same region. The MTAs detected at 154.2 cM were associated with KW/spike under C and CD and TB under C was close to the QTL found also by Varshney et al. (2012) related to biomass under control condition.

On chromosome 4H, MTAs within the genomic region of 25.7-26.4 cM are associated with KN/spike, KW/spike, TG % and NS % under both treatments. They may be related to the genes *INTERMEDIUM-SPIKE C* (*Int-C*) that inhibits lateral growth and has impact on different developmental processes in different organs including spikelets (Ramsay et al., 2011), as well as *CONSTANS 10* (*HvCO10*) which influenced barley leaf area (Alqudah et al., 2018). Within the same region, previous studies detected QTL related to KN/spike (Wehner et al., 2015) and TKW (Pasam et al., 2012;Wang et al., 2012b) demonstrating the importance of this region in barley development and yield boosting. GWAS analysis, revealed many MTAs at 53.9-56.6 cM related to KN/spike under both treatments, which was confirmed by the findings of (Honsdorf et al., 2017), who found at the same interval QTL associated with the same traits but only under drought stress. MTAs located at 103.9 and 111.3 cM associated with TB under C and CD are located within the vicinity of flowering time loci *Hv CMF4* and *RICE DWARF VIRUS MULTIPLICATION 1* (*HvRIM1*). Also, MTAs related to seed quality traits under CD were detected in the same region. Thabet et al. (2018) detected at the same position MTAs underlying germination under drought.

MTAs located at 0.1 cM on chromosome 5H associated with KN/spike under both treatments as well as TKW and TG % under C, were not reported before. In contrast, the genomic region 120.1-122.4 cM related to KN/spike and SPKL under C was reported by Honsdorf et al. (2017), where QTL related to grain number under drought stress was identified. Within the genomic region 164.7-168.9 cM MTAs were identified for TG % and NS % under both treatments. In this region the gene *HvGA20ox1* (*GIBBERELLIN 20 OXIDASE 1*) is located confirming the role of GA in seed germination. Drought stress has a major effect on the activity of phytohormones such as GA by regulating transcriptional networks (Rabbani et al., 2003) and led to decrease seed vigour (Samarah and Alqudah, 2011) which was confirmed in the current results after applying CD.

On chromosome 6H, significant associations were detected at 30.1-30.2 cM associated with TB and KN/spike under C treatment. At 54.8 cM MTAs of the same traits were found in addition to KW/spike. This is in line with the detected QTL for biological yield under drought stress by Honsdorf et al. (2017).

On chromosome 7H one MTA located at 62.0 cM and associated with KN/spike under C was detected close to the gene *Vegetative to Reproductive Transition gene 2* (*HvVRT2*) which is important to speed up floral transition in response to vernalization or long days (Trevaskis et

al., 2007). Other MTAs were identified at 70.5-71 cM associated with KN/spike, KW/spike, TG % under both treatments and TB, TKW and NS % under C. This genomic region contains CO-like family members *HvCO15* and the circadian clock-related genes *HvLHY/HvCCA*. Notably, allelic variation at this region appeared to be important in seed development and yield traits e.g. grain weight (Honsdorf et al., 2017) and percentage of germination under drought (Thabet et al., 2018).

The GWAS analysis revealed high number of MTAs under C and CD treatments associated with nine out of 12 studied traits, mainly for KN/spike, TG % and NS %. Some of these MTAs are in agreement with the findings of other studies. Up to our knowledge, high number of novel MTAs were detected for the first time in our research. Using the high dense SNP 9k chip empowered us to precisely detect drought tolerance MTAs compared with other previous studies e.g. (Varshney et al., 2012). Significant associations were also detected within the vicinity of different known genes mainly, *ppdH, HvFT, CMF* indicating the importance of heading time for yield related traits and adaptation. In addition, GA related genes were identified in our study showing once more the importance of these genes for yield related traits under drought stress in barley.

Applying drought in two experiments imposed by water stress under high throughput phenotyping platform (pre-anthesis) and by chemical desiccation under filed conditions (post-anthesis) provide evidence about the complexity of drought tolerance. This is shown by the low number of common MTAs between both experiments. Common MTAs were mainly associated with KN/spike and TG % and NS % detected under C and CD as well as DTH and SN under D. Despite of the low number of common MTAs, these regions are very important for breeding programs under drought stress, in addition to the high number of MTAs that have been not detected before.

4.5 Candidate genes of pre-anthesis drought stress experiment

4.5.1 Digital biomass

On chromosome 1H, the candidate gene *HORVU1Hr1G064200.1* encodes a RNA-binding KH domain-containing protein, which has a key role in regulating heat stress and thermo-tolerance response (Guan et al., 2013). In *Arabidopsis* a K homology (KH)-domain RNA-binding protein, *HOS5* (High Osmotic Stress Gene Expression 5), was found as a stress gene regulator responsible for stress tolerance (Chen et al., 2013). The candidate gene *HORVU1Hr1G064020.1* annotates GDSL esterase/lipase. This annotation appeared also for the maturity traits on chromosome 3H. The GDSL esterase/lipase has a crucial role in abiotic stress responses and pathogen defenses as well as plant development morphogenesis and secondary metabolism. The AtGELP (Arabidopsis thaliana GDSL-type esterase/lipase protein) showed an impact on germination rate and early seedling growth (Lai et al., 2017a).

One candidate gene *HORVU3Hr1G085290.*1 was identified on chromosome 3H associated with DB under DP annotating ARID/BRIGHT DNA-binding domain a ELM2 domain protein. This gene was also identified for maturity traits associated with SN under D treatment. Our findings may confirm the importance of the allelic variation of this gene in barley development.

Three candidate genes were detected on chromosome 5H associated with DB under DP. Gene *HORVU5Hr1G111120.2* encodes remorin family protein genes which are highly expressed under abiotic stresses as osmotic and drought stresses pressure (Raffaele et al., 2007). *HORVU5Hr1G050160.1* gene annotates asparagine-tRNA ligase, which is known to have an important role in amino acid and nitrogen metabolism in plants and was found to be highly accumulated under different abiotic and biotic stresses (Curtis et al., 2018). It was found to be achieved in different Hordeum species under salt stress (Garthwaite et al., 2005). In addition, gene *HORVU5Hr1G050570.2* was found to be related to cystathionine beta-synthase (CBS) family protein that have a crucial function in plant development and stress tolerance. The transcript levels of some proteins in root and shoot tissues change due to different stresses e.g. drought, salinity and wounding stress in *Arabidopsis thaliana* and *Oryza sativa* as reported by (Kushwaha et al., 2009).

Chromosome 6H hosts the candidate gene *HORVU6Hr1G079150.1* encoding a protein belonging to Adenine nucleotide alpha hydrolases-like superfamily proteins which is a universal stress protein domain (Jung et al., 2015). It was found to have a role in in flooding tolerance and to be involved in leaf senescence in switchgrass (Ayyappan et al., 2017).

Two candidate genes were identified on chromosome 7H. *HORVU7Hr1G107760.1* gene encodes pentatricopeptide repeat containing protein (PPR). This family includes many proteins that have an important role in biotic and abiotic stresses (Xing et al., 2018). In the current study, the PPR also appeared to be associated with the trait SN under drought treatment. So, in addition to its general role under stress it is seems to be involved in plant development.as well. The second candidate gene *HORVU7Hr1G056490.1* encodes basic-leucine zipper (bZIP) transcription family proteins. In legumes, Wang et al. (2015) reported that bZIP appeared at different seed and tissues developmental stages and was highly expressed in leaves and shoots under drought and salt stresses.

4.5.2 Traits at maturity

Six candidate genes were identified on chromosome 1H. *HORVU1Hr1G052890.4* encodes sterol C4-methyl oxidase 1-2, that has a role in plant growth and development, also in NADPH oxidases which are important in stomatal responses and for the regulation of reactive oxygen species and tolerance to drought (Pose et al., 2009). Furthermore, Kumar et al. (2015b) provided evidence about the importance of phytosterol in drought stress. Stigmasterol and β-sitosterol were observed to be increased in rice as seedlings matured. In addition, β-sitosterol was found to increase proportionately with the severity of drought stress in N22 (drought tolerant) rice seedlings. Three candidate genes related to DTH were identified. *HORVU1Hr1G058500.1* encodes Histone H2B.1. Several authors reported specific histone modifications that are altered synchronously in response to environmental stress through particular modification patterns linked with specific transcriptional processes. In particular Histone deacetylase (Sridha and Wu, 2006) and Histone acetyltransferase (Papaefthimiou et al., 2010) were shown to be related to drought stress tolerance. *HORVU1Hr1G064950.1* annotates a signal sensing machinery as Two-component Responses (TCS) regulators. The presence of TCS enables plants to sense different environmental inducements. TCS consists

of three main components: sensory histidine kinase proteins (HKs), histidine phosphotransfer proteins (Hpts) and response regulator proteins (RRs) which are biochemically related to His-to-Asp phosphorelay (Singh et al., 2015a). The role of TCS is to set up signaling, mainly cytokinin signalling, ethylene transduction and osmosensing. For instance, the developmental processes in *Arabidopsis thaliana* and flowering in rice were found to be influenced by TCS mechanism (Grefen and Harter, 2004). The third candidate gene related to DTH is *HORVU1Hr1G072810.4*, encoding the transcription factor ILR3. It is known to regulate iron deficiency response and interact with other transcriptional factors which have a role in response to stresses such as pathogen infection (Samira et al., 2018). The candidate gene *HORVU1Hr1G072490.2*, encodes ATP-dependent zinc metalloprotease FtsH which is involved in a degradation and assembly of several protein complexes in the photosynthetic electron-transport pathways. Protein quality control mechanisms are applied in order to remove any misfolded or photodamaged proteins. FtsH is a major thylakoid membrane protease playing an important role in the biogenesis of thylakoid membranes and quality control in the photosystem II repair cycle. FtsH is also contributing in the degradation and assembly of several protein complexes in the photosynthetic electron-transport pathways (Kato and Sakamoto, 2018). *HORVU1Hr1G074410.4* is encoding a protein of unknown function (DUF668). In eukaryotes, a number of gene families that encode functionally uncharacterized proteins were identified as domains of unknown function (DUF) and evolutionary conservation suggested that many DUFs have important functions (Goodacre et al., 2013).

On chromosome 2H, two putative genes were associated with DTH. *HORVU2Hr1G089970.3* annotates Aquaporin-like superfamily protein. In plants, aquaporins (AQPs) have a role in regulating water flow inside and outside of the cells as it located in plasmalemma and tonoplast membranes of leaf and root cells (Shekoofa and Sinclair, 2018). They are responsible for the hydraulic conductance in roots and leaves by affecting stomatal aperture and gas exchange (McAdam and Brodribb, 2014). The influence of AQPs on hydraulic conductance in plants is particularly important in regulating plant transpiration rate, particularly under soil water-deficit stress and elevated atmospheric vapor pressure deficit (VPD) (Devi and Reddy, 2018). The transmembrane proteins (AQPs) preserve water movement through the plant. Under any abiotic stress as drought these proteins are expressed to keep the plant alive (Kapilan et al., 2018). The second candidate gene *HORVU2Hr1G090010.1* annotates Defensin-2peptides. Defensins are stimulated by different types of biotic and abiotic stresses. First members of plant defensins were separated from barley and wheat grains. They are involved in defense against different fungi as well as drought, salt and cold stresses. Defensins have multiple functions in defense mechanisms but are also involved in growth and development of plants (Stotz et al., 2009). Another candidate gene on chromosome 2H was *HORVU2Hr1G111050.1* annotating a protein kinase superfamily (protein phosphorylation) that is important at early and late stages of the signaling pathways leading to plant defense responses. It is known to implicate a prominent role in many signal transduction pathways in plants especially in defense responses (Stone and Walker, 1995).

The detected candidate genes identified on chromosome 3H are mainly annotated proteins related to abiotic stresses such as drought. Gene *HORVU3Hr1G051000.1* encodes HSP20-like chaperones superfamily protein (Hsps). In general, the expression of Hsps is accumulated in response to heat and other stresses such as cold, salinity and osmotic stress (Swindell et al., 2007). It was reported that Hsp20 has a role in protein refolding under stress which assists plant growth (Zenda et al., 2018). Another candidate gene *HORVU3Hr1G053760.3* encodes the GDSL esterase/lipase. In rice, GDSL was reported to have defense responses under abiotic stress including drought. In addition, they play a role in plant development, morphogenesis and synthesis of secondary metabolites. (Chepyshko et al., 2012). *HORVU3Hr1G085270.8* gene annotates Fructose-1,6-bisphosphatase class 1 (FBA genes). Studies showed that fructose is generated under stresses (Xie et al., 2019). FBA genes are differently expressed according to stress conditions, for instances drought, salt and heat stresses and are involved in glycolysis and gluconeogenesis in the cytoplasm but also in the Calvin cycle pathway in plastids (Lu et al., 2012). The gene *HORVU3Hr1G085290.1* annotates ARID/BRIGHT DNA-binding domain (ELM2 domain protein) playing a role in different biological processes such as cell development and differentiation. It has a major role in forming sperm cells in Arabidopsis (Zheng et al., 2014).

On chromosome 4H gene *HORVU3Hr1G096830.4* annotates Carboxypeptidase Y homolog A which plays a major role in increasing the tolerance to oxidative stress. In fact, some peptidases, such as serine carboxypeptidase in *G. herbaceum* and oligopeptidase in *O. sativa*, were increased in leaves under drought stress (Wang et al., 2016).

On Chromosome 5H the candidate gene *HORVU4Hr1G063980.6* annotates senescence/dehydration associated protein (ERD7) also known as EARLY-RESPONSIVE TO DEHYDRATION 7 and identified as drought-regulated gene in Arabidopsis (Kiyosue et al., 1994). It is also involved in hormone signaling in response to progressive drought stress (Espinoza et al., 2007).

Chromosome 6H is carrying the gene *HORVU4Hr1G081670.1* annotating respiratory burst oxidase homologue D. The plant respiratory burst oxidase homolog (*rboh*) gene family is known to have a major role in plant development, defense reactions and hormone signaling. Additionally, several genes from this family were linked directly to stress tolerance. It was reported that under salt and drought treatments *VvrbohA*, *VvrbohB* and *VvrbohC1* were highly expressed in grape, showing the important role of this gene family (Cheng et al., 2013). The candidate gene *HORVU6Hr1G012040.1* was related to spike number and annotated Pentatricopeptide proteins which have an important role in plants as defense proteins to abiotic stress (Jiang et al., 2015). Pentatricopeptide repeat (PPR) proteins are a large family that has diverse functions in plant development such as organellar RNA metabolism and organ development in Arabidopsis and rice (Xing et al., 2018).

Two candidate genes were identified on chromosome 7H, *HORVU5Hr1G000590.2* associated with DTH annotating ethylene receptor. The plant phytohormone have a major impact in drought tolerance and in responses to other biotic stresses. This hormone mediates the signaling pathway under drought in soybean (Arraes et al., 2015). The candidate gene

HORVU7Hr1G018230.3 encodes for protein of unknown function (DUF630 and DUF632). Interestingly, a recent study reported that another gene, *REL2* encoding DUF630 and DUF632 domains containing protein, regulates leaf rolling and bending (Yang et al., 2016).

4.6 Candidate genes of post-anthesis drought stress experiment

On chromosome 1H the candidate gene *HORVU1Hr1G051470.3* annotates an S-adenosyl-L-methionine-dependent methyltransferases superfamily protein. It is one of the key enzymes in phenylpropanoid flavonoid (Joshi and Chiang, 1998). Another identified candidate gene is *HORVU1Hr1G051660.8*, encoding the MADS-box transcription factor 56 which is related to different developmental processes, mainly influencing the reproductive development as inducement of flowering and inflorescence setting but also in seed and embryo development (Grimplet et al., 2016). The candidate gene *HORVU1Hr1G058500.1* encodes Histone H2B.1 which is known to be a defence response protein in plants (Hu et al., 2014). It was also associated with DTH under pre-anthesis drought stress. This genomic region appeared in both experiments and therefore holds a candidate gene with a major role in response to drought stress. Two more candidate genes were also hosted on chromosome 1H. The gene *HORVU1Hr1G076110.4* encodes a protein kinase superfamily and is involved in cellular regulation and metabolism in addition to the response to different signals such as light, pathogens, hormones, temperature stress and nutrient deprivation (Stone and Walker, 1995). The protein kinase superfamily was also reported in the pre-anthesis drought stress experiment. The second gene *HORVU1Hr1G067110.1* encodes ethylene-responsive transcription factor 8 and appears in response to different stresses including drought (Arraes et al., 2015). Ethylene response genes were also detected under pre-anthesis drought stress in our study confirming the importance of this hormone under drought stress at different developmental stages.

On chromosome 2H the gene *HORVU2Hr1G041320.2* annotating the 3'(2'), 5’-bisphosphate nucleotidase was found. Based on several studies, this protein plays a role in metal detoxification in plants. It was reported that the overexpression of yeast gene (HAL2) encodes a 3'(2') 5’-bisphosphate nucleotidase conferring a reduction in free radical production and in heavy metal toxicity in plants exposed to various oxidative stresses. It was suggested that this protein may play a role in salinity stress as it was reported that the over expression of HAL2 increase salinity tolerance in yeast (Murguia et al., 1995). Another candidate gene on chromosome 2H, *HORVU2Hr1G013400.32*, is annotated for the pseudo-response regulator 7 reported to be a transcriptional repressor in the Arabidopsis Circadian clocks (Nakamichi et al., 2010). Other genes for post-anthesis drought stress include *HORVU2Hr1G091010.*annotating WD repeat-containing protein 44, having a role in regulating plant development. This includes cell division and movement ability in addition to its role in flowering meristem arrangement (van Nocker and Ludwig, 2003). Another candidate gene is *HORVU2Hr1G091030.9* annotating RNA polymerase II C-terminal domain phosphatase-like 1. This protein playing a role in different abiotic stresses where it increases the tolerance (Koiwa et al., 2002). The candidate gene *HORVU2Hr1G084790.1* has unknown function.

In summary, the highly significant SNPs associated with different traits identified under pre- and post-anthesis drought stress experiments which were further studied according to their physical position in the database for putative candidate genes, were involved in various abiotic stresses mainly drought. This is a clear indication that the GWAS approach applied in the current study is convenient for the genetic dissection of different traits in barley. Some of the associated markers like e.g. SCRI_RS_21483 located in chromosome 1H were identified in both experiments under drought and chemical desiccation treatments. This underlines that gene *HORVU1Hr1G058500.1* encoding Histone H2B.1 plays an important role in response to drought stress as already described by Papaefthimiou et al. (2010). Two other important candidate genes *HORVU1Hr1G067110.1* and *HORVU5Hr1G000590.2* encoding ethylene-responsive transcription factor 8 and ethylene receptor 1, respectively, were also identified in both experiments. It is well known, that ethylene has a major role in in response to abiotic stresses generally and to drought stress specifically (Arraes et al., 2015). The results showed that the identified candidate genes having high potential of drought stress tolerance provide a good resource for future breeding programs.

4.7 SNP-gene based haplotypes

The highly significant SNPs within the identified candidate genes were validated by SNP-gene based haplotype analyses, using statistical comparison of alleles at each SNP with the associated traits. The results demonstrated that SNPs within the candidate genes showed significant differences between alleles of each associated trait considered. The genotypes of the panel could be differentiated according to these alleles, showing their impact on the traits and effectiveness in future breeding. For example, the allelic variation (A, G) at SNP SCRI_RS_167877 underlines the gene *HORVU1Hr1G052890.4*, showed the importance of allele A in increasing SN/plant under pre-anthesis drought stress. This allele is mostly present in 2-rowed European cultivars in our panel, suggesting the allele potential in improving grain yield under drought. Another example of SNP gene-based haplotypes on chromosome 2H is SNP SCRI_RS_17898 located within the gene *HORVU2Hr1G089970.3.* It showed significant allelic variation (C, T) in DTH. The genotypes carrying allele C representing mainly the European cultivars, which were early heading under pre-anthesis drought compared to the ones carrying allele T. This indicates importance of this allele in the reduction of the time to heading, helping plants to escape from drought stress.

Interestingly, the SNP SCRI_RS_21483, located within the interval of the gene *HORVU1Hr1G058500.1* was detected under pre-anthesis and post-anthesis drought stress, related to DTH and TG %, respectively. A highly significant difference between alleles A and C was evident by the SNP analysis. The 6-rowed Ethiopian landraces carrying allele A showed early heading and low TG % under drought. The allelic effect showed the importance of this allele in heading to escape from drought but affected seed quality negatively.

Many of the identified SNPs showed pleotropic effects (associated with different traits) for instance, the SNP SCRI_RS_80331 co-located within the candidate gene *HORVU3Hr1G085270.8.* Here allelic variation (C, T) showed the importance of allele C in increasing SPKL and spike number in 6-rowed Ethiopian landraces under pre-anthesis

drought stress. Another SNP SCRI_RS_2961 identified in the interval of *HORVU2Hr1G091010.1* carrying alleles (C, T). Allele C affected positively TG % and NS % but adversely KN/spike and TB. Based on these results, we can confirm that haplotype analysis showed evidence that some genes associated with the studied traits gave a general insight of the variation explained by the SNP.

5 Outlook

The results of the current study demonstrate that pre- and post-anthesis drought stress affected barley development and yield. Understanding the nature of the phenotypic variation is essential for breeding to maximize yield potential. We identified genetic resources (genotypes) showing high drought tolerance at different developmental stages such as the genotypes HOR6382, HOR2441, HOR6974 and HOR2571 to be used in future plant breeding. Identified candidate genes could be considered as potential genes for drought tolerance. The next-generation sequencing technology will enable us to increase map resolution of MTAs underlying candidate genes. Further validation and functional characterization such as RNA expression analysis by quantitative real-time PCR to detect gene expression, gene silencing approaches, like RNA interference (RNAi) are required to elucidate the role of these genes under drought stress in barley. Our results put step forward for future studies in breeding to figure out the possible function of these genes under drought stress.

6 Summary

Drought is one of the most important limiting factors for crop production, affecting food security worldwide. The main objective of the present study was to identify marker trait association (MTAs) and putative candidate genes related to different, morphological, agronomical and seed quality traits under pre- and post-anthesis drought stress by performing genome-wide association study (GWAS) using a diverse panel (EcoSeed) of 184 spring barley accessions.

Pre-anthesis drought stress experiment was done based on high-throughput phenotyping using the automated phenotyping and imaging platform LemnaTec-Scanalyzer 3D in a greenhouse. In a control experiment, plants received a daily watering (90 % FC) for 58 days. Under drought treatment, watering was reduced from day 27 after sowing until day 45 to 10% FC. In both experiments, plants were kept until maturity in a greenhouse. Digital biomass (DB) in each experiment was determined independently for each day from the images report. Different agronomical traits were measured after maturity: plant height (PH), spike length (SPKL), spike number (SN), tiller number (TN), number of unproductive tiller (UNT), total biomass (TB), kernel number per plant (KN/plant), kernel weight per plant (KW/plant), thousand kernel weight (TKW), straw yield (SY) and harvest index (HI).

Post-anthesis drought stress experiment was conducted at IPK experimental fields in two growing seasons, 2016 and 2017, where drought stress was simulated using chemical desiccation by spraying 1% KI ten days after anthesis. Growing degree days (GDD) were calculated for both years together with days to heading (DTH), plant height (PH), spike length (SPKL), total biomass (TB), kernel number per spike (KN/spike), kernel weight per spike (KW/spike), thousand kernel weight (TKW), straw yield (SY), harvest index (HI), drought susceptibility index (DSI), injury%, percentage of total germination (TG %) and percentage of normal seedlings (NS %).

The current study showed the impact of drought on barley growth and development and finally the yield. The response of plants to drought stress is complex. In this study, applying drought stress at different phases (pre- and post-anthesis), under high throughput phenotyping platform and field conditions, respectively, showed high natural variation in the traits studied. GWAS analyses under pre- and post-anthesis drought stress provided explanations for the genetic background of drought stress tolerance in barley revealed high number of MTAs on different chromosomes. Common MTAs were detected under both stress application time points. For instance, MTAs identified on chromosome 3H were associated with SN, DTH, SPKL and SY under pre-anthesis drought stress as well as TG % and NS % under post-anthesis drought were determined. Several trait loci identified in the current study were found to be in highly comparable positions of already known genes/QTL. Using the iSelect 9K chip, the resolution of mapping was highly increased and, therefore, a high number of novel MTAs was found.

Highly significant SNPs associated with measured traits under pre- and post-anthesis drought stress were localized according to their physical position, as stated in the latest barley reference genome sequence, in order to identify potential candidate genes. Many candidate

genes were identified for associated traits, particularly genes involved in defense and drought tolerance. For instance, SCRI_RS_21483 located on chromosome 1H was identified in both experiments under drought and chemical desiccation treatments underling *HORVU1Hr1G058500.1* gene encoding Histone H2B.1 which play an important role in response to drought. Results demonstrated that many identified candidate genes have high potential of stress tolerance and provide a good resource for future, breeding programs.

Haplotype SNP-gene based analysis was applied for highly significant SNPs, co-located within the physical position of the candidate gene. Many of the detected SNPs had pleiotropic effects (associated with different traits), for instance, the SNP SCRI_RS_80331 co-located within the candidate gene *HORVU3Hr1G085270.8.* carrying C and T alleles showed the importance of allele C in increasing SPKL and SN in 6-rowed Ethiopian landraces under pre-anthesis drought stress. Our results confirm that the SNP-gene based haplotypes could be considered as a primary screening manner to validate the SNPs within the candidate genes and to discover favorable alleles. Important genomic regions identified can be further validated using expression analysis in order to be used for breeding and genetic improvement in plants.

7 Zusammenfassung

Trockenheit ist einer der am meisten limitierenden Faktoren in der Pflanzenproduktion und beeinflusst die Nahrungsmittelproduktion weltweit. Hauptaufgabe der vorliegenden Studie war das Auffinden von Marker-Merkmals-Assoziationen (MTAs) und möglichen Kandidatengenen, verantwortlich für verschiedene morphologische, agronomische und Saatgut-Qualitätsmerkmale unter Trockenstress vor und nach der Blüte. Dazu wurde eine genomweite Assoziationsstudie (GWAS) unter Verwendung einer Serie von 184 Sommergerstenakzessionen (ECOSEED) durchgeführt.

Das Trockenstressexperiment vor der Blüte wurde mittels einer Hoch-Durchsatz Phänotypisierung auf der automatischen Phänotypisierungsplattform LemnaTec-Scanalyzer 3D, stationiert in einem Gewächshaus, durchgeführt. In einem Kontrollexperiment wurden die Pflanzen 58 Tage lang täglich bewässert (90 % FC). Bei dem Trockenstressexperiment wurde die Wasserzufuhr vom Tag 27 bis zum Tag 45 auf 10% FC reduziert. In beiden Experimenten wurden die Pflanzen in einem Gewächshaus bis zur Reife weiter kultiviert. Zunächst wurde täglich die digitale Biomasse (DB) bestimmt. Nach der Abreife wurden weitere agronomische Merkmale erfasst: Pflanzenhöhe (PH), Ährenlänge (SPKL), Ährenanzahl (SN), Anzahl Halme (TN), Anzahl nicht produktiver Halme (UNT), Gesamtbiomasse (TB), Kornzahl pro Pflanze (KN/plant), Korngewicht pro Pflanze (KW/plant), Tausendkorngewicht (TKW), Strohertrag (SY) und Ernteindex (HI).

Das Trockenstressexperiment nach der Blüte wurde auf den Versuchsfeldern des IPK in den Vegetationsperioden 2016 und 2017 durchgeführt. Trockenstress wurde simuliert mittels chemischer Desiccation, indem die Pflanzen mit einer 1 %igen KJ Lösung 10 Tage nach der Blüte besprüht wurden. In beiden Versuchsjahren wurden folgende Merkmale erfasst: Wachstumstage (GDD), Tage bis zur Blüte (DTH), Pflanzenhöhe (PH), Ährenlänge (SPKL), Gesamtbiomasse (TB), Kornzahl pro Ähre (KN/spike), Korngewicht pro Ähre (KW/spike), Tausenkorngewicht (TKW), Strohertrag (SY), Ernteindex (HI), Trockenheit-Empfindlichkeits Index (DSI), Prozent gesamte Keimung (TG %) und Prozent normale Sämlinge (NS %).

Die vorliegende Studie hat gezeigt, dass Trockenheit einen deutlichen Effekt auf Wachstum und Entwicklung, und schließlich auf den Ertrag von Gerste hat. Der Reaktion der Pflanzen auf Trockenstress ist komplex. In der vorliegenden Studie wurde der Trockenstress in verschiedenen Wachstumsphasen appliziert (vor und nach der Blüte) auf einer automatischen Phänotypisierungsplattform beziehungsweise unter Freiland Bedingungen. Die Variation der untersuchten Merkmale war hoch.

Die GWAS Analysen für Trockenstress appliziert vor und nach der Blüte führte zur Aufklärung der genetischen Ursachen der Stresstoleranz. Eine große Anzahl von MTAs wurde auf verschiedenen Chromosomen gefunden. Auch wurden gemeinsame MTAs unter beiden Applikationszeiten entdeckt. So wurden beispielsweise auf Chromosom 3H mehrere MTAs für SN, DTH, SPKL und SY nach Stress vor und für TG % und NS % nach der Blüte entdeckt. Verschiedene Loci, die in der vorliegenden Arbeit identifiziert wurden, befinden

sich in vergleichbaren Regionen, in denen bereits Gene oder QTL für die entsprechenden Merkmale bekannt sind. Die Verwendung des iSelect 9K chip für die Genotypisierung führte zu einer verbesserten Auflösung der Kartierung und damit zum Auffinden vieler neuer MTAs.

Hoch signifikante SNPs, gekoppelt zu Merkmalen, die nach Stressapplikation vor und nach der Blüte aufgefunden wurden, konnten unter Verwendung der Gersten Referenzgenomsequenzen physikalisch annotiert werden. Das ermöglichte die Identifikation von potenziellen Kandidatengenen. Es konnte eine Reihe von Kandidatengenen identifiziert werden, insbesondere Gene, die für Abwehrmechanismen oder Trockentoleranz verantwortlich sind. So konnte zum Beispiel SCRI_RS_21483, lokalisiert auf Chromosom 1H und identifiziert nach Stressapplikation vor und nach der Blüte dem Kandidatengen *HORVU1Hr1G058500.1* zugeordnet werden. Dieses Gen kodiert Histon H2B.1, welches eine wichtige Rolle in der Reaktion auf Trockenheit spielt. Die Ergebnisse zeigen, dass viele der identifizierten Kandidatengene ein hohes Potenzial für die Verbesserung der Stresstoleranz haben und damit eine wichtige Ressource für künftige Züchtungsprogramme sind.

Für hoch signifikannte SNPs, lokalisiert innerhalb der physikalischen Position von Kandidatengenen, wurde eine SNP-basierte Haplotypanalyse durchgeführt. Viele dieser SNPs zeigten pleiotrope Effekte (zuständig für verschiedene Merkmale). Zum Beispiel zeigte SCRI_RS_8033 (Allele C und T; Kandidatengen *HORVU3Hr1G085270.8.*) eine Erhöhung für SPKL and SN nach Stress vor der Blüte, durch die Präsenz von Allel C, vorhanden insbesondere in den mehrzeiligen äthiopischen Gersten. Unsere Ergebnisse bestätigen, dass die SNP basierte Haplotypanalyse genutzt werden kann, um SNPs innerhalb von Kandidatengenen zu validieren und vorteilhafte Allele zu identifizieren. Damit können wichtige Regionen innerhalb des Genoms identifiziert und validiert, und somit für Züchtung und genetische Verbesserung von Pflanzen genutzt werden.

8 References

Abdel-Ghani, A.H., Neumann, K., Wabila, C., Sharma, R., Dhanagond, S., Owais, S.J., Börner, A., Graner, A., and Kilian, B. (2014). Diversity of germination and seedling traits in a spring barley (*Hordeum vulgare* L.) collection under drought simulated conditions. *Genet Resour Crop Evol* 62**,** 275-292.

Abdel-Ghani, A.H., Sharma, R., Wabila, C., Dhanagond, S., Owais, S.J., Duwayri, M.A., Al-Dalain, S.A., Klukas, C., Chen, D., Lubberstedt, T., Von Wiren, N., Graner, A., Kilian, B., and Neumann, K. (2019). Genome-wide association mapping in a diverse spring barley collection reveals the presence of QTL hotspots and candidate genes for root and shoot architecture traits at seedling stage. *BMC Plant Biol* 19**,** 216.

Al-Ajlouni, Z.I., Al-Abdallat, A.M., Al-Ghzawi, A.L.A., Ayad, J.Y., Abu Elenein, J.M., Al-Quraan, N.A., and Baenziger, P.S. (2016). Impact of pre-anthesis water deficit on yield and yield components in barley (*Hordeum vulgare* L.) plants grown under controlled conditions. *Agronomy-Basel* 6.

Al-Tamimi, N., Brien, C., Oakey, H., Berger, B., Saade, S., Ho, Y.S., Schmockel, S.M., Tester, M., and Negrao, S. (2016). Salinity tolerance loci revealed in rice using high-throughput non-invasive phenotyping. *Nat Commun* 7**,** 13342.

Alqudah, A.M., Koppolu, R., Wolde, G.M., Graner, A., and Schnurbusch, T. (2016). The genetic achitecture of barley plant stature. *Front Genet* 7**,** 117.

Alqudah, A.M., Samarah, N.H., and Mullen, R.E. (2011). Drought Stress Effect on Crop Pollination, Seed Set, Yield and Quality. 193-213.

Alqudah, A.M., and Schnurbusch, T. (2014). Awn primordium to tipping is the most decisive developmental phase for spikelet survival in barley. *Funct Plant Biol* 41**,** 424-436.

Alqudah, A.M., and Schnurbusch, T. (2017). Heading dat is not flowering time in spring Barley. *Front Plant Sci* 8**,** 896.

Alqudah, A.M., Sharma, R., Pasam, R.K., Graner, A., Kilian, B., and Schnurbusch, T. (2014). Genetic dissection of photoperiod response based on GWAS of pre-anthesis phase duration in spring barley. *PLoS One* 9**,** 113-120.

Alqudah, A.M., Youssef, H.M., Graner, A., and Schnurbusch, T. (2018). Natural variation and genetic make-up of leaf blade area in spring barley. *Theor Appl Genet* 131**,** 873-886.

Arraes, F.B., Beneventi, M.A., Lisei De Sa, M.E., Paixao, J.F., Albuquerque, E.V., Marin, S.R., Purgatto, E., Nepomuceno, A.L., and Grossi-De-Sa, M.F. (2015). Implications of ethylene biosynthesis and signaling in soybean drought stress tolerance. *BMC Plant Biol* 15**,** 213.

Ayyappan, V., Saha, M.C., Thimmapuram, J., Sripathi, V.R., Bhide, K.P., Fiedler, E., Hayford, R.K., and Kalavacharla, V.K. (2017). Comparative transcriptome profiling of upland (VS16) and lowland (AP13) ecotypes of switchgrass. *Plant Cell Rep* 36**,** 129-150.

Badr, A., Muller, K., Schafer-Pregl, R., El Rabey, H., Effgen, S., Ibrahim, H.H., Pozzi, C., Rohde, W., and Salamini, F. (2000). On the origin and domestication history of Barley (*Hordeum vulgare*). *Mol Biol Evol* 17**,** 499-510.

Bai, X., Huang, Y., Mao, D., Wen, M., Zhang, L., and Xing, Y. (2016). Regulatory role of FZP in the determination of panicle branching and spikelet formation in rice. *Sci Rep* 6**,** 19022.

Baik, B.K., and Ullrich, S.E. (2008). Barley for food: Characteristics, improvement, and renewed interest. *Journal of Cereal Science* 48**,** 233-242.

Baum, M., Grando, S., Backes, G., Jahoor, A., Sabbagh, A., and Ceccarelli, S. (2003). QTLs for agronomic traits in the Mediterranean environment identified in recombinant inbred lines of the cross 'Arta' x H. spontaneum 41-1. *Theor Appl Genet* 107**,** 1215-1225.

Bayer, M.M., Rapazote-Flores, P., Ganal, M., Hedley, P.E., Macaulay, M., Plieske, J., Ramsay, L., Russell, J., Shaw, P.D., Thomas, W., and Waugh, R. (2017). Development and evaluation of a barley 50k iSelect SNP Array. *Front Plant Sci* 8**,** 1792.

Bendix, C., Mendoza, J.M., Stanley, D.N., Meeley, R., and Harmon, F.G. (2013). The circadian clock-associated gene gigantea1 affects maize developmental transitions. *Plant Cell Environ* 36**,** 1379-1390.

Blattner, F.R. (2009). Progress in phylogenetic analysis and a new infrageneric classification of the barley genus Hordeum (Poaceae: Triticeae). *Breeding Science* 59**,** 471-480.

Blum, A. (1998). Improving wheat grain filling under stress by stem reserve mobilisation (Reprinted from Wheat: Prospects for global improvement. *Euphytica* 100**,** 77-83.

Blum, A. (2011). Drought resistance is it really a complex trait? *Funct Plant Biol* 38**,** 753-757.

Blum, A., Mayer, J., and Golan, G. (1983a). Chemical desiccation of wheat plants as a simulator of post-anthesis stress. *Field Crop Res* 6**,** 149-155.

Blum, A., Poiarkova, H., Golan, G., and Mayer, J. (1983b). Chemical desiccation of wheat plants as a simulator of post-anthesis stress .1. effects on translocation and kernel growth. *Field Crop Res* 6**,** 51-58.

Boden, S.A., Weiss, D., Ross, J.J., Davies, N.W., Trevaskis, B., Chandler, P.M., and Swain, S.M. (2014). Early flowering3 regulates flowering in spring barley by mediating gibberellin production and flowering expression *Plant Cell* 26**,** 1557-1569.

Börner, A., Misheva, S., Nagel, M., A. Rehman Arif, M., Allam, M., Agacka-Mołdoch, M., Doroszewska, T., and Lohwasser, U. (2014). *Plant genetic resources for food and agriculture (PGRFA) maintenance and research*

Börner, A., Schumann, E., Furste, A., Coster, H., Leithold, B., Roder, S., and Weber, E. (2002). Mapping of quantitative trait loci determining agronomic important characters in hexaploid wheat (*Triticum aestivum* L.). *Theor Appl Genet* 105**,** 921-936.

Brachi, B., Faure, N., Horton, M., Flahauw, E., Vazquez, A., Nordborg, M., Bergelson, J., Cuguen, J., and Roux, F. (2010). Linkage and association mapping of Arabidopsis thaliana flowering time in nature. *PLoS Genet* 6**,** e1000940.

Brachi, B., Morris, G., and O Borevitz, J. (2011). *Genome-wide association studies in plants: the missing Heritability is in the feld.*

Breseghello, F., and Sorrells, M.E. (2006). Association mapping of kernel size and milling quality in wheat (*Triticum aestivum* L.) cultivars. *Genetics* 172**,** 1165-1177.

Brisson, N., Gate, P., Gouache, D., Charmet, G., Oury, F.-X., and Huard, F. (2010). Why are wheat yields stagnating in Europe? A comprehensive data analysis for France. *Field Crop Res* 119**,** 201-212.

Budakli, E. (2007). effects of post-anthesis drought stress on the stem-reserve mobilization supporting grain filling of two-rowed barley cultivars at different levels of nitrogen *Journal of Biological Sciences*

Bull, H., Casao, M.C., Zwirek, M., Flavell, A.J., Thomas, W.T.B., Guo, W., Zhang, R., Rapazote-Flores, P., Kyriakidis, S., Russell, J., Druka, A., Mckim, S.M., and Waugh, R. (2017). Barley six-rowed spike3 encodes a putative Jumonji C-type H3K9me2/me3 demethylase that represses lateral spikelet fertility. *Nat Commun* 8**,** 936.

Busemeyer, L., Mentrup, D., Moller, K., Wunder, E., Alheit, K., Hahn, V., Maurer, H.P., Reif, J.C., Wurschum, T., Muller, J., Rahe, F., and Ruckelshausen, A. (2013). BreedVision--a multi-sensor platform for non-destructive field-based phenotyping in plant breeding. *Sensors (Basel)* 13**,** 2830-2847.

Cattivelli, L., Ceccarelli, S., Romagosa, I., and Stanca, M. (2011). "Abiotic Stresses in Barley: Problems and Solutions," in *Barley*. Wiley-Blackwell), 282-306.

Ceccarelli, S., Grando, S., and Impiglia, A. (1998). Choice of selection strategy in breeding barley for stress environments. *Euphytica* 103**,** 307-318.

Chaves, M.M., Maroco, J.P., and Pereira, J.S. (2003). Understanding plant responses to drought - from genes to the whole plant. *Funct Plant Biol* 30**,** 239-264.

Chen, D., Neumann, K., Friedel, S., Kilian, B., Chen, M., Altmann, T., and Klukas, C. (2014). Dissecting the phenotypic components of crop plant growth and drought responses based on high-throughput image analysis. *Plant Cell* 26**,** 4636-4655.

Chen, T., Cui, P., Chen, H., Ali, S., Zhang, S., and Xiong, L. (2013). A KH-domain RNA-binding protein interacts with FIERY2/CTD phosphatase-like 1 and splicing factors and is important for pre-mRNA splicing in *Arabidopsis*. *PLoS Genet* 9**,** e1003875.

Cheng, C., Xu, X., Gao, M., Li, J., Guo, C., Song, J., and Wang, X. (2013). Genome-wide analysis of respiratory burst oxidase homologs in grape (Vitis vinifera L.). *Int J Mol Sci* 14**,** 24169-24186.

Chepyshko, H., Lai, C.P., Huang, L.M., Liu, J.H., and Shaw, J.F. (2012). Multifunctionality and diversity of GDSL esterase/lipase gene family in rice (Oryza sativa L. japonica) genome: new insights from bioinformatics analysis. *BMC Genomics* 13**,** 309.

Chew, W., Hrmova, M., and Lopato, S. (2013). Role of Homeodomain leucine zipper (HD-Zip) IV transcription factors in plant development and plant protection from deleterious environmental factors. *Int J Mol Sci* 14**,** 8122-8147.

Chinnusamy, V., Ohta, M., Kanrar, S., Lee, B.H., Hong, X., Agarwal, M., and Zhu, J.K. (2003). ICE1: a regulator of cold-induced transcriptome and freezing tolerance in *Arabidopsis*. *Genes Dev* 17**,** 1043-1054.

Chono, M., Honda, I., Zeniya, H., Yoneyama, K., Saisho, D., Takeda, K., Takatsuto, S., Hoshino, T., and Watanabe, Y. (2003). A semidwarf phenotype of barley uzu results from a nucleotide substitution in the gene encoding a putative brassinosteroid receptor. *Plant Physiol* 133**,** 1209-1219.

Clarke, J.H., Mithen, R., Brown, J.K., and Dean, C. (1995). QTL analysis of flowering time in *Arabidopsis thaliana*. *Mol Gen Genet* 248**,** 278-286.

Cockram, J., Thiel, T., Steuernagel, B., Stein, N., Taudien, S., Bailey, P.C., and O'sullivan, D.M. (2012). Genome dynamics explain the evolution of flowering time CCT domain gene families in the Poaceae. *PLoS One* 7**,** e45307.

Cockram, J., White, J., Leigh, F.J., Lea, V.J., Chiapparino, E., Laurie, D.A., Mackay, I.J., Powell, W., and O'sullivan, D.M. (2008). Association mapping of partitioning loci in barley. *BMC Genet* 9**,** 16.

Collard, B.C.Y., Jahufer, M.Z.Z., Brouwer, J.B., and Pang, E.C.K. (2005). An introduction to markers, quantitative trait loci (QTL) mapping and marker-assisted selection for crop improvement: The basic concepts. *Euphytica* 142**,** 169-196.

Comadran, J., Kilian, B., Russell, J., Ramsay, L., Stein, N., Ganal, M., Shaw, P., Bayer, M., Thomas, W., Marshall, D., Hedley, P., Tondelli, A., Pecchioni, N., Francia, E., Korzun, V., Walther, A., and Waugh, R. (2012). Natural variation in a homolog of Antirrhinum CENTRORADIALIS contributed to spring growth habit and environmental adaptation in cultivated barley. *Nat Genet* 44**,** 1388-1392.

Curtis, T.Y., Bo, V., Tucker, A., and Halford, N.G. (2018). Construction of a network describing asparagine metabolism in plants and its application to the identification of genes affecting asparagine metabolism in wheat under drought and nutritional stress. *Food Energy Secur* 7**,** e00126.

David, B.L., and Christopher, B.F. (2007). Global scale climate–crop yield relationships and the impacts of recent warming. *Environ Res Lett* 2**,** 014002.

Dawson, I.K., Russell, J., Powell, W., Steffenson, B., Thomas, W.T., and Waugh, R. (2015). Barley a translational model for adaptation to climate change. *New Phytol* 206**,** 913-931.

Devi, M.J., and Reddy, V.R. (2018). Transpiration Response of Cotton to Vapor Pressure Deficit and Its Relationship With Stomatal Traits. *Front Plant Sci* 9**,** 1572.

Diab, A.A., Teulat-Merah, B., This, D., Ozturk, N.Z., Benscher, D., and Sorrells, M.E. (2004). Identification of drought-inducible genes and differentially expressed sequence tags in barley. *Theor Appl Genet* 109**,** 1417-1425.

Dobrovolskaya, O., Pont, C., Sibout, R., Martinek, P., Badaeva, E., Murat, F., Chosson, A., Watanabe, N., Prat, E., Gautier, N., Gautier, V., Poncet, C., Orlov, Y.L., Krasnikov, A.A., Berges, H., Salina, E., Laikova, L., and Salse, J. (2015). Frizzy panicle drives supernumerary spikelets in bread wheat. *Plant Physiol* 167**,** 189-199.

Dodig, D., Kandic, V., Zoric, M., Nikolic-Doric, E., Nikolic, A., Mutavdzic, B., Perovic, D., and Surlan-Momirovic, G. (2018). Comparative kernel growth and yield components of two- and six-row barley (*Hordeum vulgare*) under terminal drought simulated by defoliation. *Crop Pasture Sci* 69**,** 1215-1224.

Dodig, D., Zoric, M., Kobiljski, B., Savic, J., Kandic, V., Quarrie, S., and Barnes, J. (2012). Genetic and association mapping study of wheat agronomic traits under contrasting water regimes. *Int J Mol Sci* 13**,** 6167-6188.

Dogan, R., Kacar, O., Carpici, E.B., and Goksu, E. (2012). Effects of drought stress post-anthesis stageon mobilization of stem-reserves supporting grain filling of some triticale cultivar and lines. *Bulg J Agric Sci* 18**,** 325-329.

Dong, Y., Liu, J., Zhang, Y., Geng, H., Rasheed, A., Xiao, Y., Cao, S., Fu, L., Yan, J., Wen, W., Zhang, Y., Jing, R., Xia, X., and He, Z. (2016). Genome-wide association of stem water soluble carbohydrates inbread wheat. *PLoS One* 11**,** e0164293.

Edae, E.A., Byrne, P.F., Haley, S.D., Lopes, M.S., and Reynolds, M.P. (2014). Genome-wide association mapping of yield and yield components of spring wheat under contrasting moisture regimes. *Theor Appl Genet* 127**,** 791-807.

Edae, E.A., Byrne, P.F., Manmathan, H., Haley, S.D., Moragues, M., Lopes, M.S., and Reynolds, M.P. (2013). Association mapping and nucleotide sequence variation in five drought tolerance candidate genes in spring wheat. *Plant Genome* 6**,** 0.

Ehrenreich, I.M., Hanzawa, Y., Chou, L., Roe, J.L., Kover, P.X., and Purugganan, M.D. (2009). Candidate gene association mapping of *Arabidopsis* flowering time. *Genetics* 183**,** 325-335.

El-Ashry, M.S., and El-Kholy, M.A. (2005). Response of Wheat Cultivars to Chemical Desiccants under Water Stress Conditions. *Journal of Applied Sciences Research*.

Espinoza, C., Medina, C., Somerville, S., and Arce-Johnson, P. (2007). Senescence-associated genes induced during compatible viral interactions with grapevine and *Arabidopsis*. *J Exp Bot* 58**,** 3197-3212.

Estrada-Campuzano, G., Miralles, D., and Slafer, G. (2008). *Genotypic variability and response to water stress of pre- and post-anthesis phases in triticale.*

Fabre, J., Dauzat, M., Negre, V., Wuyts, N., Tireau, A., Gennari, E., Neveu, P., Tisne, S., Massonnet, C., Hummel, I., and Granier, C. (2011). PHENOPSIS DB: an information

system for *Arabidopsis* thaliana phenotypic data in an environmental context. *BMC Plant Biol* 11**,** 77.

Fan, Y., Shabala, S., Ma, Y., Xu, R., and Zhou, M. (2015). Using QTL mapping to investigate the relationships between abiotic stress tolerance (drought and salinity) and agronomic and physiological traits. *BMC Genomics* 16**,** 43.

Fan, Y., Zhou, G., Shabala, S., Chen, Z.H., Cai, S., Li, C., and Zhou, M. (2016). Genome-wide association study reveals a new QTL for salinity tolerance in barley (*Hordeum vulgare* L.). *Front Plant Sci* 7**,** 946.

Fang, Y., Du, Y., Wang, J., Wu, A., Qiao, S., Xu, B., Zhang, S., Siddique, K.H.M., and Chen, Y. (2017). Moderate Drought Stress Affected Root Growth and Grain Yield in Old, Modern and Newly Released Cultivars of Winter Wheat. *Front Plant Sci* 8**,** 672.

Fang, Y., and Xiong, L. (2015). General mechanisms of drought response and their application in drought resistance improvement in plants. *Cell Mol Life Sci* 72**,** 673-689.

Faostat (2016). "Food and agriculture organization of the united nations, satatistical database". (Italy).

Farooq, M., Hussain, M., and Siddique, K.H.M. (2014). Drought stress in wheat during flowering and grain-filling periods. *Crit Rev Plant Sci* 33**,** 331-349.

Farooq, M., Wahid, A., Kobayashi, N., Fujita, D., and Basra, S.M.A. (2009). Plant drought stress: effects mechanisms and management. *Agron Sustain Dev* 29**,** 185-212.

Fischer, R.A., and Maurer, R. (1978). Drought resistance in spring wheat cultivars. I. Grain yield responses. *Australian Journal of Agricultural Research* 29.

Fischer, R.a.T., and Edmeades, G.O. (2010). Breeding and Cereal Yield Progress. *Crop Science* 50**,** S85-S98.

Fleury, D., Jefferies, S., Kuchel, H., and Langridge, P. (2010). Genetic and genomic tools to improve drought tolerance in wheat. *J Exp Bot* 61**,** 3211-3222.

Flint-Garcia, S.A., Thornsberry, J.M., and Buckler, E.S.T. (2003). Structure of linkage disequilibrium in plants. *Annu Rev Plant Biol* 54**,** 357-374.

Flint-Garcia, S.A., Thuillet, A.C., Yu, J., Pressoir, G., Romero, S.M., Mitchell, S.E., Doebley, J., Kresovich, S., Goodman, M.M., and Buckler, E.S. (2005). Maize association population: a high-resolution platform for quantitative trait locus dissection. *Plant J* 44**,** 1054-1064.

Franco-Navarro, J.D., Brumos, J., Rosales, M.A., Cubero-Font, P., Talon, M., and Colmenero-Flores, J.M. (2016). Chloride regulates leaf cell size and water relations in tobacco plants. *J Exp Bot* 67**,** 873-891.

Friedrichsen, D.M., Joazeiro, C.A., Li, J., Hunter, T., and Chory, J. (2000). Brassinosteroid-insensitive-1 is a ubiquitously expressed leucine-rich repeat receptor serine/threonine kinase. *Plant Physiol* 123**,** 1247-1256.

Furbank, R.T., and Tester, M. (2011). Phenomics--technologies to relieve the phenotyping bottleneck. *Trends Plant Sci* 16**,** 635-644.

Gahlaut, V., Jaiswal, V., Tyagi, B.S., Singh, G., Sareen, S., Balyan, H.S., and Gupta, P.K. (2017). QTL mapping for nine drought-responsive agronomic traits in bread wheat under irrigated and rain-fed environments. *PLoS One* 12**,** e0182857.

Garthwaite, A.J., Von Bothmer, R., and Colmer, T.D. (2005). Salt tolerance in wild Hordeum species is associated with restricted entry of Na+ and Cl- into the shoots. *J Exp Bot* 56**,** 2365-2378.

Goddard, M.E., Kemper, K.E., Macleod, I.M., Chamberlain, A.J., and Hayes, B.J. (2016). Genetics of complex traits: prediction of phenotype, identification of causal polymorphisms and genetic architecture. *Proc Biol Sci* 283.

Golzarian, M.R., Frick, R.A., Rajendran, K., Berger, B., Roy, S., Tester, M., and Lun, D.S. (2011). Accurate inference of shoot biomass from high-throughput images of cereal plants. *Plant Methods* 7**,** 2.

Gonzalez, A., Martin, I., and Ayerbe, L. (2008). Yield and osmotic adjustment capacity of barley under terminal water-stress conditions. *Journal of Agronomy and Crop Science* 194**,** 81-91.

Goodacre, N.F., Gerloff, D.L., and Uetz, P. (2013). Protein domains of unknown function are essential in bacteria. *MBio* 5**,** e00744-00713.

Goyal, K., Walton, L.J., and Tunnacliffe, A. (2005). LEA proteins prevent protein aggregation due to water stress. *Biochem J* 388**,** 151-157.

Grefen, C., and Harter, K. (2004). Plant two-component systems: principles, functions, complexity and cross talk. *Planta* 219**,** 733-742.

Grimplet, J., Martinez-Zapater, J.M., and Carmona, M.J. (2016). Structural and functional annotation of the MADS-box transcription factor family in grapevine. *BMC Genomics* 17**,** 80.

Guan, Q., Wen, C., Zeng, H., and Zhu, J. (2013). A KH domain-containing putative RNA-binding protein is critical for heat stress-responsive gene regulation and thermotolerance in *Arabidopsis*. *Mol Plant* 6**,** 386-395.

Gupta, P.K., Balyan, H.S., and Gahlaut, V. (2017). QTL analysis for drought tolerance in wheat: present status and future possibilities. *Agronomy-Basel* 7**,** 5.

Gupta, P.K., Rustgi, S., and Kulwal, P.L. (2005). Linkage disequilibrium and association studies in higher plants: present status and future prospects. *Plant Mol Biol* 57**,** 461-485.

Hairmansis, A., Berger, B., Tester, M., and Roy, S.J. (2014). Image-based phenotyping for non-destructive screening of different salinity tolerance traits in rice. *Rice* 7**,** 16.

Haley, S.D., and Quick, J.S. (1998). Methodology for evaluation of chemical desiccation tolerance in winter wheat. *Cereal Research Communications* 26**,** 73-79.

Harlan, J.R., and De Wet, J.M.J. (1971). Toward a Rational Classification of Cultivated Plants. *Taxon* 20**,** 509-517.

Harris, D.R. (1990). 3. Vavilov's concept of centres of origin of cultivated plants: its genesis and its influence on the study of agricultural origins. *Biological Journal of the Linnean Society* 39**,** 7-16.

Hartmann, A., Czauderna, T., Hoffmann, R., Stein, N., and Schreiber, F. (2011). HTPheno: an image analysis pipeline for high-throughput plant phenotyping. *BMC Bioinformatics* 12**,** 148.

Hemming, M.N., Peacock, W.J., Dennis, E.S., and Trevaskis, B. (2008). Low-temperature and daylength cues are integrated to regulate FLOWERING LOCUS T in barley. *Plant Physiol* 147**,** 355-366.

Heuzé, V., Tran G., Lebas F., Nozière P (2013). "Animal feed resources information system (AFRIS)".).

Honsdorf, N., March, T.J., Hecht, A., Eglinton, J., and Pillen, K. (2014). Evaluation of juvenile drought stress tolerance and genotyping by sequencing with wild barley introgression lines. *Mol Breed* 34**,** 1475-1495.

Honsdorf, N., March, T.J., and Pillen, K. (2017). QTL controlling grain filling under terminal drought stress in a set of wild barley introgression lines. *PLoS One* 12**,** e0185983.

Hu, M., Pei, B.L., Zhang, L.F., and Li, Y.Z. (2014). Histone H2B monoubiquitination is involved in regulating the dynamics of microtubules during the defense response to Verticillium dahliae toxins in *Arabidopsis*. *Plant Physiol* 164**,** 1857-1865.

Huang, Y., Haas, M., Heinen, S., Steffenson, B.J., Smith, K.P., and Muehlbauer, G.J. (2018). QTL mapping of Fusarium head blight and correlated agromorphological traits in an elite barley cultivar Rasmusson. *Front Plant Sci* 9**,** 1260.

Huang, Y., Wang, X., Ge, S., and Rao, G.Y. (2015). Divergence and adaptive evolution of the gibberellin oxidase genes in plants. *BMC Evol Biol* 15**,** 207.

Huo, Y., Wang, M., Wei, Y., and Xia, Z. (2015). Overexpression of the Maize psbA gene enhances drought tolerance through regulating antioxidant system, photosynthetic capability, and stress defense gene expression in tobacco. *Front Plant Sci* 6**,** 1223.

International Barley Genome Sequencing, C., Mayer, K.F., Waugh, R., Brown, J.W., Schulman, A., Langridge, P., Platzer, M., Fincher, G.B., Muehlbauer, G.J., Sato, K., Close, T.J., Wise, R.P., and Stein, N. (2012). A physical, genetic and functional sequence assembly of the barley genome. *Nature* 491**,** 711-716.

Islamovic, E., Obert, D.E., Oliver, R.E., Marshall, J.M., Miclaus, K., Hang, A., Chao, S., Lazo, G.R., Harrison, S.A., Ibrahim, A., Jellen, E.N., Maughan, P.J., Brown, R.H., and Jackson, E.W. (2013). A new genetic linkage map of barley (*Hordeum vulgare* L.) facilitates genetic dissection of height and spike length and angle. *Field Crop Res* 154**,** 91-99.

ISTA (2014). International rules for seed testing. International Seed Testing Association, Bassersdorf.

Jabbari, M., Fakheri, B.A., Aghnoum, R., Mahdi Nezhad, N., and Ataei, R. (2018). GWAS analysis in spring barley (*Hordeum vulgare* L.) for morphological traits exposed to drought. *PLoS One* 13**,** e0204952.

Jennings, H.S. (1917). The Numerical Results of Diverse Systems of Breeding, with Respect to Two Pairs of Characters, Linked or Independent, with Special Relation to the Effects of Linkage. *Genetics* 2**,** 97-154.

Jiang, S.C., Mei, C., Liang, S., Yu, Y.T., Lu, K., Wu, Z., Wang, X.F., and Zhang, D.P. (2015). Crucial roles of the pentatricopeptide repeat protein SOAR1 in *Arabidopsis* response to drought, salt and cold stresses. *Plant Mol Biol* 88**,** 369-385.

Joshi, C.P., and Chiang, V.L. (1998). Conserved sequence motifs in plant S-adenosyl-L-methionine-dependent methyltransferases. *Plant Mol Biol* 37**,** 663-674.

Jung, Y.J., Melencion, S.M., Lee, E.S., Park, J.H., Alinapon, C.V., Oh, H.T., Yun, D.J., Chi, Y.H., and Lee, S.Y. (2015). Universal stress protein exhibits a redox-dependent chaperone function in *Arabidopsis* and enhances plant tolerance to heat shock and oxidative stress. *Front Plant Sci* 6**,** 1141.

Kamal, N.M., Gorafi, Y.S.A., Mega, R., and Tsujimoto, H. (2018). Physiological response of wheat to chemical desiccants used to simulate post-anthesis drought stress. *Agronomy-Basel* 8**,** 44.

Kang, H.M., Zaitlen, N.A., Wade, C.M., Kirby, A., Heckerman, D., Daly, M.J., and Eskin, E. (2008). Efficient control of population structure in model organism association mapping. *Genetics* 178**,** 1709-1723.

Kant, S., Thoday-Kennedy, E., Joshi, S., Vakani, J., Hughes, J., Maphosa, L., Sadler, A., Menidis, M., Slater, A., and Spangenberg, G. (2017). Automated Rainout Shelter's Design for Well-Defined Water Stress Field Phenotyping of Crop Plants. *Crop Science* 57**,** 327-331.

Kapilan, R., Vaziri, M., and Zwiazek, J.J. (2018). Regulation of aquaporins in plants under stress. *Biol Res* 51**,** 4.

Kato, Y., and Sakamoto, W. (2018). FtsH Protease in the thylakoid membrane: physiological functions and the regulation of protease activity. *Front Plant Sci* 9**,** 855.

Kikuchi, R., and Handa, H. (2009). Photoperiodic control of flowering in barley. *Breeding Science* 59**,** 546-552.

Kirby, E., and Appleyard, M. (1987). *Cereal development guide.* Stoneleigh, UK: NAC Cereal Unit.

Kiyosue, T., Yamaguchi-Shinozaki, K., and Shinozaki, K. (1994). Cloning of cDNAs for genes that are early-responsive to dehydration stress (ERDs) in *Arabidopsis thaliana* L.: identification of three ERDs as HSP cognate genes. *Plant Mol Biol* 25**,** 791-798.

Klukas, C., Chen, D., and Pape, J.M. (2014). Integrated analysis platform: an open-source information system for high-throughput plant phenotyping. *Plant Physiol* 165**,** 506-518.

Koiwa, H., Barb, A.W., Xiong, L., Li, F., Mccully, M.G., Lee, B.H., Sokolchik, I., Zhu, J., Gong, Z., Reddy, M., Sharkhuu, A., Manabe, Y., Yokoi, S., Zhu, J.K., Bressan, R.A., and Hasegawa, P.M. (2002). C-terminal domain phosphatase-like family members (AtCPLs) differentially regulate *Arabidopsis thaliana* abiotic stress signaling, growth, and development. *Proc Natl Acad Sci U S A* 99**,** 10893-10898.

Komatsuda, T., Maxim, P., Senthil, N., and Mano, Y. (2004). High-density AFLP map of nonbrittle rachis 1 (btr1) and 2 (btr2) genes in barley (*Hordeum vulgare* L.). *Theor Appl Genet* 109**,** 986-995.

Komatsuda, T., Pourkheirandish, M., He, C., Azhaguvel, P., Kanamori, H., Perovic, D., Stein, N., Graner, A., Wicker, T., Tagiri, A., Lundqvist, U., Fujimura, T., Matsuoka, M., Matsumoto, T., and Yano, M. (2007). Six-rowed barley originated from a mutation in a homeodomain-leucine zipper I-class homeobox gene. *Proc Natl Acad Sci U S A* 104**,** 1424-1429.

Koppolu, R., Anwar, N., Sakuma, S., Tagiri, A., Lundqvist, U., Pourkheirandish, M., Rutten, T., Seiler, C., Himmelbach, A., Ariyadasa, R., Youssef, H.M., Stein, N., Sreenivasulu, N., Komatsuda, T., and Schnurbusch, T. (2013). *Six-rowed spike4* (*Vrs4*) controls spikelet determinacy and row-type in barley. *Proc Natl Acad Sci U S A* 110**,** 13198-13203.

Korte, A., and Farlow, A. (2013). The advantages and limitations of trait analysis with GWAS: a review. *Plant Methods* 9**,** 29.

Kuijt, S.J., Greco, R., Agalou, A., Shao, J., T Hoen, C.C., Overnas, E., Osnato, M., Curiale, S., Meynard, D., Van Gulik, R., De Faria Maraschin, S., Atallah, M., De Kam, R.J., Lamers, G.E., Guiderdoni, E., Rossini, L., Meijer, A.H., and Ouwerkerk, P.B. (2014). Interaction between the GROWTH-REGULATING FACTOR and KNOTTED1-LIKE HOMEOBOX families of transcription factors. *Plant Physiol* 164**,** 1952-1966.

Kumar, B., Abdel-Ghani, A.H., Pace, J., Reyes-Matamoros, J., Hochholdinger, F., and Lubberstedt, T. (2014). Association analysis of single nucleotide polymorphisms in candidate genes with root traits in maize (Zea mays L.) seedlings. *Plant Sci* 224**,** 9-19.

Kumar, J., Pratap, A., and Kumar, S. (2015a). Plant Phenomics: An Overview. 1-10.

Kumar, M.S., Ali, K., Dahuja, A., and Tyagi, A. (2015b). Role of phytosterols in drought stress tolerance in rice. *Plant Physiol Biochem* 96**,** 83-89.

Kushwaha, H.R., Singh, A.K., Sopory, S.K., Singla-Pareek, S.L., and Pareek, A. (2009). Genome wide expression analysis of CBS domain containing proteins in *Arabidopsis thaliana* (L.) Heynh and Oryza sativa L. reveals their developmental and stress regulation. *BMC Genomics* 10**,** 200.

Lai, C.P., Huang, L.M., Chen, L.O., Chan, M.T., and Shaw, J.F. (2017a). Genome-wide analysis of GDSL-type esterases/lipases in *Arabidopsis*. *Plant Mol Biol* 95**,** 181-197.

Lai, Y.P., Yu, Y., Liu, X., Wan, H., Zhang, Z., Wang, L., Leng, Y., Ma, L., Yang, W., and Feng, Z. (2017b). Association mapping of grain weight, length and width in barley (*Hordeum vulgare*) beeding germplasm. *INT J AGRIC BIOL* 19**,** 1175-1186.

Lander, E.S., and Botstein, D. (1989). Mapping mendelian factors underlying quantitative traits using RFLP linkage maps. *Genetics* 121**,** 185-199.

Langridge, P. (2018). "Economic and Academic Importance of Barley," in *The Barley Genome*, eds. N. Stein & G.J. Muehlbauer. (Cham: Springer International Publishing), 1-10.

Lazar, T. (2003). Taiz, L. and Zeiger, E. Plant physiology. 3rd edn. *Annals of Botany* 91**,** 750-751.

Li, J., Jiang, J., Qian, Q., Xu, Y., Zhang, C., Xiao, J., Du, C., Luo, W., Zou, G., Chen, M., Huang, Y., Feng, Y., Cheng, Z., Yuan, M., and Chong, K. (2011). Mutation of rice BC12/GDD1, which encodes a kinesin-like protein that binds to a GA biosynthesis gene promoter, leads to dwarfism with impaired cell elongation. *Plant Cell* 23**,** 628-640.

Long, N.V., Dolstra, O., Malosetti, M., Kilian, B., Graner, A., Visser, R.G., and Van Der Linden, C.G. (2013). Association mapping of salt tolerance in barley (*Hordeum vulgare* L.). *Theor Appl Genet* 126**,** 2335-2351.

Lu, W., Tang, X., Huo, Y., Xu, R., Qi, S., Huang, J., Zheng, C., and Wu, C.A. (2012). Identification and characterization of fructose 1,6-bisphosphate aldolase genes in *Arabidopsis* reveal a gene family with diverse responses to abiotic stresses. *Gene* 503**,** 65-74.

M. Ezzat Ahmadi, G.N., M. Kafi (2009). Effects of water deficit and spraying of dessicant on yield, yield components and water use efficiency of wheat genotypes.

Maiti, R.K., and Satya, P. (2014). Research advances in major cereal crops for adaptation to abiotic stresses. *GM Crops Food* 5**,** 259-279.

Mansour, E., Casas, A.M., Gracia, M.P., Molina-Cano, J.L., Moralejo, M., Cattivelli, L., Thomas, W.T.B., and Igartua, E. (2013). Quantitative trait loci for agronomic traits in an elite barley population for Mediterranean conditions. *Mol Breed* 33**,** 249-265.

Maroco, J.P., Pereira, J.S., and Manuela Chaves, M. (2000). Growth, photosynthesis and water-use efficiency of two C4Sahelian grasses subjected to water deficits. *Journal of Arid Environments* 45**,** 119-137.

Marschner, H. (2012). "Preface to Second Edition," in *Marschner's Mineral Nutrition of Higher Plants*, ed. P. Marschner. (San Diego: Academic Press), ix.

Mascher, M., Gundlach, H., Himmelbach, A., Beier, S., Twardziok, S.O., Wicker, T., Radchuk, V., Dockter, C., Hedley, P.E., Russell, J., Bayer, M., Ramsay, L., Liu, H., Haberer, G., Zhang, X.Q., Zhang, Q., Barrero, R.A., Li, L., Taudien, S., Groth, M., Felder, M., Hastie, A., Simkova, H., Stankova, H., Vrana, J., Chan, S., Munoz-Amatriain, M., Ounit, R., Wanamaker, S., Bolser, D., Colmsee, C., Schmutzer, T., Aliyeva-Schnorr, L., Grasso, S., Tanskanen, J., Chailyan, A., Sampath, D., Heavens, D., Clissold, L., Cao, S., Chapman, B., Dai, F., Han, Y., Li, H., Li, X., Lin, C., Mccooke, J.K., Tan, C., Wang, P., Wang, S., Yin, S., Zhou, G., Poland, J.A., Bellgard, M.I., Borisjuk, L., Houben, A., Dolezel, J., Ayling, S., Lonardi, S., Kersey, P., Langridge, P., Muehlbauer, G.J., Clark, M.D., Caccamo, M., Schulman, A.H., Mayer, K.F.X., Platzer, M., Close, T.J., Scholz, U., Hansson, M., Zhang, G., Braumann, I., Spannagl, M., Li, C., Waugh, R., and Stein, N. (2017). A chromosome conformation capture ordered sequence of the barley genome. *Nature* 544**,** 427-433.

Mascher, M., Jost, M., Kuon, J.E., Himmelbach, A., Assfalg, A., Beier, S., Scholz, U., Graner, A., and Stein, N. (2014). Mapping-by-sequencing accelerates forward genetics in barley. *Genome Biol* 15**,** R78.

Maurer, A., Draba, V., Jiang, Y., Schnaithmann, F., Sharma, R., Schumann, E., Kilian, B., Reif, J.C., and Pillen, K. (2015). Modelling the genetic architecture of flowering time control in barley through nested association mapping. *BMC Genomics* 16**,** 290.

Maurer, A., Draba, V., and Pillen, K. (2016). Genomic dissection of plant development and its impact on thousand grain weight in barley through nested association mapping. *J Exp Bot* 67**,** 2507-2518.

Mcadam, S.A., and Brodribb, T.J. (2014). Separating active and passive influences on stomatal control of transpiration. *Plant Physiol* 164**,** 1578-1586.

Milner, S.G., Jost, M., Taketa, S., Mazon, E.R., Himmelbach, A., Oppermann, M., Weise, S., Knupffer, H., Basterrechea, M., Konig, P., Schuler, D., Sharma, R., Pasam, R.K., Rutten, T., Guo, G., Xu, D., Zhang, J., Herren, G., Muller, T., Krattinger, S.G., Keller, B., Jiang, Y., Gonzalez, M.Y., Zhao, Y., Habekuss, A., Farber, S., Ordon, F., Lange, M., Borner, A., Graner, A., Reif, J.C., Scholz, U., Mascher, M., and Stein, N. (2019). Genebank genomics highlights the diversity of a global barley collection. *Nat Genet* 51**,** 319-326.

Mishra, P., and Panigrahi, K.C. (2015). GIGANTEA - an emerging story. *Front Plant Sci* 6**,** 8.

Mitra, J. (2001). Genetics and genetic improvement of drought resistance in crop plants. *Current Science* 80**,** 758-763.

Mulki, M.A., Bi, X., and Von Korff, M. (2018). Flowering locusT3 controls spikelet initiation but not floral development. *Plant Physiol* 178**,** 1170-1186.

Muraya, M.M., Chu, J., Zhao, Y., Junker, A., Klukas, C., Reif, J.C., and Altmann, T. (2017). Genetic variation of growth dynamics in maize (Zea mays L.) revealed through automated non-invasive phenotyping. *Plant J* 89**,** 366-380.

Murguia, J.R., Belles, J.M., and Serrano, R. (1995). A salt-sensitive 3'(2'),5'-bisphosphate nucleotidase involved in sulfate activation. *Science* 267**,** 232-234.

Mwadzingeni, L., Shimelis, H., Rees, D.J., and Tsilo, T.J. (2017). Genome-wide association analysis of agronomic traits in wheat under drought-stressed and non-stressed conditions. *PLoS One* 12**,** e0171692.

Nagel, K.A., Putz, A., Gilmer, F., Heinz, K., Fischbach, A., Pfeifer, J., Faget, M., Blossfeld, S., Ernst, M., Dimaki, C., Kastenholz, B., Kleinert, A.K., Galinski, A., Scharr, H., Fiorani, F., and Schurr, U. (2012). GROWSCREEN-Rhizo is a novel phenotyping robot enabling simultaneous measurements of root and shoot growth for plants grown in soil-filled rhizotrons. *Funct Plant Biol* 39**,** 891-904.

Nagel, M., Alqudah, A.M., Bailly, M., Rajjou, L., Pistrick, S., Matzig, G., Borner, A., and Kranner, I. (2019). Novel loci and a role for nitric oxide for seed dormancy and preharvest sprouting in barley. *Plant Cell Environ* 42**,** 1318-1327.

Nagel, M., Navakode, S., Scheibal, V., Baum, M., Nachit, M., Roder, M.S., and Borner, A. (2014). The genetic basis of durum wheat germination and seedling growth under osmotic stress. *Biologia Plantarum* 58**,** 681-688.

Nakamichi, N., Kiba, T., Henriques, R., Mizuno, T., Chua, N.H., and Sakakibara, H. (2010). PSEUDO-RESPONSE REGULATORS 9, 7, and 5 are transcriptional repressors in the *Arabidopsis* circadian clock. *Plant Cell* 22**,** 594-605.

Nawaz, A., Farooq, M., Alam, S., Yasmeen, A., and Wahid, A. (2013). *Stay green character at grain filling ensures resistance against terminal drought in wheat.*

Neumann, K., Klukas, C., Friedel, S., Rischbeck, P., Chen, D., Entzian, A., Stein, N., Graner, A., and Kilian, B. (2015). Dissecting spatiotemporal biomass accumulation in barley under different water regimes using high-throughput image analysis. *Plant Cell Environ* 38**,** 1980-1996.

Neumann, K., Kobiljski, B., Denčić, S., Varshney, R.K., and Börner, A. (2010). Genome-wide association mapping: a case study in bread wheat (*Triticum aestivum* L.). *Mol Breed* 27**,** 37-58.

Neumann, K., Zhao, Y., Chu, J., Keilwagen, J., Reif, J.C., Kilian, B., and Graner, A. (2017). Genetic architecture and temporal patterns of biomass accumulation in spring barley revealed by image analysis. *BMC Plant Biol* 17**,** 137.

Nezhad, K.Z., Weber, W.E., Roder, M.S., Sharma, S., Lohwasser, U., Meyer, R.C., Saal, B., and Borner, A. (2012). QTL analysis for thousand-grain weight under terminal drought stress in bread wheat (*Triticum aestivum* L.). *Euphytica* 186**,** 127-138.

Nicolas, M.E., and Turner, N.C. (1993). Use of chemical desiccants and senescing agents to select wheat lines maintaining stable grain size during post-anthesis drought. *Field Crop Res* 31**,** 155-171.

Nordborg, M., Borevitz, J.O., Bergelson, J., Berry, C.C., Chory, J., Hagenblad, J., Kreitman, M., Maloof, J.N., Noyes, T., Oefner, P.J., Stahl, E.A., and Weigel, D. (2002). The extent of linkage disequilibrium in *Arabidopsis thaliana*. *Nat Genet* 30**,** 190-193.

Ongom, P.O., Volenec, J.J., and Ejeta, G. (2016). Selection for drought tolerance in sorghum using desiccants to simulate post-anthesis drought stress. *Field Crop Res* 198**,** 312-321.

Papaefthimiou, D., Likotrafiti, E., Kapazoglou, A., Bladenopoulos, K., and Tsaftaris, A. (2010). Epigenetic chromatin modifiers in barley: III. Isolation and characterization of the barley GNAT-MYST family of histone acetyltransferases and responses to exogenous ABA. *Plant Physiol Biochem* 48**,** 98-107.

Pasam, R.K., Sharma, R., Malosetti, M., Van Eeuwijk, F.A., Haseneyer, G., Kilian, B., and Graner, A. (2012). Genome-wide association studies for agronomical traits in a world wide spring barley collection. *BMC Plant Biol* 12**,** 16.

Pasam, R.K., Sharma, R., Walther, A., Ozkan, H., Graner, A., and Kilian, B. (2014). Genetic diversity and population structure in a legacy collection of spring barley landraces adapted to a wide range of climates. *PLoS One* 9**,** e116164.

Pearce, S., Vanzetti, L.S., and Dubcovsky, J. (2013). Exogenous gibberellins induce wheat spike development under short days only in the presence of VERNALIZATION1. *Plant Physiol* 163**,** 1433-1445.

Pins, J.J., and Kaur, H. (2006). A review of the effects of barley beta-glucan on cardiovascular and diabetic risk. *Cereal Foods World* 51**,** 8-11.

Plaut, Z., Butow, B.J., Blumenthal, C.S., and Wrigley, C.W. (2004). Transport of dry matter into developing wheat kernels and its contribution to grain yield under post-anthesis water deficit and elevated temperature. *Field Crop Res* 86**,** 185-198.

Poland, J.A., Brown, P.J., Sorrells, M.E., and Jannink, J.L. (2012). Development of high-density genetic maps for barley and wheat using a novel two-enzyme genotyping-by-sequencing approach. *PLoS One* 7**,** e32253.

Pose, D., Castanedo, I., Borsani, O., Nieto, B., Rosado, A., Taconnat, L., Ferrer, A., Dolan, L., Valpuesta, V., and Botella, M.A. (2009). Identification of the *Arabidopsis* dry2/sqe1-5 mutant reveals a central role for sterols in drought tolerance and regulation of reactive oxygen species. *Plant J* 59**,** 63-76.

Pourkheirandish, M., and Komatsuda, T. (2007). The importance of barley genetics and domestication in a global perspective. *Ann Bot* 100**,** 999-1008.

Price, A.L., Patterson, N.J., Plenge, R.M., Weinblatt, M.E., Shadick, N.A., and Reich, D. (2006). Principal components analysis corrects for stratification in genome-wide association studies. *Nat Genet* 38**,** 904-909.

Pritchard, J.K., Stephens, M., and Donnelly, P. (2000a). Inference of population structure using multilocus genotype data. *Genetics* 155**,** 945-959.

Pritchard, J.K., Stephens, M., Rosenberg, N.A., and Donnelly, P. (2000b). Association mapping in structured populations. *Am J Hum Genet* 67**,** 170-181.

Probert, R.J., Daws, M.I., and Hay, F.R. (2009). Ecological correlates of ex situ seed longevity: a comparative study on 195 species. *Ann Bot* 104**,** 57-69.

Qaseem, M.F., Qureshi, R., Muqaddasi, Q.H., Shaheen, H., Kousar, R., and Roder, M.S. (2018). Genome-wide association mapping in bread wheat subjected to independent and combined high temperature and drought stress. *PLoS One* 13**,** e0199121.

Qin, P., Lin, Y., Hu, Y., Liu, K., Mao, S., Li, Z., Wang, J., Liu, Y., Wei, Y., and Zheng, Y. (2016). Genome-wide association study of drought-related resistance traits in Aegilops tauschii. *Genet Mol Biol* 39**,** 398-407.

Quinde, Z., Ullrich, S.E., and Baik, B.K. (2004). Genotypic variation in color and discoloration potential of barley-based food products. *Cereal Chemistry* 81**,** 752-758.

Rabbani, M.A., Maruyama, K., Abe, H., Khan, M.A., Katsura, K., Ito, Y., Yoshiwara, K., Seki, M., Shinozaki, K., and Yamaguchi-Shinozaki, K. (2003). Monitoring expression profiles of rice genes under cold, drought, and high-salinity stresses and abscisic acid application using cDNA microarray and RNA gel-blot analyses. *Plant Physiol* 133**,** 1755-1767.

Raffaele, S., Mongrand, S., Gamas, P., Niebel, A., and Ott, T. (2007). Genome-wide annotation of remorins, a plant-specific protein family: evolutionary and functional perspectives. *Plant Physiol* 145**,** 593-600.

Rahaman, M.M., Ahsan, M.A., Gillani, Z., and Chen, M. (2017). Digital Biomass Accumulation Using High-Throughput Plant Phenotype Data Analysis. *J Integr Bioinform* 14.

Ramsay, L., Comadran, J., Druka, A., Marshall, D.F., Thomas, W.T., Macaulay, M., Mackenzie, K., Simpson, C., Fuller, J., Bonar, N., Hayes, P.M., Lundqvist, U., Franckowiak, J.D., Close, T.J., Muehlbauer, G.J., and Waugh, R. (2011). *INTERMEDIUM-C,* a modifier of lateral spikelet fertility in barley, is an ortholog of the maize domestication gene *TEOSINTE BRANCHED 1*. *Nat Genet* 43**,** 169-172.

Regan, K.L., Whan, B.R., and Turner, N.C. (1993). Evaluation of chemical desiccation as a selection technique for drought resistance in a dryland wheat breeding program. *AUST J AGR RES* 44**,** 1683-1691.

Rollins, J.A., Drosse, B., Mulki, M.A., Grando, S., Baum, M., Singh, M., Ceccarelli, S., and Von Korff, M. (2013a). Variation at the vernalisation genes Vrn-H1 and Vrn-H2 determines growth and yield stability in barley (*Hordeum vulgare*) grown under dryland conditions in Syria. *Theor Appl Genet* 126**,** 2803-2824.

Rollins, J.A., Habte, E., Templer, S.E., Colby, T., Schmidt, J., and Von Korff, M. (2013b). Leaf proteome alterations in the context of physiological and morphological responses to drought and heat stress in barley (*Hordeum vulgare* L.). *J Exp Bot* 64**,** 3201-3212.

Ross-Ibarra, J., Morrell, P.L., and Gaut, B.S. (2007). Plant domestication, a unique opportunity to identify the genetic basis of adaptation. *Proc Natl Acad Sci U S A* 104 Suppl 1**,** 8641-8648.

Roy, J.K., Smith, K.P., Muehlbauer, G.J., Chao, S., Close, T.J., and Steffenson, B.J. (2010). Association mapping of spot blotch resistance in wild barley. *Mol Breed* 26**,** 243-256.

Russell, J., Mascher, M., Dawson, I.K., Kyriakidis, S., Calixto, C., Freund, F., Bayer, M., Milne, I., Marshall-Griffiths, T., Heinen, S., Hofstad, A., Sharma, R., Himmelbach, A., Knauft, M., Van Zonneveld, M., Brown, J.W., Schmid, K., Kilian, B., Muehlbauer, G.J., Stein, N., and Waugh, R. (2016). Exome sequencing of geographically diverse barley landraces and wild relatives gives insights into environmental adaptation. *Nat Genet* 48**,** 1024-1030.

Saisho, D., and Takeda, K. (2011). Barley: emergence as a new research material of crop science. *Plant Cell Physiol* 52**,** 724-727.

Samarah, N., and Alqudah, A. (2011). Effects of late-terminal drought stress on seed germination and vigor of barley (*Hordeum vulgare*L.). *Archives of Agronomy and Soil Science* 57**,** 27-32.

Samarah, N.H. (2005). Effects of drought stress on growth and yield of barley. *Agron Sustain Dev* 25**,** 145-149.

Samarah, N.H., Alqudah, A.M., Amayreh, J.A., and Mcandrews, G.M. (2009). The effect of late-terminal drought stress on yield components of four barley cultivars. *J Agron Crop Sci* 195**,** 427-441.

Samira, R., Li, B., Kliebenstein, D., Li, C., Davis, E., Gillikin, J.W., and Long, T.A. (2018). The bHLH transcription factor ILR3 modulates multiple stress responses in *Arabidopsis*. *Plant Mol Biol* 97**,** 297-309.

Sanchez-Bragado, R., Molero, G., Reynolds, M.P., and Araus, J.L. (2016). Photosynthetic contribution of the ear to grain filling in wheat: a comparison of different methodologies for evaluation. *J Exp Bot* 67**,** 2787-2798.

Sawhney, V., and Singh, D.P. (2002). Effect of chemical desiccation at the post-anthesis stage on some physiological and biochemical changes in the flag leaf of contrasting wheat genotypes. *FIield Crop Res* 77**,** 1-6.

Senapati, N., Stratonovitch, P., Paul, M.J., and Semenov, M.A. (2019). Drought tolerance during reproductive development is important for increasing wheat yield potential under climate change in Europe. *J Exp Bot* 70**,** 2549-2560.

Shakhatreh, Y., Kafawin, O., Ceccarelli, S., and Saoub, H. (2001). Selection of barley lines for drought tolerance in low-rainfall areas. *J Agron Crop Sci* 186**,** 119-127.

Shekoofa, A., and Sinclair, T.R. (2018). Aquaporin Activity to Improve Crop Drought Tolerance. *Cells* 7.

Si, L., Chen, J., Huang, X., Gong, H., Luo, J., Hou, Q., Zhou, T., Lu, T., Zhu, J., Shangguan, Y., Chen, E., Gong, C., Zhao, Q., Jing, Y., Zhao, Y., Li, Y., Cui, L., Fan, D., Lu, Y., Weng, Q., Wang, Y., Zhan, Q., Liu, K., Wei, X., An, K., An, G., and Han, B. (2016). OsSPL13 controls grain size in cultivated rice. *Nat Genet* 48**,** 447-456.

Sinclair, T.R., and Jamieson, P.D. (2006). Grain number, wheat yield, and bottling beer: An analysis. *Field Crop Res* 98**,** 60-67.

Singh, A., Kushwaha, H.R., Soni, P., Gupta, H., Singla-Pareek, S.L., and Pareek, A. (2015a). Tissue specific and abiotic stress regulated transcription of histidine kinases in plants is also influenced by diurnal rhythm. *Front Plant Sci* 6**,** 711.

Singh, A.K., Singh, A., Singh, A.K., Shamim, M., Vikram, P., Singh, S., and Chaturvedi, G. (2012). Application of potassium iodide as a new agent for screening of drought tolerance upland rice genotypes at flowering stage. *PKJ* 1**,** 25.

Singh, B., Bohra, A., Mishra, S., Joshi, R., and Pandey, S. (2015b). Embracing new-generation 'omics' tools to improve drought tolerance in cereal and food-legume crops. *Biol. Plant* 59**,** 413-428.

Slafer, G., Molina, J., Savin, R., Araus, J., and Romagosa, I. (2002). *Barley science: recent advances from molecular biology to agronomy of yield and quality*. New York: Food Products Press. The Harworth Press.

Sonah, H., O'donoughue, L., Cober, E., Rajcan, I., and Belzile, F. (2015). Identification of loci governing eight agronomic traits using a GBS-GWAS approach and validation by QTL mapping in soya bean. *Plant Biotechnol J* 13**,** 211-221.

Sreenivasulu, N., and Schnurbusch, T. (2012). A genetic playground for enhancing grain number in cereals. *Trends Plant Sci* 17**,** 91-101.

Sridha, S., and Wu, K. (2006). Identification of AtHD2C as a novel regulator of abscisic acid responses in *Arabidopsis*. *Plant J* 46**,** 124-133.

Stone, J.M., and Walker, J.C. (1995). Plant protein kinase families and signal transduction. *Plant Physiol* 108**,** 451-457.

Storey, J.D. (2003). The positive false discovery rate: A Bayesian interpretation and the q-value. *Annals of Statistics* 31**,** 2013-2035.

Storey, J.D., and Tibshirani, R. (2003). Statistical significance for genomewide studies. *Proc Natl Acad Sci U S A* 100**,** 9440-9445.

Stotz, H.U., Thomson, J.G., and Wang, Y. (2009). Plant defensins: defense, development and application. *Plant Signal Behav* 4**,** 1010-1012.

Stracke, S., Haseneyer, G., Veyrieras, J.B., Geiger, H.H., Sauer, S., Graner, A., and Piepho, H.P. (2009). Association mapping reveals gene action and interactions in the determination of flowering time in barley. *Theor Appl Genet* 118**,** 259-273.

Sunohara, H., Kawai, T., Shimizu-Sato, S., Sato, Y., Sato, K., and Kitano, H. (2009). A dominant mutation of TWISTED DWARF 1 encoding an alpha-tubulin protein causes severe dwarfism and right helical growth in rice. *Genes Genet Syst* 84**,** 209-218.

Swindell, W.R., Huebner, M., and Weber, A.P. (2007). Transcriptional profiling of *Arabidopsis* heat shock proteins and transcription factors reveals extensive overlap between heat and non-heat stress response pathways. *BMC Genomics* 8**,** 125.

Szira, F., Balint, A.F., Borner, A., and Galiba, G. (2008). Evaluation of drought-related traits and screening methods at different developmental stages in spring barley. *Journal of Agronomy and Crop Science* 194**,** 334-342.

Tanksley, S.D., and Mccouch, S.R. (1997). Seed banks and molecular maps: unlocking genetic potential from the wild. *Science* 277**,** 1063-1066.

Tarawneh, R.A., Szira, F., Monostori, I., Behrens, A., Alqudah, A.M., Thumm, S., Lohwasser, U., Roder, M.S., Borner, A., and Nagel, M. (2019). Genetic analysis of drought response of wheat following either chemical desiccation or the use of a rain-out shelter. *J Appl Genet* 60**,** 137-146.

Tardieu, F., Cabrera-Bosquet, L., Pridmore, T., and Bennett, M. (2017). Plant phenomics from sensors to knowledge. *Curr Biol* 27**,** R770-R783.

Teulat, B., Zoumarou-Wallis, N., Rotter, B., Ben Salem, M., Bahri, H., and This, D. (2003). QTL for relative water content in field-grown barley and their stability across Mediterranean environments. *Theor Appl Genet* 108**,** 181-188.

Thabet, S.G., Moursi, Y.S., Karam, M.A., Graner, A., and Alqudah, A.M. (2018). Genetic basis of drought tolerance during seed germination in barley. *PLoS One* 13**,** e0206682.

Thorp , A.L.T., , S.J.H., , A.N.F.A., and Ward, R.W. (2017). High Throughput Phenotyping of Blueberry Bush Morphological Traits Using Unmanned Aerial Systems. *Remote Sensing* 9.

Trevaskis, B., Tadege, M., Hemming, M.N., Peacock, W.J., Dennis, E.S., and Sheldon, C. (2007). Short vegetative phase-like MADS-box genes inhibit floral meristem identity in barley. *Plant Physiol* 143**,** 225-235.

Tuberosa, R., and Salvi, S. (2006). Genomics-based approaches to improve drought tolerance of crops. *Trends Plant Sci* 11**,** 405-412.

Turner, A., Beales, J., Faure, S., Dunford, R.P., and Laurie, D.A. (2005). The pseudo-response regulator Ppd-H1 provides adaptation to photoperiod in barley. *Science* 310**,** 1031-1034.

Tyagi, R., and Agrawal, A. (2013). *Genebank standards -revised guidelines adopted by FAO.*

Ugarte, C., Calderini, D.F., and Slafer, G.A. (2007). Grain weight and grain number responsiveness to pre-anthesis temperature in wheat, barley and triticale. *Field Crop Res* 100**,** 240-248.

Van Nocker, S., and Ludwig, P. (2003). The WD-repeat protein superfamily in *Arabidopsis*: conservation and divergence in structure and function. *BMC Genomics* 4**,** 50.

Varshney, R.K., Paulo, M.J., Grando, S., Van Eeuwijk, F.A., Keizer, L.C.P., Guo, P., Ceccarelli, S., Kilian, A., Baum, M., and Graner, A. (2012). Genome wide association analyses for drought tolerance related traits in barley (*Hordeum vulgare* L.). *Field Crop Res* 126**,** 171-180.

Voorrips, R.E. (2002). MapChart: software for the graphical presentation of linkage maps and QTLs. *J Hered* 93**,** 77-78.

Vsn International (2013). "GenStat for Windows 18th edition". (Hemel Hempstead, UK. Web page: GenStat.co.uk: VSN International,Ltd, UK).

Wallsten, J., and Martinsson, K. (2009). Effects of maturity stage and feeding strategy of whole crop barley silage on intake, digestibility and milk production in dairy cows. *Livestock Science* 121**,** 155-161.

Walsh, K., O'kiely, P., Moloney, A.P., and Boland, T.M. (2008). Intake, digestibility, rumen fermentation and performance of beef cattle fed diets based on whole-crop wheat or barley harvested at two cutting heights relative to maize silage or ad libitum concentrates. *Animal Feed Science and Technology* 144**,** 257-278.

Wang, G., Schmalenbach, I., Von Korff, M., Leon, J., Kilian, B., Rode, J., and Pillen, K. (2010). Association of barley photoperiod and vernalization genes with QTLs for flowering time and agronomic traits in a BC2DH population and a set of wild barley introgression lines. *Theor Appl Genet* 120**,** 1559-1574.

Wang, H., Smith, K.P., Combs, E., Blake, T., Horsley, R.D., and Muehlbauer, G.J. (2012a). Effect of population size and unbalanced data sets on QTL detection using genome-wide association mapping in barley breeding germplasm. *Theor Appl Genet* 124**,** 111-124.

Wang, M., Jiang, N., Jia, T., Leach, L., Cockram, J., Comadran, J., Shaw, P., Waugh, R., and Luo, Z. (2012b). Genome-wide association mapping of agronomic and morphologic traits in highly structured populations of barley cultivars. *Theor Appl Genet* 124**,** 233-246.

Wang, X., Cai, X., Xu, C., Wang, Q., and Dai, S. (2016). Drought responsive mechanisms in plant leaves revealed by proteomics. *Int J Mol Sci* 17.

Wang, Z., Cheng, K., Wan, L., Yan, L., Jiang, H., Liu, S., Lei, Y., and Liao, B. (2015). Genome-wide analysis of the basic leucine zipper (bZIP) transcription factor gene family in six legume genomes. *BMC Genomics* 16**,** 1053.

Ward, B., Brien, C., Oakey, H., Pearson, A., Negrao, S., Schilling, R.K., Taylor, J., Jarvis, D., Timmins, A., Roy, S.J., Tester, M., Berger, B., and Van Den Hengel, A. (2019). High-throughput 3D modelling to dissect the genetic control of leaf elongation in barley (*Hordeum vulgare*). *Plant J* 98**,** 555-570.

Wardlaw, I.F. (1972). Responses of Plants to Environmental Stresses. J. Levitt. Academic Press, New York, 1972. xiv, 698 pp., illus. $32.50. Physiological Ecology. *Science* 177**,** 786-786.

Waugh, R., Jannink, J.L., Muehlbauer, G.J., and Ramsay, L. (2009). The emergence of whole genome association scans in barley. *Curr Opin Plant Biol* 12**,** 218-222.

Wehner, G.G., Balko, C.C., Enders, M.M., Humbeck, K.K., and Ordon, F.F. (2015). Identification of genomic regions involved in tolerance to drought stress and drought stress induced leaf senescence in juvenile barley. *BMC Plant Biol* 15**,** 125.

Weight, C., Parnham, D., and Waites, R. (2008). LeafAnalyser: a computational method for rapid and large-scale analyses of leaf shape variation. *Plant J* 53**,** 578-586.

Wojcik-Jagla, M., Fiust, A., Koscielniak, J., and Rapacz, M. (2018). Association mapping of drought tolerance-related traits in barley to complement a traditional biparental QTL mapping study. *Theor Appl Genet* 131**,** 167-181.

Xie, H., Wang, Y., Ding, Y., Qiu, C., Sun, L., Gai, Z., Gu, H., and Ding, Z. (2019). Global Ubiquitome Profiling Revealed the Roles of Ubiquitinated Proteins in Metabolic Pathways of Tea Leaves in Responding to Drought Stress. *Sci Rep* 9**,** 4286.

Xing, H., Fu, X., Yang, C., Tang, X., Guo, L., Li, C., Xu, C., and Luo, K. (2018). Genome-wide investigation of pentatricopeptide repeat gene family in poplar and their expression analysis in response to biotic and abiotic stresses. *Sci Rep* 8**,** 2817.

Xu, X., Sharma, R., Tondelli, A., Russell, J., Comadran, J., Schnaithmann, F., Pillen, K., Kilian, B., Cattivelli, L., Thomas, W.T.B., and Flavell, A.J. (2018). Genome-wide association analysis of grain Yield associated traits in a pan-European barley cultivar collection. *Plant Genome* 11.

Yamasaki, Y., Gao, F., Jordan, M.C., and Ayele, B.T. (2017). Seed maturation associated transcriptional programs and regulatory networks underlying genotypic difference in seed dormancy and size/weight in wheat (*Triticum aestivum* L.). *BMC Plant Biol* 17**,** 154.

Yang, J., and Zhang, J. (2006). Grain filling of cereals under soil drying. *New Phytol* 169**,** 223-236.

Yang, S.Q., Li, W.Q., Miao, H., Gan, P.F., Qiao, L., Chang, Y.L., Shi, C.H., and Chen, K.M. (2016). REL2, a gene encoding an unknown function protein which contains DUF630 and DUF632 domains controls leaf rolling in rice. *Rice* 9**,** 37.

Yang, W., Guo, Z., Huang, C., Duan, L., Chen, G., Jiang, N., Fang, W., Feng, H., Xie, W., Lian, X., Wang, G., Luo, Q., Zhang, Q., Liu, Q., and Xiong, L. (2014). Combining high-throughput phenotyping and genome-wide association studies to reveal natural genetic variation in rice. *Nat Commun* 5**,** 5087.

Youssef, H.M., Eggert, K., Koppolu, R., Alqudah, A.M., Poursarebani, N., Fazeli, A., Sakuma, S., Tagiri, A., Rutten, T., Govind, G., Lundqvist, U., Graner, A., Komatsuda, T., Sreenivasulu, N., and Schnurbusch, T. (2017). VRS2 regulates hormone-mediated inflorescence patterning in barley. *Nat Genet* 49**,** 157-161.

Zadoks, J.C., Chang, T.T., and Konzak, C.F. (1974). Adecimal code for the growth stages. *weed research*.

Zenda, T., Liu, S., Wang, X., Jin, H., Liu, G., and Duan, H. (2018). Comparative proteomic and physiological analyses of two Divergent maize Inbred Lines provide more insights into drought stress tolerance mechanisms. *Int J Mol Sci* 19.

Zeng, Z.B. (1993). Theoretical basis for separation of multiple linked gene effects in mapping quantitative trait loci. *Proc Natl Acad Sci U S A* 90**,** 10972-10976.

Zheng, B., He, H., Zheng, Y., Wu, W., and Mccormick, S. (2014). An ARID domain-containing protein within nuclear bodies is required for sperm cell formation in *Arabidopsis thaliana*. *PLoS Genet* 10**,** e1004421.

Zhou, G.F., Johnson, P., Ryan, P.R., Delhaize, E., and Zhou, M.X. (2012). Quantitative trait loci for salinity tolerance in barley (*Hordeum vulgare* L.). *Mol Breed* 29**,** 427-436.

Zhu, C.S., Gore, M., Buckler, E.S., and Yu, J.M. (2008). Status and Prospects of Association Mapping in Plants. *Plant Genome* 1**,** 5-20.

Zohary, D., and M, H. (2000). "Domestication of plants in the old world". Oxford University Press, Oxford, UK).

Rasha Tarawneh

Curriculum Vitae

Education

Oct. 2015 –present **PhD Candidate**

Martin-Luther University Halle-Wittenberg, Germany und Leibniz Institut für Pflanzengenetik und Kulturpflanzenforschung (IPK), Germany
PhD thesis: „Mapping and Identifying Genes for Drought Tolerance in Barley (*Hordeum Vulgare* L.)"

Feb. 2008 – Feb. 2010 **MSc Plant Crops Protection**

Mutah University, Jordan
MSc thesis: „Physiological and Biochemical Aspects of Two Olive Cultivars as Influenced by Deficit Irrigation and Irrigation Water Salinity"

Sept. 2001 – Jun. 2005 **BSc Plant Protection**

Mutah University, Jordan

Professional Experience

Apr. 2011 – Apr. 2015 **Project Coordinator**

Jordan Hashemite Fund for Human Development, Jordan

Apr. 2010 – Apr. 2011 **Administrative Assistant**

Arab Group for Education and Training, Jordan

Feb. 2006 – Feb. 2008 **Research Assistant**

Plant Production Department, Mutah University Jordan

Courses

- Statistics and Figures with R, Apr. 2017; IPK Gatersleben, Germany
- Proposal Writing, Mar. 2017; IPK Gatersleben, Germany
- Plant in Vitro Propagation and Cryopreservation, Sep. 2016; IPK Gatersleben, Germany
- Statistics Based on R, Aug. 2016; IPK Gatersleben, Germany
- Academic Writing: How to create good texts, May 2019; IPK Gatersleben, Germany

Lectures and Conferences

- Lecture series in Genebank Department, Oct. 2015- present, IPK Gatersleben, Germany
- Lecture series for PhD students, Oct. 2015- present, IPK Gatersleben, Germany
- "Genome-Wide Association Analysis Controlled Seed Deterioration Using Barley Genebank Accessions" (Poster), Arbeitstagung der Arbeitsgemeinschaft Saatgut- und Sortenwesen, Apr. 2016, Universität Regensburg, Germany
- „Controlled Deterioration Affects Viability of Barley Genebank Accessions"(Oral Presentation), The 12th Plant Science Student Conference (PSSC), Jul. 2017, IPK Gatersleben, Germany
- "Quantitative Mapping of Barley Sees Viability After Controlled Deterioration" (Oral Presentation), The International Biodiversity and Sustainable Development Conference, Oct. 2016, Helwan University, Egypt
- "Genome-Wide Association Mapping Studies Reveal Loci for Agronomical Traits in Spring Wheat under Drought Stress" (Poster), The 5th Quedlinburger Pflaznezüchtungstage, GPZ Meeting of AG Genomanalyse and the 18th Kurt von Rümker Symposium. Status of Translating Genomics into Application, Mar. 2017, IPK Gatersleben, Germany
- "Studies on Drought Stress in a Spring Wheat Genebank Collection Using Genome-Wide Association Mapping" (Poster), Crop Diversification in a Changing World. Mobilizing the Green Gold of Plant Genetic Resources, May 2017, Montpellier, France
- „Controlled Deterioration Affects Viability of Barley Genebank Accessions"(Oral Presentation), The 8th International Triticeae Symposium 2017, Jun. 2017, Wernigerode, Germany
- "Genome-Wide Association Mapping to Identify Candidate Genes for Drought Tolerance in Barley (Oral Presentation), The International Cereal Conference, May 2018, Lublin, Poland

Languages

- English: fluent
- German: Intermediate level (B1)
- Arabic: Mother tongue
-

Gatersleben,

Eidesstattliche Erklärung / Declaration under Oath

Ich erkläre an Eides statt, dass ich die Arbeit selbstständig und ohne fremde Hilfe verfasst, keine anderen als die von mir angegebenen Quellen und Hilfsmittel benutzt und die den benutzten Werken wörtlich oder inhaltlich entnommenen Stellen als solche kenntlich gemacht habe.

I declare under penalty of perjury that this thesis is my own work entirely and has been written without any help from other people. I used only the sources mentioned and included all the citations correctly both in word or content.

_____ _____

Datum / Date Unterschrift des Antragstellers / *Signature of the applicant*

Erklärung über bestehende Vorstrafen und anhängige Ermittlungsverfahren /

Declaration concerning Criminal Record and Pending Investigations

Hiermit erkläre ich, dass ich weder vorbestraft bin noch dass gegen mich Ermittlungsverfahren anhängig sind. */ I hereby declare that I have no criminal record and that no preliminary investigations are pending against me.*

_____ _____

Datum / Date Unterschrift des Antragstellers / *Signature of the applicant*